THE DYNAMIC RESPONSE OF FLOATING BRIDGES TO TRANSIENT LOADS

By

J. P. Romualdi - Project Engineer
E. D'Appolonia - Associate Professor
F. T. Mavis - Head

Department of Civil Engineering
Carnegie Institute of Technology

For

Office of Naval Research

Contract No. Nonr - 760(03)

August, 1954

THE DYNAMIC RESPONSE OF FLOATING BRIDGES TO TRANSIENT LOADS

By

J. P. Romualdi - Project Engineer

E. D'Appolonia - Associate Professor

F. T. Mavis - Head

Department of Civil Engineering

Carnegie Institute of Technology

August 1954

This work was sponsored by the Army, Navy and Air Force through the Joint Services Advisory Committee for Research Groups in Applied Mathematics and Statistics by Contract No. Nonr-760(03).

TABLE OF CONTENTS

LIST OF FIGURES

LIST OF FIGURES (continued)

LIST OF FIGURES (continued)

LIST OF FIGURES (continued)

ACKNOWLEDGMENTS

This research project described herein was sponsored by the Army, Navy and Air Force through the Joint Services Advisory Committee for Research Groups in Applied Mathematics and Statistics by Contract No. Nonr-760(03). The authors acknowledge their indebtedness to the members of the Civil Engineering Department for their helpful suggestions, and to Robert Hagaman and Dayton Cook for their aid in carrying out the computations. They are also grateful to Dr. H. M. Trent and Dr. W. A. McCool, both of the Naval Research Laboratories, Washington, D. C., for their kindness in making available the analog computor at the Naval Research Laboratories.

INTRODUCTION

A floating bridge is essentially a continuous bridge on n intermediate supports which act as elastic springs. The resistance of a support, brought about by the buoyant force of the water, may be linear or non-linear with respect to displacement depending upon the geometry of the support. A study of the dynamic behavior of such structures is complicated by the fact that the mass of a floating support, or ponton, is not constant. This is due to the virtual mass of the ponton which must be considered in the case of bodies accelerating in fluids. The virtual mass of the ponton is the mass of the ponton in air plus the added mass which is usually expressed in terms of the mass of displaced water. The added mass arises from the vertical acceleration of the ponton through the water. However, as the ponton is displaced the quantity of displaced water changes and hence, the added mass changes. We are then confronted with the problem of a mass which varies with displacement. In the literature there is little treatment of this type of non-linear problem. By formal mathematical methods solutions of engineering problems of this type are intractable. Most non-linear problems treat the case of mass varying with time, as in the problems associated with rocket flight.

The most important application of a dynamic analysis of floating bridges, at present, is in the design of military ponton bridges. A brief survey of existing design standards indicates that these bridges are designed for static loads only whereas, as will be subsequently

shown, the dynamic displacements for a given moving load can be twice as great as the corresponding static displacement! This is important not only with respect to the maximum permissible displacement before swamping but also with respect to the stresses set up in the ponton shell.

This investigation, however, is concerned with displacements and results are presented in terms of impact factors. The impact factor is defined as the ratio of the maximum dynamic displacement of the bridge due to a moving load to the maximum static displacement that can be caused by the same load if it were applied statically to the bridge. For bridges with an odd number of pontons the maximum static displacement occurs when the load is at the center ponton. The maximum dynamic displacement, however, usually occurs after the moving load has passed the center ponton. If the maximum stresses due to a moving load are desired, they can be calculated to a good approximation from the dynamic deflected load line by determining the static forces necessary to produce the same displacements. The stresses can then be calculated from the bending moments produced by these loads.

A floating ponton bridge is a series of discrete floating units normally with some degree of articulation between the deck structure and the pontons. Articulation is not considered in this work. It is assumed that the bridge is floating at its dead weight displacement which is 5.2 in. for an M-4 ponton bridge. All displacements presented in this work are measured from this datum and the structure is considered continuous. This means that the resistance to displacements due to moving loads comes from three sources; (1) the flexural

rigidity of the continuous deck structure, (2) the buoyant force of the water and (3) the inertia of the structure. The buoyant resistance of a ponton to displacement is 1500 lbs/in. The combined resistance to displacement of a single ponton bridge of 30 ft span, due to the buoyant force of the water and the flexural rigidity of the bridge, is 34420 lbs/in. These figures give the relative order of magnitude of the resistance of the deck structure to resistance of the water. The capacity of a single ponton before swamping is about 60000 lbs which is about eight times the weight of a ponton plus one-half the adjoining spans. The mass of the loads supported by a ponton bridge, therefore, is large in comparison to the mass of the bridge. This study has been extended to take into account the mass of the load for loads up to 78000 lbs.

The natural period of vibration for ponton bridges ranges from 0.150 sec for a single ponton bridge to 0.64 sec for a five ponton bridge. These values neglect virtual mass. The actual periods are less due to the effect of virtual mass and are different at different depths of submergence. However, to serve as a basis of comparison, the time for a moving load to cross a given structure is given in terms of the natural fundamental period of that structure neglecting virtual mass. In general the maximum dynamic effects occur when the load crosses the bridge in about one or two times the fundamental period of the bridge. For a three ponton bridge, for example, with a natural fundamental period of 0.37 sec and a span length of 60 ft the speed of the moving load will be 55 mph if the load crosses in twice the fundamental period. For a five ponton bridge (span length = 90 ft) the corresponding speed is 49 mph. The range of

times of crossing studied was selected to include this normal range of operation.

In general, a ponton bridge consists of many pontons. But the analysis of bridges of more than four or five pontons is extremely laborious. The number of simultaneous differential equations describing the behavior of such structures is equal to the number of pontons. This work, however, is concerned only with bracketing the effects of the different variables that affect the behavior of such floating structures and to establish trends and show relative variations. The study of bridges of from one to five pontons is considered sufficient for this purpose.

A continuous floating bridge on n intermediate supports, subjected to a load P moving across the span with velocity v, is shown in Fig. 1.

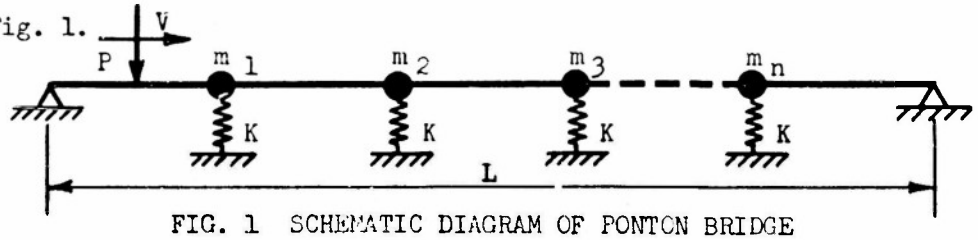

FIG. 1 SCHEMATIC DIAGRAM OF PONTON BRIDGE

The general equations describing the displacement of each support, 1, 2, 3...n, due to the moving load P, are

$$\begin{aligned} m_1\ddot{y}_1 + (a_{11}+K)y_1 + a_{12}y_2 + \cdots + a_{1n}y_n &= F_1(t) \\ m_2\ddot{y}_2 + a_{21}y_1 + (a_{22}+K)y_2 + \cdots + a_{2n}y_n &= F_2(t) \\ \vdots \\ m_n\ddot{y}_n + a_{n1}y_1 + a_{n2}y_2 + \cdots + (a_{nn}+K)y_n &= F_n(t) \end{aligned} \qquad (1)$$

or

$$\sum_{i=1}^{n} \left\{ m_i\ddot{y}_i + \sum_{j=1}^{n} (a_{ij}+\delta_{ij}K)y_j - F_j(t) \right\} = 0 \qquad (2)$$

where δ_{ij}, the Kronecker Delta, is 0 when $i \neq j$
and 1 when $i=j$

m_i is the equivalent concentrated mass at support i, (lbs-sec^2/in.)

a_{ij} is the reaction at support i due to a unit displacement at support j, (lbs/in.)

K is the slope of the buoyant force-displacement relationship of the floating support, (lbs/in.)

y_i is the displacement of support i, (in.)

$F_i(t)$ is the external force at support i due to the load P at any time t, (lbs)

The general cases considered in this work are:

(a) m_i and K are constants. The load P is a constant force (its mass is neglected). F_i is a linear function of the position of the load P on the span; and since P moves across the span with constant velocity F_i is linearly time dependant. The equations then appear as in (2).

(b) m_i' is the virtual mass and is given by

$$m_i' = M_i + \xi y_i$$

The equations of motion then become

$$\sum_{i=1}^{n} \left\{ \left[M_i + \xi y_i \right] \ddot{y}_i + \sum_{j=1}^{n} (a_{ij} + \delta_{ij} K) y_j - F_i(t) \right\} = 0 \quad (3)$$

(c) The mass of the moving load P is considered. Hence, F_i is a function of time and the inertia force of the moving load, P. The equations of motion can then be represented as

$$\sum_{i=1}^{n} \left\{ m_i \ddot{y}_i + \sum_{j=1}^{n} (a_{ij} + \delta_{ij} K) y_j - F_i(t, \ddot{y}_p) \right\} = 0 \qquad (4)$$

where $\ddot{y}_p$ is the vertical acceleration of the bridge at the position of the load P.

(d) Viscous damping is considered. Letting C be the coefficient of viscous damping the equations are

$$\sum_{i=1}^{n} \left\{ m_i \ddot{y}_i + C\dot{y}_i + \sum_{j=1}^{n} (a_{ij} + \delta_{ij} K) y_j - F_i(t) \right\} = 0 \qquad (5)$$

(e) The most general case includes virtual mass, damping, and the mass of the moving load. The equations, assuming a linear spring constant K, are

$$\sum_{i=1}^{n} \left\{ \left[M_i + \gamma_i \right] \ddot{y}_i + C\dot{y}_i + \sum_{j=1}^{n} (a_{ij} + \delta_{ij} K) y_j - F_i(t, \ddot{y}_p) \right\} = 0 \qquad (6)$$

In this thesis a numerical procedure developed by J. M. Bonetti [1] is applied to the solution of these problems. The method is based on the concept of impulse-momentum and the solution is carried out by successive integration over short time intervals. The method is extended to the non-linear class of problems of cases (b), (c), and (e).

(1) Numbers in raised parentheses refer to Bibliography

Problems in each of the above five categories were solved by this numerical method as illustrations. The bulk of the solutions, however, were obtained on the electronic analog computor which is installed at the Naval Research Laboratories in Washington, D. C. The method of solution by the analog computor is discussed and in a few cases the analog and numerical solutions are compared. Exact solutions of the differential equations of motion by formal mathematical methods are obtained to check the analog and numerical solutions.

Experimental tests were conducted to verify the importance of the influence of virtual mass on the transient oscillations of floating structures. From known impulses calculated solutions were obtained neglecting virtual mass and damping and considering virtual mass and damping. These results are compared with experimental results. An experimental procedure for determining virtual mass is also presented.

PREVIOUS WORK

The behavior of a floating bridge subjected to moving loads falls into the broader classification of moving loads on simple span bridges. Indeed, a floating bridge can be thought of as a simple span bridge whose flexural rigidity is augmented by the addition of intermediate springs.

Early investigations of the effect of moving loads on bridges were conducted by Sir G. G. Stokes who was concerned with the deflection of a simply supported girder subjected to a concentrated mass moving with constant speed [2]. Applications of his treatment are

limited because the mass of the load is assumed large compared to the mass of the girder which is neglected in his method of solution

The case of a constant force moving across a simply supported girder was studied by Sir C. E. Inglis[3] and by S. Tomoshenko[4]. In this case the differential equation of motion for a simple span, subjected to a moving load P whose mass is neglected, is

$$\frac{\partial^4 y}{\partial x^4} + k^2 \frac{\partial^2 y}{\partial t^2} = \frac{1}{EI} P(x,t) \qquad (7)$$

where w is the weight per unit length of girder

EI is the flexural stiffness of the girder

$k^2 = w/EIg$

y is the vertical displacement at distance x along the span.

In general, the moving force P(x,t) can be expressed as an harmonic series whence, equation (7) becomes

$$\frac{\partial^4 y}{\partial x^4} + k^2 \frac{\partial^2 y}{\partial t^2} = \frac{2P}{EIL} \sum_{i=1}^{n} \sin \frac{i\pi x}{L} \sin \frac{i\pi vt}{L} \qquad (8)$$

where L is the length of the span

v is the velocity of the moving load P

The general case in which the mass of the load and the mass of the beam are considered was first investigated by H. H. Jeffcott[5]. The method, however, based on successive approximations, was cumbersome and did not converge in many cases. A more complete analysis, based on the method of Inglis, was afforded by A. Hillerborg[6]. He also expressed the forcing function as an harmonic series and obtained

the differential equations of motion for a simple span in the form

$$\frac{\partial^4 y}{\partial x^4} + k^2 \frac{\partial^2 y}{\partial t^2} = \frac{2m_L}{EIL}\left[g - \frac{d^2 y(vt,t)}{dx^2}\right]\sum_{i=1}^{n} \sin\frac{i\pi vt}{L} \sin\frac{i\pi x}{L} \qquad (9)$$

where m_L is the mass of the moving load.

This is essentially the same as the equation obtained by Inglis except that the reaction of the load against the beam is changed by the amount

$$\frac{g - \dfrac{d^2 y(vt,t)}{dx^2}}{g}$$

This is due to the effect of the beam "falling away" from beneath the moving load.

The solution of problems by these methods is laborious and is often a needless refinement over quicker numerical methods which yield approximate solutions to sufficient accuracy for engineering purposes. One of these methods consists of representing the actual structure by an analog as shown in Fig. 2.

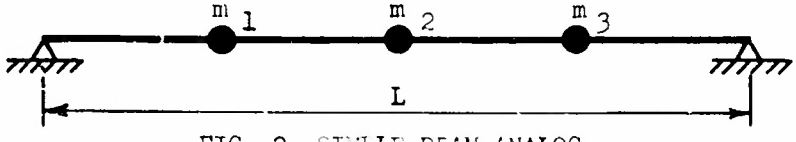

FIG. 2 SIMPLE BEAM ANALOG

The mass of the beam is assumed concentrated at n intermediate supports. The remaining portions of the span are considered weightless but otherwise retain their elastic properties. Considering the external force, reaction and inertia force at each concentrated mass, n equations are obtained for the n intermediate points in the form

$$
\begin{aligned}
m_1\ddot{y}_1 + a_{11}y_1 + a_{12}y_2 + \cdots\cdots a_{1n}y_n &= F_1(t) \\
m_2\ddot{y}_2 \quad a_{21}y_1 \quad a_{22}y_2 \qquad\qquad a_{2n}y_n &= F_2(t) \\
&\vdots \\
m_n\ddot{y}_n + a_{n1}y_1 + a_{n2}y_2 + \cdots\cdots a_{nn}y_n &= F_2(t)
\end{aligned}
\tag{10}
$$

The greater the number of intermediate points n, at which the mass of the beam is assumed concentrated, the closer will be the approximation to the actual span.

A convenient stepwise method of solution for equations (10) was developed by J. M. Bonetti[1]. The method consists, essentially, of assuming the impulse at each intermediate point to be linear over a short time interval Δt and equating this impulse to the change in momentum of the corresponding concentrated mass at each intermediate point. The displacement y_i of any intermediate mass m_i at time $t+\Delta t$ is found in terms of its displacement and velocity at time t.

The extension of this method to floating bridges is easily performed. Equations (10) are the same as equations (1) for a floating bridge with the exception of the K values of equations (1). Moreover, the analog described above, which is only an approximation of a simple span bridge, is actually a much closer approximation of a floating bridge since part of the mass of the bridge is actually concentrated at the intermediate supports due to the presence of the pontons. The major difference lies in the fact that the concentrated masses of the floating bridge are not constant but vary with displacement. The numerical method mentioned above has been extended to take into account these varying masses.

NUMERICAL SOLUTIONS

General

The numerical procedure used is based upon the principle of impulse - momentum. The integration of the resultant force on a body over a time interval is equal to the net change in the momentum of the body. In this case the integration is performed numerically - that is, the integration is carried out successively over short time intervals.

Consider the mass m suspended from a spring with spring constant K shown in Fig. 3.

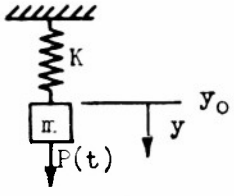

FIG. 3 SINGLE MASS OSCILLATOR

If a force P, which varies with time, is applied in the positive (downward) y direction the equation of motion for the mass is

$$P(t) - Ky = m\frac{dV}{dt} \tag{11}$$

The unbalanced force at any instant is the difference between the applied force P and the tension in the spring Ky, or

$$\Sigma F = P(t) - Ky \tag{12}$$

Introducing this expression in (11) and rearranging terms we have

$$\Sigma F\, dt = m dV \tag{13}$$

The integral of the unbalanced force from time t_1 to time t_2 is equal to the total change in momentum over that time interval.

$$\int_{t_1}^{t_2} UF \; dt = m\,(V_2 - V_1) = m\Delta V \tag{14}$$

If the time interval, $t_2 - t_1$, is very small it can be assumed that the unbalanced force varies linearly with time. With this assumption, letting $\Delta t = t_2 - t_1$, the impulse is

$$\int_{t_1}^{t_2} UF \; dt = \frac{UF_2 + UF_1}{2}\Delta t \tag{15}$$

The integral of the velocity of the mass from t_1 to t_2 is equal to the change in displacement, $y_2 - y_1$, during the time interval.

$$\int_{t_1}^{t_2} V \; d \; t = y_2 - y_1 \tag{16}$$

Assuming that the velocity varies linearly with time over the interval Δt equation (16) becomes

$$\int_{t_1}^{t_2} V \; d \; t = \frac{V_2 + V_1}{2}\Delta t = y_2 - y_1$$

and this allows the change in velocity ΔV to be expressed in the form

$$\Delta V = V_2 - V_1 = \frac{2}{\Delta t}\,(y_2 - y_1 - V_1\Delta t) \tag{17}$$

Substituting equations (15) and (17) into equation (14) the impulse and change in momentum over a short time interval Δt are related by

$$\frac{UF_2 + UF_1}{2}\Delta t = \frac{2m}{\Delta t}\,(y_2 - y_1 - V_1\Delta t) \tag{18}$$

Using expression (12) and rearranging terms the equation for the

displacement at time t_2 is

$$\left(\frac{4m}{\Delta t^2}+K\right)y_2 = \left(\frac{4m}{\Delta t^2} - K\right)y_1 + \frac{4m}{\Delta t^2} V_1\Delta t + P_1 + P_2 \qquad (19)$$

Thus the displacement at the end of any time interval is expressed in terms of the displacement and velocity at the beginning of the time interval and the applied load.

Single Ponton Bridge

Fig. 4 represents a single ponton bridge.

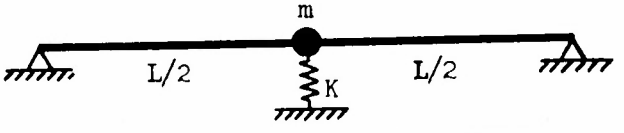

FIG.4 SINGLE PONTON BRIDGE

The spring constant K due to the buoyant force of the displaced water is obtained from Fig. 5 which shows the displaced weight of water as a function of displacement for a full M-4 Ponton. Fig. 5 is appended at the end of this thesis. The curve is not linear but a value for K of 1500 lbs/in. is a good approximation. The force K' to produce unit displacement of the ponton is resisted by the buoyant force and the flexural rigidity of the span. For a 30-foot span with EI = 320×10^8 lb-in.^{2} the value for K' is 34420 lbs/in. The mass of the ponton plus one-half the mass of the span is 20.2 lb-sec^2/in. Choosing the time interval Δt as one-twentieth of the fundamental period of the bridge, that is

$$\Delta t = T_0/20 = \frac{\pi}{10}\sqrt{\frac{m}{K'}}$$

The coefficient of $4m/\Delta t^2$ becomes $400K'/\Delta t^2$

Substituting these numerical values into (19) the displacement at time t_2, neglecting virtual mass, is

$$(\frac{400}{\pi^2} + 1)y_2 = (\frac{400}{\pi^2} - 1)y_1 + \frac{400}{\pi^2} V_1 \Delta t + \frac{P_1+P_2}{K'} \qquad (20)$$

The reaction of the load P on the ponton, as the load moves across the span, is assumed to vary linearly. The beam force which transmits the effect of the load to the ponton is the same as that of a span completely articulated at the ponton. In other words continuity is neglected when computing the force at a ponton due to a moving load. It must be emphasized, however, that in computing the resistance to displacement by this force continuity is not neglected. Letting H be the time for a moving load to cross the span the reaction of the load P on the ponton, as a function of time, is represented by Fig. 6

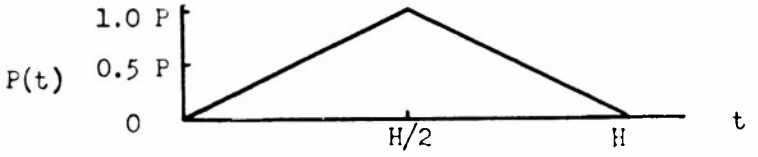

FIG. 6 REACTION ON PONTON DUE TO MOVING LOAD P

The results for a load P = 23,400 lbs (three times the weight of the ponton and one-half the deck structure concentrated at the center) for different speeds of crossing are shown in Fig. 7. The ordinate is the ratio of the dynamic displacement to the static displacement that would occur if the load P were applied statically at the center of the span. The abscissa is time in multiples of the fundamental period, T_0. Example calculations for $H = T_0$ are given in Appendix A.

If the virtual mass is considered equation (19) becomes

$$(\frac{4m'}{\Delta t^2} + K')y_2 = (\frac{4m'}{\Delta t^2} - K')y_1 + \frac{4m'}{\Delta t^2} K' V_1 \Delta t + P_1 + P_2 \qquad (21)$$

Keeping T_0 as the time scale and choosing Δt as one-twentieth the fundamental period T_0 equation (21) becomes

$$(40.568 \frac{m'}{m} + 1)y_2 = (40.568 \frac{m'}{m} - 1)y_1 + 40.568 \frac{m'}{m} V_1 \Delta t + \frac{P_1 + P_2}{K'} \quad (22)$$

Fig. 8 shows the virtual mass-displacement relationship for an M-4 Ponton. The data were obtained experimentally from a one-twelfth scale model. Since added mass is a function of shape, mass of displaced fluid and direction of motion, the added mass of the full scale ponton, at a given displacement, is obtained from the added mass of the scale model at the corresponding displacement. The shape and direction of motion is the same in each case. The added mass of the model, therefore, is multiplied by the ratio of the mass of displaced water of the full scale ponton at the given displacement to the mass of displaced water of the model at the corresponding displacement to obtain the added mass of the full scale ponton.

The observed added mass of the ponton is a linear function of displacement. A more detailed description of the method of obtaining these values if given in a later section.

From Fig. 8 the virtual mass for the ponton is

$$m' = 74 + 2.23y$$

when the initial dead weight displacement of the ponton is 5.2 in. Choosing m = 20.2 lbs-sec^2/in., the coefficient

$$40.568 \frac{m'}{m} = 148.613 + 4.478\ y$$

Equation (22) becomes

$$(149.613 + 4.478y_1)y_2 = (147.613 + 4.478y_1)y_1 + (148.613 + 4.478y_1)\, V_1\Delta t + \frac{P_1 + P_2}{K'} \qquad (23)$$

It is assumed that the virtual mass during any interval of time, Δt, is a function only of the displacement at the beginning of the time interval.

Results of solutions of equation (23) are given in Fig. 9 for $H = T_0$, for a moving load P of 39,000 and 234,000 lbs (five and thirty times the concentrated weight at the ponton, respectively). An example solution is shown in Appendix A. Fig. 10 summarizes solutions of equation (23) for a moving load P of three times the concentrated weight at the center of the span and for different times of crossing. The ordinate is the impact factor, and the abscissa is the ratio of the time of crossing to the natural period of the structure ignoring virtual mass.

If the mass of the moving load is considered the vertical displacement of the bridge at the point of application of the moving load must be known in terms of the displacement at the center of the bridge. Assume a linear relation between the deflection y_x at any position x along the bridge and the displacement y of the ponton.

$$y_x = \alpha y$$

where $\alpha = 2x/L$ when $0 < x < L/2$

and $\alpha = 2(L-x)/L$ when $L/2 < x < L$

If the load is assumed to follow the deflection curve of the bridge, the acceleration of the load, when $0 < x < L/2$, is

$$\ddot{y}_x = \alpha \ddot{y} + \frac{4v}{L} V \qquad (24)$$

and when $L/2 < x < L$

$$\ddot{y}_x = \alpha \ddot{y} - \frac{4v}{L} V \qquad (24a)$$

where v is the horizontal velocity of the moving load as it crosses the bridge and V is the vertical velocity of the ponton. The last term in equations (24) and (24a), when multiplied by the mass of the moving load, is the Coriolis force which is due to the precession of the velocity vector v as the span displaces. In general this force will not have much effect at low velocities of the moving load.

The force of the moving load P applied to the bridge at any position x is given by

$$F_x = P - m_L \ddot{y}_x$$

assuming, as above, that the force F at the ponton due to the force F_x varies linearly with x

$$F = F_x \alpha = (P - m_L \ddot{y}_x)\alpha$$

The unbalanced force on the ponton is the difference between this downward force of the moving load and the upward force due to the flexural rigidity of the span and the buoyant force of the water. These latter forces depend on displacement.

$$\Delta F = F - K'y = (P - m_L \ddot{y}_x)\alpha - K'y \qquad (25)$$

If the Coriolis force in equations (24) and (24a) is neglected, equation (25) becomes

$$\Delta F = P\alpha - m_L \alpha^2 \ddot{y} - K'y$$

Substituting this expression into equation (14)

$$\int_{t_1}^{t_2} (P\alpha - K'y)dt = (m + m_L \alpha^2)\Delta V$$

and integrating we have

$$P\alpha_1 - K'y_1 + P\alpha_2 - K'y_2 = \frac{4}{\Delta t^2}\ (m + m_L\alpha^2)(y_2 - y_1 - V_1\Delta t)$$

Simplifying, the expression for the displacement at time t_2 is

$$(\frac{4m}{\Delta t^2} + \frac{4m_L}{\Delta t^2}\alpha^2 + K')y_2 = (\frac{4m}{\Delta t^2} + \frac{4m_L}{\Delta t^2}\alpha^2 - K')y_1$$

$$+ (\frac{4m}{\Delta t^2} + \frac{4m_L}{\Delta t^2}\alpha^2)V_1\Delta t + P(\alpha_1 + \alpha_2)$$

Letting $m_L = \beta m$

$$\Delta t = \eta T_0 = 2\eta\pi\sqrt{\frac{m}{K'}}$$

$$(1 + \beta\alpha^2 + \eta^2\pi^2)y_2 = (1 + \beta\alpha^2 - \eta^2\pi^2)y_1 + (1 + \beta\alpha^2)V_1\Delta t$$

$$+ \frac{\eta^2\pi^2}{K'}P(\alpha_1 + \alpha_2) \qquad (26)$$

Solutions of equation (26) are shown in Fig. 11 for β = 1, 3, 5, and 10 and for different speeds of crossing. An example solution of equation (26) is given in Appendix A.

If the Coriolis force in equations (24) and (24a) is not neglected equation (25) becomes

$$UF = P\alpha - m_L\alpha^2\ddot{y} - 4m_L\alpha v\, V/L - K'y$$

for $0 < x < L/2$ and

$$UF = P\alpha - m_L\alpha^2\ddot{y} + 4m_L\alpha v\, V/L - K'y$$

for $L/2 < x < L$

Substituting these expressions into equation (14)

$$\int_{t_1}^{t_2} (P\alpha - K'y)dt = (m + m_L\alpha^2)\Delta V + \frac{4m_L v}{L}\alpha\int_{t_1}^{t_2} V\,dt$$

for $0 < x < L/2$ and

$$\int_{t_1}^{t_2} (P\alpha - K'y)dt = (m + m_L\alpha^2)\Delta V - \frac{4m_L v}{L}\alpha\int_{t_1}^{t_2} V dt$$

for $L/2 < x < L$

Integrating and rearranging terms we have

$$(1 + \beta\alpha^2 + \frac{2\beta\eta}{\mu}\alpha + \eta^2\pi^2)y_2 = (1 + \beta\alpha^2 + \frac{2\beta\eta}{\mu}\alpha - \eta^2\pi^2)y_1 + (1 + \beta\alpha^2)V_1\Delta t + \frac{\eta^2\pi^2}{K'} P(\alpha_1 + \alpha_2) \qquad (27)$$

for $0 < x < L/2$ and

$$(1 + \beta\alpha^2 + \frac{2\beta\eta}{\mu}\alpha + \eta^2\pi^2)y_2 = (1 + \beta\alpha^2 - \frac{2\beta\eta}{\mu}\alpha - \eta^2\pi^2)y_1 + (1 + \beta\alpha^2)V_1\Delta t + \frac{\eta^2\pi^2}{K'} P(\alpha_1 + \alpha_2) \qquad (27a)$$

where $H = \mu T_0$

Results of equations (27) and (27a) for $\beta = 5$ and for different times of crossing are shown by curve A in Fig. 11a. These results are compared to solutions of equations (26) which neglects the Coriolis force for $\beta = 5$ and different times of corssing (curve B of Fig. 11a). The maximum impact factor remains essentially the same in both cases.

Bridges of More Than One Floating Support

Linear Behavior.- Consider the two ponton bridge shown schematically in Fig. 12.

FIG. 12 TWO PONTON BRIDGE

At any time t the unbalanced force at any one of the concentrated masses is the difference between the applied force and the ponton reaction

$$UF_{1-t} = P_{1-t} - R_{1-t} \qquad (28)$$

$$UF_{2-t} = P_{2-t} - R_{2-t}$$

For a continuous structure of this type the reaction of either ponton depends on the displacement of both pontons. Assuming linear elastic behavior, the reaction at each ponton expressed in matrix notation is

$$\begin{vmatrix} (a_{11}+K) & a_{12} \\ a_{21} & (a_{22}+K) \end{vmatrix} \begin{vmatrix} y_{1-t} \\ y_{2-t} \end{vmatrix} = \begin{vmatrix} R_{1-t} \\ R_{2-t} \end{vmatrix} \qquad (29)$$

Substituting these expressions for the reactive forces into equation (28)

$$UF_{1-t} = P_{1-t} - (a_{11}+K)y_{1-t} - a_{12}y_{2-t}$$

$$UF_{2-t} = P_{2-t} - a_{21}y_{1-t} - (a_{22}+K)y_{2-t}$$

As before, from impulse - momentum considerations, the integral of the unbalanced force at ponton 1 over the short time interval Δt is

$$\int_{t_1}^{t_2} F\,dt = \frac{P_{1-1}-\left[(a_{11}+K)y_{1-1}+a_{12}y_{2-1}\right]+P_{1-2}-\left[a_{11}y_{1-2}+(a_{12}+K)y_{2-2}\right]}{2}\Delta t$$

The corresponding change in momentum of ponton 1 is

$$m_1 \Delta V = \frac{2m_1}{\Delta t}(y_{1-2} - y_{1-1} - V_{1-1}\Delta t)$$

Equating impulse to change in momentum the expression for the displacement of ponton 1 in terms of the displacements of pontons 1 and 2 at time t_2 is

$$(\frac{4m_1}{\Delta t^2} + a_{11} + K)y_{1-2} + a_{12}\,y_{2-2} = K_1$$

where the load coefficient for ponton 1 is

$$K_1 = P_{1-1} + P_{1-2} + (\frac{4m_1}{\Delta t^2} - a_{11} - K)y_{1-1} - a_{12}y_{2-1} + \frac{4m_1}{\Delta t^2}V_{1-1}\Delta t$$

Following a similar procedure for ponton 2 the simultaneous linear equations, written in matrix form, are

$$\begin{vmatrix} (\frac{4m_1}{\Delta t^2}+a_{11}+K) & a_{12} \\ a_{21} & (\frac{4m_1}{\Delta t^2}+a_{22}+K) \end{vmatrix} \begin{vmatrix} y_{1-2} \\ y_{2-2} \end{vmatrix} = \begin{vmatrix} K_{1-1} \\ K_{2-1} \end{vmatrix}$$

or

$$|a'|\,|y| = |K| \qquad (30)$$

The effect of virtual mass is neglected in this expression.

To express the displacements y in explicit form it is necessary to invert the matrix $|a'|$. Letting $|\Psi|$ be the inverse matrix equation of $|a'|$ equation (30) becomes

$$\begin{vmatrix} \Psi_{11} & \Psi_{12} \\ \Psi_{21} & \Psi_{22} \end{vmatrix} \begin{vmatrix} K_{1-1} \\ K_{2-1} \end{vmatrix} = \begin{vmatrix} y_{1-2} \\ y_{2-2} \end{vmatrix}$$

or

$$|\Psi|\,|K| = |y| \qquad (31)$$

A convenient tabular scheme can then be used to successively compute the displacements of the pontons at any time t_m in terms of the displacements and velocities at time t_{m-1}. Fig. 13 shows solutions of equations (31) for different times of crossing. The physical constants for the two ponton bridge are the same as for the single ponton bridge treated earlier with the exception that the span length is increased to 45 feet.

This method of analysis is readily extended to ponton bridges with more than two pontons. Fig. 14 shows results for a three ponton bridge when the time of crossing of the moving load is equal to T_0. Virtual mass is neglected.

Non-Linear Behavior.- The linear problems discussed above consist, essentially, of solving the linear matrix equation

$$|a'|\,|y| = |K|$$

which would allow a direct calculation of the displacement of each ponton from the matrix equation

$$|y| = |\Psi|\,|K|$$

If virtual mass is considered the solution is complicated by the fact that the matrix $|a'|$ is displacement dependent. After each step in the numerical computation the diagonal elements of the matrix $|a'|$ change by the amount

$$\frac{4\,\xi\,\Delta y}{\Delta t^2}$$

where ξ is the slope of the virtual mass-displacement

relationship at time t_m and Δy is the difference in displacement over the time interval $\Delta t = t_{m+1}-t_m$. In other words, $|a'|$ is changed to

$$|a'|^* = |a'| + |b| \tag{33}$$

where $|b|$ is a diagonal matrix.

For engineering purposes it is sufficient to consider the change in $|a'|$ only during the time interval t_m-t_{m-1} when calculations are being made for the time interval $t_{m+1}-t_m$. This procedure maintains linearity of the simultaneous linear equations and avoids the occurence of terms of an order higher than one.

The problem, therefore, is to find a new inverse matrix

$$|\Psi|^* = |a'|^{*-1} \tag{34}$$

It would be laborious to invert $|a'|^*$ to get $|\Psi|^*$ at each step in the computation. Instead it is expedient to express $|\Psi|^*$ in terms of a series and consider only the first few terms[7]. This is procedure can be used only if the corrections $|b|$ are small relative to $|a'|$ so that adequate accuracy is obtained from the first few terms in the series.

From equations (33) and (34)

$$|\Psi|^* = (|a'| + |b|)^{-1} \tag{35}$$

and since

$$(|a'| + |b|) = |a'| (I+|a'|^{-1}|b|) \tag{36}$$

the right hand side of equation (35) becomes

$$(|a'| + |b|)^{-1} = \left\{|a'| \ (I + |a'|^{-1}|b|)\right\}^{-1}$$

$$= \left\{(I + |a'|^{-1}|b|)^{-1}\right\}|a|^{-1} \quad ** \qquad (37)$$

The first term in (37) can be expressed as the continuous series

$$\sum_{n=1}^{\infty} \left[I + (-1)^n \ (|a'|^{-1}|b|)^n\right.$$

Therefore,

$$|\Psi|^* = (|a'| + |b|)^{-1} = \sum_{n=1}^{\infty} \left[I + (-1)^n (|a'|^{-1}|b|)^n\right] |a'|^{-1}$$

$$= |\Psi| - |\Psi||b||\Psi| + |\Psi||b||\Psi||b||\Psi| + \cdots$$

or

$$|\Psi|^* = |\gamma||\Psi| \qquad (38)$$

where

$$|\gamma| = I - |\Psi||b| + (|\Psi||b|)^2 + \cdots \qquad (39)$$

Consider an example of this procedure.

$$|a'| = \begin{vmatrix} 4 & 2 & 1 \\ 2 & 3 & 2 \\ 1 & 2 & 4 \end{vmatrix}; \qquad |\Psi| = \begin{vmatrix} 0.3810 & -0.2860 & 0.0476 \\ -0.2860 & 0.7150 & -0.2860 \\ 0.0476 & -0.2860 & 0.3810 \end{vmatrix}$$

$$|a'|^* = \begin{vmatrix} 4.1 & 2 & 1 \\ 2 & 3.1 & 2 \\ 1 & 2 & 4.2 \end{vmatrix}; \quad |b| = \begin{vmatrix} 0.1 & 0 & 0 \\ 0 & 0.1 & 0 \\ 0 & 0 & 0.2 \end{vmatrix}$$

$$|\Psi||b| = \begin{vmatrix} 0.0381 & -0.0286 & 0.0095 \\ -0.0286 & 0.0715 & -0.0572 \\ 0.0048 & -0.0286, & 0.0762 \end{vmatrix}$$

** This follows from the fundamental rule in matrix operation that $(|A||B|)^{-1} = |B|^{-1}\,|A|^{-1}$

$$(|\psi||b|)^2 = \begin{vmatrix} 0.0023 & -0.0034 & 0.0027 \\ -0.0034 & 0.0076 & -0.0087 \\ 0.0014 & -0.0044 & 0.0075 \end{vmatrix}$$

$$= I - |\psi||b| + (|\psi||b|)^2 = \begin{vmatrix} 0.964 & 0.0252 & -0.0068 \\ 0.0252 & 0.9361 & 0.0485 \\ -0.0034 & 0.0242 & 0.9313 \end{vmatrix}$$

$$|\psi|^* = |\gamma||\psi| = \begin{vmatrix} 0.3598 & -0.2558 & 0.0361 \\ -0.2558 & 0.6482 & -0.2480 \\ 0.0361 & -0.2480 & 0.3477 \end{vmatrix}$$

The correct value of $|\psi|^*$ determined by inverting $|a'|^*$ directly is

$$|\psi|^* = \begin{vmatrix} 0.3596 & -0.2552 & 0.0359 \\ -0.2552 & 0.6467 & -0.2472 \\ 0.0359 & -0.2472 & 0.3473 \end{vmatrix}$$

The average error of the elements of the matrix $|\psi|^*$ as computed by the series compared to their exact values is 1.72% with a maximum (at ψ_{22}^*) of 2.20%.

Considering only the first two terms in the series

$$|\gamma| = I - |\psi||b| = \begin{vmatrix} 0.9619 & 0.0286 & -0.0095 \\ 0.0286 & 0.9285 & 0.0572 \\ -0.0048 & 0.0286 & 0.9238 \end{vmatrix}$$

and

$$|\psi|^* = |\gamma||\psi| = \begin{vmatrix} 0.3579 & -0.2519 & 0.0340 \\ -0.2519 & 0.6393 & -0.2424 \\ 0.0340 & -0.2424 & 0.3436 \end{vmatrix}$$

The average error considering only the first two terms of the series is 12.05% with a maximum of 16.2%.

Fig. 15 shows the results of applying this method to a three ponton bridge for different times of crossing. The virtual mass, for each change in the $|a'|$ matrix, was determined for each ponton from Fig. 8. In general it is not always necessary to compute a new inverse matrix $|\psi|^*$ after each step in the computations. If the slope of the virtual mass-displacement diagram is small it may only be necessary to correct for the change in virtual mass after every second or third step. This is mostly a matter of judgment since the change in virtual mass (which is a function of displacement) during one step in the computations also depends on the magnitude of the moving load. The corrected inverse matrix $|\psi|^*$, for the solutions shown in Fig. 15, was computed after every second step in the computations.

Damping

The numerical methods described above, for either the linear or non-linear problems, are easily extended to include the effect of viscous damping. The damping force is added to the buoyant resistance of the ponton and; from equation (12),

$$UF = P(t) - K\dot{y} - CV \qquad (40)$$

where C is the coefficient of viscous damping. The unbalanced force over a short time interval becomes

$$I = \frac{P(t) - K\dot{y}_1 - CV_1 + P_2(t) - K\dot{y}_2 - CV_2}{2} \Delta t$$

Equating this impulse to the change in momentum and rearranging terms

$$(\frac{4M}{\Delta t^2}+K')y_2 = P_1 + P_2 - C(V_1+V_2) + (\frac{4M}{\Delta t^2}-K')y_1 + \frac{4M}{\Delta t^2}V_1\Delta t \quad (41)$$

and from equation (16)

$$V_1 + V_2 = \frac{2}{\Delta t}(y_2 - y_1)$$

With this value for V_1+V_2 equation (41) becomes

$$(\frac{4M}{\Delta t^2}+K'+\frac{2C}{\Delta t})y_2 = (\frac{4M}{\Delta t^2}-K'+\frac{2C}{\Delta t})y_1 + \frac{4M}{\Delta t^2}V_1\Delta t + P_1+P_2 \quad (42)$$

The analysis is easily extended to bridges of more than one ponton. Fig. 16, for example, shows results for a three ponton bridge for C=100 and 1000 lb-sec/in. The logarithmic decrement corresponding to these values of C can be computed from the equation

$$\tau = \frac{2\pi C}{C_{cr}}$$

where τ is the logarithmic decrement

C_{cr} is the critical damping

The critical damping can be computed from

$$C_{cr} = \frac{4m\pi}{T_o}$$

For a three ponton bridge, neglecting virtual mass, T_o is 0.370 seconds and C_{cr} = 2060 lb-sec/in. The logarithmic decrements corresponding to C = 100 and 1000 lb-sec/in. are 0.304 and 3.04 respectively.

Accuracy of Numerical Procedure

The stepwise solution of the initial value problems discussed above consists of the evaluation of an integral at pivotal points

along its interval of definition. Consider the function f(t) shown in Fig. 17a. The integral of f(t) from t_m to t_{m+1} is given by

$$\int_{t_m}^{t_{m+1}} f(t)dt = \frac{f_{m+1}(t) + f_m(t)}{2} \Delta t + e \qquad (43)$$

where e is the small shaded area in Fig. 17a. For a second degree curve this error is

$$e = 2/3\, d\Delta t \qquad (44)$$

where d is the maximum vertical ordinate between the actual curve of f(t) and a straight line relationship from $f_m(t)$ to $f_{m+1}(t)$. In the derivation of the numerical procedure used above it was assumed that f(t) varies linearly over the small time interval Δt. The correction e, therefore, indicates the discrepancy between the correct and the approximate values of the solution for one step of the stepwise integration process. These "truncation errors" accumulate and the results after a number of steps become more inaccurate than at the origin.

An estimate for e, however, can be included in each step of the numerical integration. If this estimate is conservative enough to include the largest expected value of e the results thus obtained would constitute an "upper bound" to the solution. The correct solution then lies between the values obtained by including e and those obtained by neglecting e.

A safe estimate for the ordinate d between the actual and assumed curve of f(t) over the time interval Δt is obtained from Fig. 17b. Let S_m be the slope of f(t) at time t_m. This slope can

be approximated by

$$S_m = \frac{f_{m+1}(t) - f_{m-1}(t)}{2\Delta t} \tag{45}$$

The distance b of Fig. 17b at time $t_m + \Delta t/2$ is then

$$b = S_m \Delta t/2 = \frac{f_{m+1}(t) - f_{m-1}(t)}{4} \tag{46}$$

The distance c is

$$c = \frac{f_{m+1}(t) - f_m(t)}{2} \tag{47}$$

The difference between b and c is a value, d', that is always larger than d for a function f(t) of any degree. The error e can then be approximated by

$$e' = 2/3\ d'\Delta t \tag{48}$$

where $d' = b - c$

From equations (46) and (47)

$$d' = \frac{1}{4}\left[2f_m(t) - f_{m+1}(t) - f_{m-1}(t)\right]$$

and

$$e' = \frac{\Delta t}{6}\left[2f_m(t) - f_{m+1}(t) - f_{m-1}(t)\right] \tag{49}$$

As an example consider the single mass oscillator shown on page 9. From equations (13) and (14)

$$\int_{t_1}^{t_2} (P(t) - Ky)\ dt = m\Delta V$$

or

$$\int_{t_1}^{t_2} P(t)dt - K\int_{t_1}^{t_2} ydt = m(V_2 - V_1) \tag{50}$$

From equation (43)

$$\int_{t_1}^{t_2} V dt = y_2 - y_1 = \frac{V_2+V_1}{2}\Delta t + e_v \qquad (51)$$

and from equation (49)

$$e_v = \frac{\Delta t}{6}\left[2V_1 - V_2 - V_0\right] \qquad (52)$$

Substituting equation (52) into equation (51) the expression for the change in velocity becomes

$$V_2 - V_1 = \frac{3}{\Delta t}(y_2 - y_1) - {}^7/_2 V_1 + {}^1/_2 V_0 \qquad (53)$$

The integral of the external force over the time interval t_2-t_1 becomes, from equation (43),

$$\int_{t_1}^{t_2} P(t)dt = \frac{P_1(t) + P_2(t)}{2}\Delta t + \frac{\Delta t}{6}\left[2P_1(t) - P_2(t) - P_0(t)\right]$$

$$= \frac{\Delta t}{6}\left[2P_2(t) + 5P_1(t) - P_0(t)\right] \qquad (54)$$

and in a similar manner

$$K\int_{t_1}^{t_2} y dt = -\frac{Ky_1 + Ky_2}{2}\Delta t + \frac{K\Delta t}{6}(2y_1 - y_2 - y_0)$$

$$= \frac{K\Delta t}{6}(2y_2 + 5y_1 - y_0) \qquad (55)$$

Substituting equations (53), (54) and (55) into equation (50) and rearranging terms, the equation for the displacement of a single mass oscillator at time t_2, in terms of the displacements and velocities at times t_1 and t_0 and the applied load, becomes

$$\left(\frac{18m}{\Delta t^2}+2K\right)y_2 = \left(\frac{18m}{\Delta t^2}-5K\right)y_1 + \frac{21m}{\Delta t^2}V_1\Delta t - \frac{3m}{\Delta t^2}V_0\Delta t$$

$$+ Ky_0 + 2P_2 + 5P_1 - P_0 \qquad (56)$$

Numerical Example.- Again considering the single mass oscillator shown on page 11 and assuming that m = 1 lbs-sec^2/in. and K = 64 lbs/in., the fundamental period is

$$T_0 = 2\pi\sqrt{\frac{m}{K}} = \frac{\pi}{4}$$

The external force P is chosen to vary parabolically with time from t=0 to t=T_0, or

$$P(t) = \frac{4P'}{T_0}t - \frac{4P'}{T_0^2}t^2$$

where P' = 1000 lbs.

With these numerical values, chosing $\Delta t = T_0/20$, equation (56) becomes

$$11823y_2 = 11375y_1 + 13645V_1\Delta t - 1949V_0\Delta t$$

$$+ 64y_0 + 2P_2 + 5P_1 - P_0 \qquad (57)$$

The displacement-time relationship for the single mass oscillator calculated from equation (57) is shown in Fig. 18. This solution includes the corrections e'. When the corrections e' are neglected equation (19) becomes

$$2658y_2 = 2530y_1 + 2594V_1\Delta t + P_1 + P_2 \qquad (58)$$

Solutions from equation (58) are shown in Fig. 18. The difference between the maximum ordinates of the two solutions for a time interval $\Delta t = T_0/20$ is 1.13%. The exact solution, shown in Fig. 18, lies halfway between the two curves.

Fig. 18 also shows results of the numerical procedure for $\Delta t = T_{0/10}$. The difference between the maximum ordinates for solutions including the corrections e' and for solutions neglecting this correction is 4.45%.

ELECTRONIC ANALOG SOLUTIONS

The solution of the types of problems discussed above by numerical or exact means is laborious and time-consuming when a large number of problems is to be considered. Mathematical equations relating measures of change (derivatives) of this type, however, are particularly amenable to solution by means of electronic analog computors[8,9]. In these computors, the variables in question are represented by d-c voltages which may vary with time. These voltages are made to obey mathematical relations in a manner analogous to those of the original problem. Time is used as the independent variable. The voltages, or machine variables, may be conveniently varied and measured in the laboratory. The magnitudes and time scale of these analogous variables can be adjusted to facilitate their measurement. The solution of the differential equations of motion of the pontons proceeds as follows:

a) When the machine is set up to solve the problem the voltages (machine variables) are set to the initial conditions of the given problem.

b) The computor is then started and forces the voltages to vary in the manner prescribed by the differential

equations. The output voltages are plotted as a function of time and constitute a solution of the problem.

A more detailed description of the basic components and programming is given in Appendix C.

Solutions were obtained by the analog computor for the following cases:

A. Single ponton bridge considering the mass of the moving load P. The deflected load line is approximated by a second degree curve through the supports and the single ponton.
   (1) Neglecting virtual mass and damping. m_L = 3m and 5m
   (2) Considering virtual mass. m_L = 3m

B. Two ponton bridge neglecting the mass of the moving load P.
   (1) Neglecting virtual mass and damping.
   (2) Considering virtual mass.
   (3) Considering virtual mass and damping. Solutions were obtained for damping coefficients of 100 and 1000 lb-sec/in.

C. Three ponton bridge neglecting the mass of the moving load P.
   (1) Neglecting virtual mass and damping and choosing the value of EI/L^3 = 85.8 lbs/in.
   (2) The same as (1) except EI/L^3 = 42.9 lbs/in.
   (3) Considering virtual mass and damping. The damping coefficients were assumed to be 100 and 1000 lb-sec/in.

D. Five ponton bridge neglecting the mass of the moving load P.
   (1) Neglecting virtual mass and damping.

In all the cases described above solutions were obtained for

different times of crossing.

Results of Analog Solutions

Case A-1.- Since the shape of the deflected load line is assumed the displacement of the bridge at any point x is known in terms of the displacement of the ponton

$$y_x = \theta(x) y_p$$

and the vertical acceleration of the bridge at point x, neglecting the Coriolis acceleration, becomes

$$\ddot{y}_x = \theta(x) \ddot{y}_p \tag{59}$$

Since the speed of the moving load is constant the position of the load can be expressed in terms of time t and equation (59) becomes

$$\ddot{y}_x = \theta(t) \ddot{y}_p \tag{60}$$

For a second degree deflection curve

$$\theta(t) = \frac{4t}{H} - \frac{4t^2}{H^2} \tag{61}$$

The force of the moving load P applied to the bridge at the point x is

$$F_x = P - m_L \ddot{y}_x \tag{62}$$

Substituting equation (60) into equation (62)

$$F_x = P - m_L \theta(t) \ddot{y}_p \tag{63}$$

The reaction $F(t,\ddot{y}_p)$ on the ponton due to the force F_x is assumed to vary linearly whence,

$$F = F_x \phi(t) = \left[P - m_L \theta(t) \ddot{y}_p\right] \phi(t) \tag{64}$$

The function $\phi(t)$ represents the influence of the force F_x at any time t on the ponton. If H is the time for the load to cross the bridge this function can be represented as shown in Fig. 19.

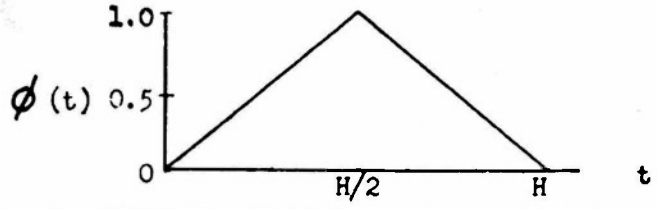

FIG. 19 INFLUENCE OF MOVING LOAD ON PONTON

Using equations (61) and (64) the equation of motion for the ponton of a single ponton bridge (n=1), considering the mass of the load and neglecting virtual mass and damping, becomes from equation (4)

$$M\ddot{y} + (a_{11}+K)y = \left[P-m_L\left(\frac{4t}{H} - \frac{4t^2}{H^2}\right)\ddot{y}\right]\phi(t) \qquad (65)$$

Introducing the following numerical values

$m_L = 3m = 60.6$ lbs-sec^2/in.

$a_{11}+K = 34422$ lbs/in.

$P = 23{,}400$ lbs

$EI = 320 \times 10^8$ lbs-in.^{2}

$L = 30$ ft

$T_o = 0.152$ sec

equation (65) becomes

$$\ddot{y} + 1704y = \left[1158.4 + \left(\frac{12t^2}{H^2} - \frac{12t}{H}\right)\ddot{y}\right]\phi(t) \qquad (66)$$

Solutions for equation (66), taken from the computor record, are shown in Fig. 20 for H=0.5, 1.0, 1.5 and 2.0 T_o.

Assuming $m_L = 5m$ equation (65) becomes

$$\ddot{y} + 1704y = \left[1931 + \left(\frac{20t^2}{H^2} - \frac{20t}{H}\right)\ddot{y}\right]\phi(t) \qquad (67)$$

Computor solutions for equation (67) are shown in Fig. 21 for H = 0.5, 1.0, 1.5, 2.0 and 2.5 T_0.

Case A-2.- From Fig. 8 the virtual mass, at the dead weight displacement of the ponton (5.2)inches), is

$$m' = M + \xi(y) = 74 + 2.23y \qquad (68)$$

With this value and using expression (64) equation (6), neglecting damping, becomes

$$(74+2.23y)\ddot{y} + 34422y = \left[23400-60.6\left(\frac{4t}{H} - \frac{4t^2}{H^2}\right)\ddot{y}\right]\phi(t) \qquad (69)$$

Solutions for equation (69) are given in Fig. 22 for H = 0.5, 1.0, 1.5, 2.0 and 2.5 T_0.

Case B-1.- From equation (2) the equations of motion of a two ponton bridge (n=2), with the following numerical constants:

P = 23,400 lbs L = 45 ft

EI = 320 x 10^8 lb-in.^{2}

K = 1500 lb/in.

m = 20.2 lbs-sec^2/in.

becomes

$$\begin{aligned} 20.2\ddot{y}_1 + 54175y_1 - 46090y_2 &= F_1(t) = 23400\,\phi_1(t) \\ 20.2\ddot{y}_2 - 46090y_1 + 54175y_2 &= F_2(t) = 23400\,\phi_2(t) \end{aligned} \qquad (70)$$

The functions $\phi_1(t)$ and $\phi_2(t)$ represent the influence of the moving load P, at any time t, on pontons 1 and 2, respectively These functions can be represented as shown below in Fig. 23.

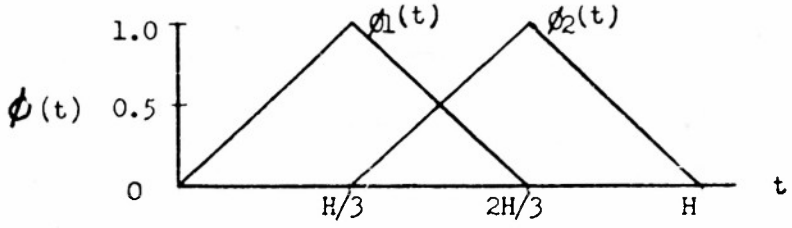

FIG. 23 INFLUENCE OF MOVING LOAD ON PONTONS 1 AND 2

Solutions for equations (70) are given in Fig. 24 for different times of crossing.

Case B-2.- With the value for the virtual mass given in expression (68) numerical values of Case B-1 equations (3) become

$$\begin{aligned}(74 + 2.23y_1)\ddot{y}_1 + 54175y_1 - 46090y_2 &= F_1(t) = 23400\ \phi_1(t)\\ (74 + 2.23y_2)\ddot{y}_2 - 46090y_1 + 54175y_2 &= F_2(t) = 23400\ \phi_2(t)\end{aligned} \tag{71}$$

Fig. 25 shows the computor solutions for equations (71) for different times of crossing.

Case B-3.- Considering virtual mass and damping and neglecting the mass of the moving load equations (6), with the numerical values of Case B-1, become

$$\begin{aligned}(74 + 2.23y_1)\ddot{y}_1 + C\dot{y}_1 + 54175y_1 - 46090y_2 &= F_1(t) = 23400\ \phi_1(t)\\ (74 + 2.23y_2)\ddot{y}_2 + C\dot{y}_2 - 46090y_1 + 54175y_2 &= F_2(t) = 23400\ \phi_2(t)\end{aligned} \tag{72}$$

Figs. 26 and 27 show solutions for equations (72) for C =100 and 1000 lb-sec/in., respectively.

Case C-1.- For a three ponton bridge (n=3), neglecting virtual mass and damping and using the same numerical values of Case B-1 with the exception that L=60 ft, equations (2) are

$$20.2\ddot{y}_1 + 55000y_1 - 49300y_2 + 20600y_3 = 23400\ \phi_1(t)$$
$$20.2\ddot{y}_2 - 49300y_1 + 75500y_2 - 49300y_3 = 23400\ \phi_2(t) \quad (73)$$
$$20.2\ddot{y}_3 + 20600y_1 - 49300y_2 + 55000y_3 = 23400\ \phi_3(t)$$

The functions $\phi_1(t)$, $\phi_2(t)$ and $\phi_3(t)$, which represent the effect of a unit load at any time t on pontons 1, 2 and 3, respectively, can be represented as shown in Fig. 28.

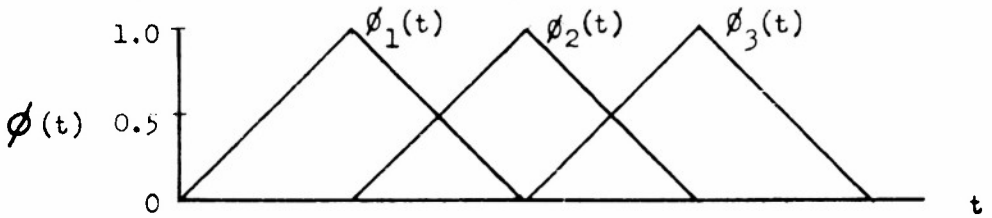

FIG. 28 INFLUENCE OF MOVING LOAD ON PONTONS 1, 2 AND 3.

Fig. 29 gives solutions for equations (73) for different times of crossing.

Case C-2.- This case is the same as Case C-1 with the exception that the value of EI is reduced from 320 x 10^8 lbs-in.^{2} to 160 x 10^8 lbs-in.^{2}. With this change equations (2) become

$$20.2\ddot{y}_1 + 28250y_1 - 24650y_2 + 10300y_3 = 23400\ \phi_1(t)$$
$$20.2\ddot{y}_2 - 24650y_1 + 38500y_2 - 24650y_3 = 23400\ \phi_2(t) \quad (74)$$
$$20.2\ddot{y}_3 + 10300y_1 - 24650y_2 + 28250y_3 = 23400\ \phi_3(t)$$

Fig. 30 gives the computor solutions for equations (74) for a range of crossing times.

Case C-3.- Considering virtual mass and damping and the numerical values from Case B-1 equations (6), neglecting the mass of the moving load, become

$$(74+2.23y_1)\ddot{y}_1 + C\dot{y}_1 + 55000y_1 - 49300y_2 + 20600y_3 = 23400\,\phi_1(t)$$
$$(74+2.23y_2)\ddot{y}_2 + C\dot{y}_2 - 49300y_1 + 75500y_2 - 49300y_3 = 23400\,\phi_2(t) \quad (75)$$
$$(74+2.23y_3)\ddot{y}_3 + C\dot{y}_3 + 20600y_1 - 49300y_2 + 55000y_3 = 23400\,\phi_3(t)$$

Figs. 31 and 32 present solutions for equations (75) for C=100 and 1000 lb-sec/in., respectively, and for times of crossing of 3.0, 4.0 and 6.0 T_o.

Case D-1.- Using the numerical values from Case B-1 equations (2) for a five ponton bridge (n=5), become

$$20.2\ddot{y}_1 + 55750y_1 - 52240y_2 + 22845y_3 - 6114\,y_4 + 1540y_5 = 23400\,\phi_1(t)$$
$$20.2\ddot{y}_2 - 52240y_1 + 78600y_2 - 58340y_3 + 24370y_4 - 6114y_5 = 23400\,\phi_2(t)$$
$$20.2\ddot{y}_3 + 22845y_1 - 58340y_2 + 80130y_3 - 58340y_4 + 22845y_5 = 23400\,\phi_3(t) \quad (76)$$
$$20.2\ddot{y}_4 - 6114\,y_1 + 24370y_2 - 58340y_3 + 78600y_4 - 52240y_5 = 23400\,\phi_4(t)$$
$$20.2\ddot{y}_5 + 1540\,y_1 - 6114\,y_2 + 22845y_3 - 52240y_4 + 55750y_5 = 23400\,\phi_5(t)$$

Fig. 33 shows computor solutions of equations (76) for different times of crossing.

Accuracy of Analog Solutions

The electronic analog computors described above are essentially electrical devices. When these devices are "set up" to solve a set of differential equations they are wired in such a way that the equations describing the variation of voltage with time are analogous to the set of differential equations whose solution is desired. The constants of these equations are represented in the computor by resistances which are adjusted to their correct value by rheostats. The accuracy of the computer (or the degree to which a record of voltage variation in the computor can be said to represent a solution

of the differential equations) is determined by the accuracy of these rheostats and the reliability of its components. These components perform the necessary mathematical operations of addition, multiplication, division, and integration.

As a check on this accuracy the exact solution of equation (70) describing the behavior of a two ponton bridge was compared to the analog solution. These results, for ponton 1, are shown in Fig. 34. There is no difference in the maximum value of displacement in each case. After the peak, however, the analog solution lags the exact solution by a small amount.

The numerical solution, from equation (31) is also shown.

IMPULSE-DISPLACEMENT TESTS

Experimental impulse-displacement tests were conducted on pontons of different shapes in an open 58-in. flume. The pontons were subjected to an arbitrary impulse which was measured and recorded. The corresponding displacements were also measured. These displacements were then compared to calculated displacements based on the known impulse to afford a measure of the reliability of the virtual mass and damping factors. Several assumptions are made in computing the displacements from the given impulse by the numerical procedure previously discussed. It is assumed that the water level does not change during the displacement - that is to say, that the transient waves formed at the sides of the pontons due to the rapid displacement of water are neglected. It is also assumed that the buoyant force-

displacement relationship is linear and equal to the slope of the buoyant force-displacement curve at the point of static dead weight displacement. The virtual mass at each step in the computations is determined from the experimental virtual mass-displacement curve for each ponton.

The experimental technique for determining the added masses for the models is based on a method developed by T. E. Stelson[10]. This method consists of connecting the object to be tested to a metal rod which is rigidly connected to the center of a simple beam. The beam is then vibrated with the object in the air and again when it is submerged to the desired depth of water.

The frequency of a simple beam with a weight concentrated at the center is given by

$$f = \frac{1}{2\pi}\sqrt{\frac{K}{m}}$$

where f = frequency, (cycles/sec)

K = spring constant, (lbs/in.)

m = mass of suspended object and equivalent concentrated weight of beam (one-half total mass of beam), (lbs-sec^2/in.)

The ratio of the mass of a ponton in water to its mass in air can then be calculated from the relationship

$$\frac{m_w}{m_a} = \frac{fa^2}{fw^2}$$

where m_w = apparent mass of ponton submerged in water

m_a = mass of ponton in air

fa = frequency of beam and ponton when vibrated in air

fw = frequency of beam and ponton when vibrated with ponton at desired submergence

The test beam is designed to have a relatively high frequency (20-30 cycles/sec) within the expected range of virtual masses. By keeping the amplitudes small the ratio of inertia forces to viscous forces is high[11].

The apparatus used to determine the added masses is shown in Fig. 35 and schematically in Fig. 36. The test beam is suspended longitudinally between two I-beams which, in turn, are cast in heavy concrete blocks. This supporting framework has a high frequency with respect to the natural frequency of the test beam to prevent the occurrence of harmonics or resonance which would distort the test results. A magnetized rod is fixed vertically near the center of the test beam. A detector coil is suspended around this rod and connected to a Brush Oscillograph. As the test beam vibrates an alternating emf is set up in the coil and is recorded on the oscillograph. The frequency of vibration is determined from the oscillograph chart.

The three types of model pontons tested are shown in Fig. 37 and schematically in Fig. 38. The corresponding bouyant force-displacement relationships are shown in Fig. 39. In order to facilitate the testing procedure the test beam is first calibrated - that is, known weights are added to the beam and the natural frequency, corresponding to each weight, is noted. The curve thus obtained is shown in Fig. 40. The ponton to be tested is then fixed to the beam and the corresponding natural frequency noted on the curve. When the ponton is then vibrated in water the effective added weight, due to the acceleration of the ponton through the water, is given by the difference between the

the points on the abscissa corresponding to the two different frequencies. The results of these tests are shown in Fig. 41 which gives the virtual mass for the model pontons as a function of displacement.

A similar procedure was followed for determining the virtual mass-displacement relationship of an M-4 ponton. A one-twelfth scale model, shown in Fig. 42, was used for this purpose. The tests were carried out, in this case, in an 18-in. flume.* The added mass, at any particular displacement, is expressed in terms of the mass of displaced water. The added mass of the full scale ponton, at the corresponding full scale displacement, is determined by multiplying the added mass of the model at that displacement by the ratio of the weight of displaced water of the full scale ponton to the weight of displaced water of the model ponton. By this method the virtual mass-displacement relationship shown in Fig. 8 was determined.

The apparatus used for the impulse-displacement tests is shown in Fig. 43 and schematically in Fig. 44. The vertical rod attached to the center of the ponton is restricted to vertical motion by the slide bearing attached to the side of one of the I-beams used in the virtual mass apparatus. The force on the ponton is determined from SR-4 electric strain gages attached to an aluminum "horseshoe" at the center of the ponton. The force is applied to the vertical

---

*The proximity of the side walls has an effect on the virtual mass coefficient. The values used for a study of a full scale ponton, however, are only meant to be representative and no effort was made to correct for this.

rod which is attached to the top of the "horseshoe" and bending stresses are induced. The "horseshoe" is calibrated so that the vertical force in the bar can be determined from the strain in the SR-4 gages due to these bending stresses.

Displacements are determined in much the same manner by a cantilevered strip of thin spring steel to which SR-4 strain gages are fastened. The spring is calibrated so that the vertical displacement of the free end can be interpreted in terms of the strains in the SR-4 gages. The end of the steel strip is deflected by a metal "finger" attached to the ponton. The spring is thin enough so that its resistance to displacement of the ponton is negligible.

Fig. 45 shows results of an impulse-displacement test on the rectangular ponton. The displacement curves calculated from the recorded impulse with virtual mass considered and with virtual mass and damping considered agree well with the experimental displacement curve.* The calculated displacement curve with the virtual mass neglected, however, shows practically no agreement with the experimental results. An inspection of Fig. 45 indicates that in this case the virtual mass is of greater importance for design considerations than damping. Neglecting damping gives results on the safe side whereas neglecting virtual mass yields results considerably on the unsafe side. Similar good agreement between calculated and experimental displacement curves for the rectangular ponton is shown in Fig. 46.

---

*The determination of the damping coefficient is shown in Appendix B.

Fig. 47, 48, and 49 present results of impulse-displacement tests on the ponton with triangular cross-section. Figs. 47 and 48 indicate the importance of damping on tests of short duration with relatively high velocity. The relatively large error (17%) between the calculated displacement curve with damping considered and the experimental displacement curve in Fig. 48 can probably be attributed to inaccuracies in determining the damping coefficients.

Results of tests on the ponton with semi-circular cross-section are shown in Figs. 50, 51 and 52. The agreement between calculated and experimental displacement curves, for the test of short duration shown in Fig. 52, is not as good as in the case of the other pontons tested.

SUMMARY

The relationship between maximum impact factor and number of pontons is shown in Fig. 53 for bridges of one, two, three and five pontons. The open circles show results neglecting virtual mass, damping, and the mass of the load. The scatter in values of impact factor with increasing number of pontons is not unreasonable. Consider the mid-span deflection of identical simple span beams of uniform section subjected to different loads which produce the same maximum fiber stress at mid-span. The ratio of the mid-span deflection of a beam subjected to equal end moments to the deflection of a beam under uniform load is 1.20. Similar ratios for beams with 2 and 4 equal, symmetrically placed concentrated loads is 1.02 and 1.01. For beams with 1, 3 and 5 equal symmetrically placed concentrated loads

the ratios are 0.80, 0.95 and 0.98. As the number of load concentrations increase the ratio approaches the limiting value of 1.0. The ratio, for odd number load concentrations, approaches the limiting value asymptotically from below; while, for even number load concentrations, the approach is from above. The plotted data of Fig.53 indicate this trend. The variations may be attributed to the contribution of the higher modes of vibration to the displacements in each case.

Fig. 54 shows the first and second modes of vibration for the four bridges summarized in Fig. 53. For a one ponton bridge only the first mode is excited by the action of the moving load P. Fib. 54b shows how the first two modes are excited in a two ponton bridge by the moving load and, moreover, how all of the concentrated mass of the bridge oscillates in this second mode. One would then expect the dynamic displacements to be greater for a two ponton bridge than a one ponton bridge due to the contribution of the second mode. This contention is supported by Fig. 53.

In the case of a three ponton bridge, however, only 66.67% of the concentrated mass oscillates in the second mode. The center mass is at a node. One would then expect, neglecting the contribution of the third mode, that the maximum dynamic displacements of a three ponton bridge would be less than a two ponton bridge but more than a one ponton bridge. This is supported by Fig. 53. For a five ponton bridge 80% of the concentrated mass oscillates in the second mode as is shown in Fig. 54 d and the maximum dynamic displacements are greater than those of a three ponton bridge (66.67% of the oscillating mass in the

second mode) and less than those of a two ponton bridge (100 of the mass oscillating in the second mode).

As the number of pontons increases the difference in the impact factor between any two consecutive values of n will decrease and eventually the relationship between impact factor and n will be consistent.

Fig. 10 shows the impact factor as a function of time of crossing for a single span bridge considering virtual mass and neglecting virtual mass. The maximum ordinate is the same in each case. The effect of the virtual mass is to cause the maximum impact factor to occur at a slower speed of crossing. Figs. 25a and 29a show similar comparisons for two and three ponton bridges, respectively. The maximum impact factor for a two ponton bridge is increased when virtual mass is considered. In the case of the three ponton bridge a consideration of virtual mass leads to lower impact factors.

These results are also summarized in Fig. 53. The open squares are results for bridges of one, two and three pontons considering virtual mass.

The effect of the mass of the moving load was considered for a single ponton bridge only. The impact factor-time of crossing relationship shown in Fig. 11 for different values of the ratio $m_L m$ indicates that the maximum impact factor is the same for all values of this ratio. The deflected load line, in this case, was assumed linear. Fig. 55 shows similar results for $m_L = 3m$ and $5m$ which are summarized in Figs. 20 and 21. In this case, however, the deflected load line was assumed to be a second degree curve. The

maximum impact factors, however, are the same as those of Fig. 11 indicating that the assumption of a linear deflection curve yields sufficiently accurate results when the mass of the load is taken into account. This is emphasized by Fig. 55 which shows a computor solution for a single ponton bridge considering virtual mass and the mass of the moving load assuming a second degree deflection curve (Fig. 22) and a numerical solution of the same problem assuming a linear deflection curve. Fig. 55 also indicates that the consideration of virtual mass leads to a lower impact factor for a single ponton bridge, when considering the mass of the load, than is obtained when virtual mass is neglected.

The effect of varying the ratio of K to EI/L^3 for a three ponton bridge is shown in Fig. 57 which is a plot of impact factor as a function of KL^3/EI. The results for values of KL^3/EI of 17.5 and 35 are obtained from Figs. 29 and 30. A value for KL^3/EI of infinity means that there is no elastic interaction between the pontons. This implies that each ponton and its adjacent spans act as single ponton bridges. The impact factor, therefore, from Fig. 53, is 1.52.

A value of KL^3/EI of zero implies that the value for K is zero. The equations for a three ponton bridge, for K=0, are then the same as equations (10) with n=3. Solutions of these equations for a moving load P and for different times of crossing are given by J. M. Bonetti.[1] The maximum impact factor obtained is 1.67.

The effect of damping on impact factor is shown in Fig. 58 for a two ponton bridge and Fig. 59 for a three ponton bridge. These plots show the relationship between impact factor and time of crossing

for damping coefficients C = 0, 100 and 1000 lb-sec/in. These curves are summarized in Fig. 60. Curve C of Fig. 59 reveals that the impact factor approaches 1.0 at large times of crossing for C=1000 lb-sec/in. Curve B of Fig. 60, which shows the relationship between impact factor and coefficient of viscous damping, for the three ponton bridge, then has the value of 1.0 at C= 1000 lb-sec/in. and also has zero slope since all the values of C above 1000 lb-sec/in. (and some below) cause an impact factor of 1.0.

CONCLUSIONS

1. The numerical procedure discussed above can be satisfactorily used for the analysis of the dynamic response of floating bridges to transient loads. The accuracy obtained compares well with that obtained by an electronic analog computor and is sufficient for engineering purposes. The method is readily extended to include damping, the mass of the moving load and non-linear behavior.
2. Virtual mass has a significant effect on the response of floating bridges to transient loads. The effect is more pronounced than the effect of viscous damping. Moreover, the omission of virtual mass in the analysis of a floating bridge leads to displacements on the unsafe side.
3. The impact factor for a single ponton bridge does not change when the mass of the load is taken into account. Varying the ratio of the mass of the moving load to the mass of the bridge merely

causes the maximum displacement to occur at a different speed of crossing.

4. The assumption of a linear deflection curve, when considering the mass of the load, is a good approximation for the shape of the deflected structure. Comparison of solutions for a single ponton bridge considering a linear deflection curve and considering a second degree (parabolic) deflection curve show complete agreement.

5. The ratio of the buoyant resistance K of the ponton to the stiffness EI/L^3 of the bridge has some effect on the impact factor. For higher values of this ratio the impact factor decreases and, neglecting virtual mass and the mass of the moving load, approaches an impact factor of 1.52. The upper limit of the impact factor for lower values of this ratio is 1.67.

6. The virtual mass and damping coefficients obtained by experiments are reliable. Calculated displacements, based on these values, compare well with experimental results.

APPENDIX A

Example Calculations

SINGLE PONTON BRIDGE

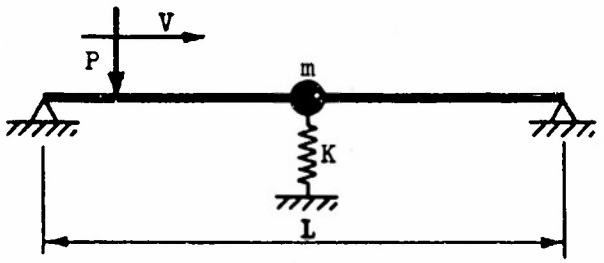

SINGLE PONTON BRIDGE

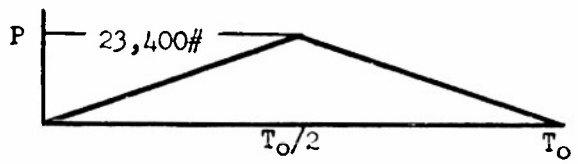

APPLIED LOAD-TIME CURVE FOR $H=T_0$

Equation of Motion:

$$(\frac{4m}{\Delta t^2}+K)y_2 = (\frac{4m}{\Delta t^2}-K)y_1 + \frac{4m}{\Delta t^2} V_1\Delta t + P_1+P_2$$

$H=T_0$ $\quad \Delta t=T_0/20$ $\quad P=23,400$ $\quad K=34,420$

Time T_0	P_1+P_2	y	$V\Delta t$
0	0	0	0
0.05	2,340	0.00164	0.00328
0.10	7,020	0.00967	0.01278
0.15	11,700	0.02986	0.02760
0.20	16,380	0.06682	0.04632
0.25	21,060	0.12354	0.06712
0.30	25,740	0.20110	0.08800
0.35	30,420	0.29858	0.10696
0.40	35,100	0.41314	0.12216
0.45	39,780	0.54029	0.13214
0.50	44,460	0.67433	0.13594
0.55	44,460	0.80562	0.12664
0.60	39,780	0.91824	0.09860
0.65	35,100	0.99480	0.05452
0.70	30,420	1.02138	-0.00036
0.75	25,740	0.98985	-0.06270
0.80	21,060	0.89572	-0.12556
0.85	16,380	0.74150	-0.18288
0.90	11,700	0.53550	-0.22912
0.95	7,020	0.29102	-0.25984
1.00	2,340	0.02506	-0.27208

SINGLE PONTON BRIDGE CONSIDERING VIRTUAL MASS

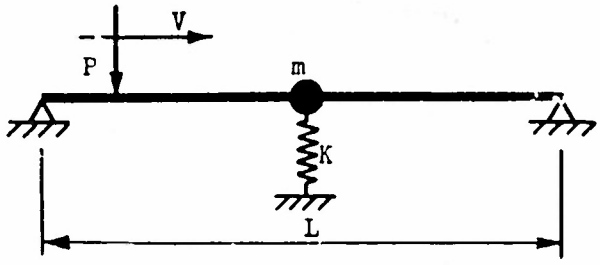

SINGLE PONTON BRIDGE

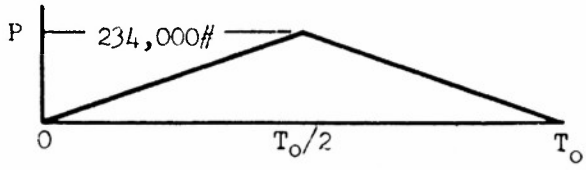

APPLIED LOAD-TIME CURVE FOR H=T_o

Equation of Motion:

$$(40.568\frac{m'}{m}+1)y_2 = (40.458\frac{m'}{m}-1)y_1+40.568\frac{m'}{m}\,V_1\Delta t+\frac{P_1+P_2}{K'}$$

or $$Ay_2 = By_1 + CV_1\Delta t + D$$

$m' = 74.+2.23y$ $\qquad$ $\Delta t = T_O/20$

Time T_O	A	B	C	D	y	$V\Delta t$
0	149.613	147.613	148.613	0	0	0
0.05	149.613	147.613	148.613	0.67984	0.00454	0.00908
0.10	149.633	147.633	148.633	2.03953	0.02713	0.03610
0.15	149.734	147.734	148.734	3.39920	0.08533	0.08030
0.20	149.995	147.995	148.995	4.75888	0.19568	0.14040
0.25	150.489	148.489	149.489	6.11856	0.37320	0.21464
0.30	151.284	149.284	150.284	7.47824	0.63092	0.30080
0.35	152.438	150.438	151.438	8.83792	0.97945	0.39626
0.40	153.999	151.999	152.999	10.19760	1.42664	0.49812
0.45	156.002	154.002	155.002	11.55728	1.97736	0.60332
0.50	158.468	156.468	157.468	12.91696	2.63343	0.70882
0.55	161.406	159.406	160.406	12.91696	3.38526	0.79484
0.60	164.773	162.773	163.773	11.55728	4.20433	0.84330
0.65	168.441	166.441	167.441	10.19760	5.05224	0.85452
0.70	172.243	170.243	171.243	8.83792	5.89543	0.82986
0.75	176.015	174.015	175.015	7.47824	6.69607	0.77142
0.80	179.600	177.600	178.600	6.11856	7.42270	0.68184
0.85	182.854	180.854	181.854	4.75888	8.04565	0.56406
0.90	185.644	183.644	184.644	3.39920	8.53830	0.42124
0.95	187.850	185.850	186.850	2.0352	8.87725	0.25666
1.00	189.368	187.368	188.368	0.67984	9.04239	0.07362

SINGLE PONTON BRIDGE CONSIDERING MASS OF LOAD

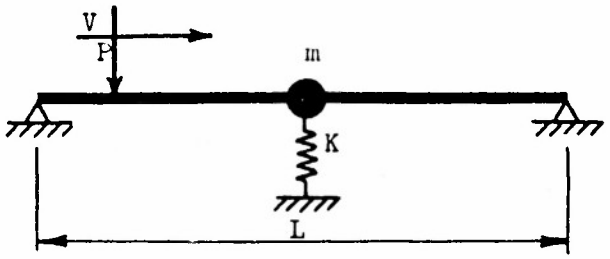

SINGLE PONTON BRIDGE

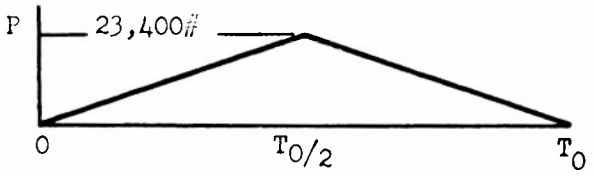

APPLIED LOAD-TIME CURVE FOR $H=T_0$

Equation of Motion:

$$(1+\beta\alpha^2+\eta^{-2}\pi^2)y_2 = (1+\beta\alpha^2-\eta^2\pi^2)y_1 + (1+\beta\alpha^2)V_1\Delta t + \eta^2\pi^2\frac{(\alpha_1+\alpha_2)}{K'}P$$

or $\quad Ay_2 = By_1 + CV_1\Delta t + D$

$\beta = 3$ $\qquad$ $\eta = 1/20$

Time T_0		A	B	C	D	y	$V\Delta t$
0	0	1.025	0.975	1.000	0	0	0
0.05	0.1	1.055	1.005	1.030	0.0017	0.0016	0.0032
0.10	0.2	1.145	1.095	1.120	0.0051	0.0918	0.0118
0.15	0.3	1.295	1.245	1.270	0.0085	0.0270	0.0238
0.20	0.4	1.505	1.455	1.480	0.0119	0.0574	0.0370
0.25	0.5	1.775	1.725	1.750	0.0153	0.1008	0.0499
0.30	0.6	2.105	2.055	2.080	0.0187	0.1566	0.0617
0.35	0.7	2.495	2.445	2.470	0.0331	0.0221	0.0719
0.40	0.8	2.945	2.895	2.920	0.0255	0.2997	0.0805
0.45	0.9	3.455	3.405	3.430	0.0289	0.3836	0.0874
0.50	1.0	4.025	3.975	4.000	0.0323	0.4738	0.0929
0.55	0.9	3.455	3.405	3.430	0.0323	0.5685	0.0965
0.60	0.8	2.945	2.895	2.920	0.0289	0.6643	0.0952
0.65	0.7	2.495	2.445	2.470	0.0255	0.7554	0.0870
0.70	0.6	2.105	2.055	2.080	0.0221	0.8340	0.0700
0.75	0.5	1.775	1.725	1.750	0.0187	0.8900	0.0421
0.80	0.4	1.505	1.455	1.480	0.0153	0.9121	0.0019
0.85	0.3	1.295	1.245	1.270	0.0119	0.8879	-0.0500
0.90	0.2	1.145	1.095	1.120	0.0085	0.8075	-0.1107
0.95	0.1	1.055	1.005	1.030	0.0051	0.6660	-0.1723
1.00	0	1.025	0.975	1.000	0.0017	0.4671	-0.2256

APPENDIX B

Determination of Damping Coefficients

Consider the single mass oscillator shown in Fig. 3. If in addition to the resistance of the spring the mass encounters a resistance proportional to velocity the equation of motion for free vibration (P=0) is

$$m\ddot{y} = Ky + C\dot{y} \tag{77}$$

The solution of this equation is of the form[4]

$$y = e^{-\frac{Ct}{2m}} (A \cos pt + B \sin pt) \tag{78}$$

where A, B and p are constants.

The solution of equation (78), for a single mass oscillator subjected to an initial displacement y_0, is shown schematically in Fig. 6la. The equation of the dotted curve connecting the maximum ordinate is

$$y = y_0 e^{-\frac{Ct}{2m}} \tag{79}$$

or, taking the natural logarithm of each side of equation (79),

$$C = \frac{2m}{t} \ln {}^{y_0}/_{y} \tag{80}$$

Equation (80) can be used for the experimental determination of the coefficient of damping C. It is only necessary to determine by experiment the ratio of the amplitudes of vibration after a period of time t.

Data from the tests conducted to determine the virtual mass coefficients were used to determine the damping coefficients for the model pontons. An example of such data is shown in Fig. 6lb. This trace is for the triangular model ponton vibrating at a displacement

of 2.06 in. Considering the two arbitrary points a and b, 0.2 seconds apart, the ratio of their amplitudes is

$$\frac{y_a}{y_b} = \frac{140}{80} = 1.75$$

The mass of the system, including the mass of the ponton plus one-half the mass of the test beam, is 0.0479 lbs-sec^2/in. whence,

$$C = \frac{(2)\ (0.0479)}{0.2} \ln 1.75$$

or

$$C = 0.268 \text{ lbs-sec}^2/\text{in.}$$

Following a similar procedure with the ponton vibrating in air a value for C of 0.030lbs-sec^2/in. is obtained. The difference between these two values of C is the damping due to the water in contact with the ponton.

Similar tests were conducted on the rectangular and semi-circular pontons at different displacements. In all cases the damping varied with displacement but, to simplify calculations, an average value was used for computations.

APPENDIX C

Electronic Analog Computors

General

An electronic analog computor deals with problems that involve the behavior of several variables. These variables are represented in the computor by d-c voltages, which are referred to as machine variables, and are usually related to the original variables on some convenient scale. The given mathematical relations between the original variables are expressed by an analagous set of relations between the machine variables. In order to deal with a wide range of problems the mathematical operations on the machine variables are performed by basic computing elements in a small number of simple operations. In general a wide variety of problems can be treated withthe following computing elements:

1. Elements which will multiply a variable by a constant coefficient.
2. Elements which will add variables.
3. Elements which will multiply two variables.
4. Elements which will integrate with respect to time.

Basic Computing Elements.- The addition of several machine variables V can be performed with the network shown in Fig. 62a. Let A be the amplifier forward gain. The voltage at the amplifier input grid is

$$E = V_o/A$$

From Kirchoff's first law the sum of all current flowing to the grid must be zero or

$$\left(\frac{V_o}{A}-V_1\right)\!\!-\!\!\bullet\left(\frac{V_o}{A}-V_2\right)\!\!-+\left(\frac{V_o}{A}-V_3\right)\!\!-+\left(\frac{V_o}{A}-V_o\right)\!\!- = 0$$

and solving for V_o

$$V_o = \left(\frac{V_1}{R_1} + \frac{V_2}{R_2} + \frac{V_3}{R_3}\right) \frac{AR_o}{(1-A) + R_o\left(\frac{1}{R_1} + \frac{1}{R_2} + \frac{1}{R_3}\right)} \qquad (81)$$

With sufficiently high amplifier gain

$$A \quad 1$$

and equation (81) becomes

$$V_o = -R_o\left(\frac{V_1}{R_1} + \frac{V_2}{R_2} + \frac{V_3}{R_3}\right)$$

or

$$V_o = -(a_1V_1 + a_2V_2 + a_3V_3)$$

where

$$a_1 = R_o/R_1 \qquad a_2 = R_o/R_2 \qquad a_3 = R_o/R_3$$

Thus the variables are not only summed but are multiplied, if necessary, by a coefficient.

Multiplication by a constant can be performed with the network shown in Fig. 62b. The voltage at the input grid of the amplifier is V_o/A. Equating the current into the grid to the current leaving the grid

$$\left(\frac{V_o}{A} - V_o\right)\frac{1}{R_o} + \left(\frac{V_o}{A} - V_1\right)\frac{1}{R_1} = 0$$

and

$$V_o = V_1 \frac{A}{(1 + A)\frac{R_1}{R_o} + 1} \qquad (82)$$

Since A 1 we have to a good approximation

$$V_o = -\frac{R_o}{R_1}V_1 = a_1V_1 \qquad (83)$$

Fig. 62c shows the network for multiplying two variables together. The voltage V_o, for a setting a of the voltage divider, is

$$V_o = aV_1$$

If the setting a is made proportional to some voltage V_2 by means of a servomechanism then the output voltage aV_1 will be proportional to the product of V_1 and V_2.

$$V_o = V_1 f(V_2)$$

Electrical integrators are based on the property of capacitors. The current through a capacitor is proportional to the derivative of the voltage E

$$i = CdE/dt = CPE$$

where

$$P = d/dt$$

Fig. 62d shows the network for an electrical integrator using a capacitor and a high gain amplifier. The equation for the currents at the input grid is

$$(\frac{V_o}{A} - V_1)\frac{1}{R} + (\frac{V_o}{A} - V_o)CP = 0$$

or

$$V_o = \frac{A}{(1-A)RCP + 1} V_1$$

For a large amplifier gain A

$$V_o = -\frac{1}{RCP} V_1 \qquad (84)$$

which corresponds to integration.

Fig. 62e shows the network of a summing integrator which is capable

of summing as well as integration. Following a similar derivation as above the output voltage is

$$V_o = -\frac{1}{CP}\left(\frac{V_1}{R_1} + \frac{V_2}{R_2} + \frac{V_3}{R_3}\right) \tag{85}$$

Block Diagrams.- In "setting up" a computor to solve a mathematical equation it is convenient to represent the relation between the computor components and voltages by means of a block diagram. The block diagram describes the relations between voltages and computing components in the same way as the mathematical equation describes relations between operators and variables. The symbols commonly used to represent the basic computing elements are shown in Fig. 62.

As an example consider the equation

$$Y_1 = Y_2 + aY_2^2 \tag{86}$$

Y_1 and Y_2 are voltages and Y_1 is a function of Y_2. The voltage Y_2 will be the input voltage to a block of computing components as shown in Fig. 63.

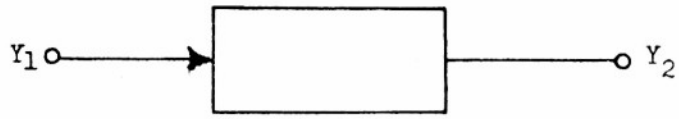

FIG. 63 BLOCK REPRESENTATION OF RELATIONSHIP BETWEEN Y_1 AND Y_2.

If the correct combination of computing elements is used Y_1 will appear as the output voltage.

Frequently it is not possible to solve explicitly for a variable

in equations like

$$Y_1 = Y_1^2 + bY_2 + cY_3 \qquad (87)$$

However, since Y_1 appears on the right of equation (87) it can be treated as an input voltage to the block of computing elements. Since Y_1 at the input terminal must equal Y_1 at the output terminal the output voltage is treated as if it were known and is "fed back" to the input terminal as shown in Fig. 64.

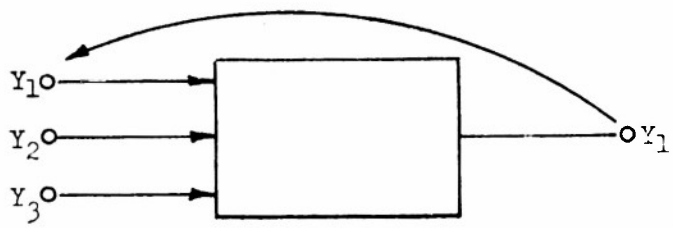

FIG. 64 BLOCK REPRESENTATION OF RELATIONSHIP BETWEEN Y_1, Y_2, AND Y_3

The correct relationship will be established if suitable computing components are used.

Application To Floating Bridges

Equation (5) for a single ponton bridge considering damping is

$$d^2y_1/dt^2 + bdy_1/dt^2 + dy_1 - f(t) = 0$$

or

$$P^2y_1 + bPy_1 + dy_1 - f(t) = 0 \qquad (88)$$

where

$$b = C/m_1$$

$$d = (a_{11}+K)/m_1$$

$$f(t) = F_1(t)/m_1$$

Solving for the highest derivative of y_1 equation (88) becomes

$$P^2y_1 = - dy_1 + bPy_1 - f(t) \qquad (89)$$

The block diagram for the solution of equation (89) is shown in Fig 65. The voltages dy_1, bPy_1, and $f(t)$ are applied to the input terminals of a summing circuit (Fig 62 a) which yields $- P^2y_1$. These input voltages, however, must be obtained from P^2y_1 by integration and multiplication by suitable constants. The voltage $- P^2y_1$ is considered known and is applied to the input of an integrater which yields Py_1. This voltage is multiplied by a constant b (see Fig 62 b) and serves as the input voltage bPy_1 applied to the summing circuit. The voltage Py_1 is also applied to the input of another integrator which yields $- y_1$. The voltage $- y_1$ is applied to a phase inverting amplifier which yields y_1. This voltage is multiplied by a constant d to provide the voltage dy_1 which must be applied to the summing circuit and is also recorded. This record constitutes a solution to the problem. The voltage $-F(t)$ applied to the summing circuit is supplied by a suitable function generator. With the computor set up in as shown in Fig 65 the machine variable y_1 is forced to vary in the manner prescribed by equation (89).

Equation (3) for a single ponton bridge considering virtual mass can be written

$$P^2y_1 + b^2y_1 P^2y_1 + dy_1 - f(t) = 0 \qquad (90)$$

where $b = \quad /M_1$

$d = (a_{11} + k) /M_1$

$f(t) = F(t) /M$

Solving for P^2y_1 equations (90) becomes

$$P^2y_1 = -by_1 P^2y_1 - dy_1 + f(t) \qquad (91)$$

Fig 66 shows the block diagram of the computer set up for the solution of equation (91). The solution is carried out in much the same way as that of equation (88) with the exception of the addition of the servomechanism. This is necessary to generate the product of by_1 and $- P^2y_1$ to yield the voltage $-by_1P^2y_1$ which is applied to the summing circuit.

The construction of block diagrams for bridge of more than one ponton presents no difficulties. Equations (2) for a two ponton bridge (n=2) becomes

$$\begin{aligned} P^2y_1 + b_{11}\, y_1 + b_{12}\, y_2 - f_1(t) &= 0 \\ P^2y_1 + b_{21}\, y_1 + b_{22}\, y_2 - f_2(t) &= 0 \end{aligned} \qquad (92)$$

where $b_{11} = (a_{11} + k)/M_1$

$b_{12} = a_{12}/M_1$

$b_{21} = a_{21}/M_1$

$b_{22} = (a_{22} + k)/M_1$

Fig 67 shows the computer set up for the solution of equations (92). A separate circuit is constructed for each equation. The input $b_{21}\, y_1$ to the summing circuit of the second equation is taken from the output of the first equation and the input $b_{12}\, y_2$ of the first equation is obtained from the output of the second equation.

BIBLIOGRAPHY

1. Bonetti, J. M.: Transients - Their Solution by Impulse-Momentum. M.S. Thesis, Carnegie Institute of Technology, 1953

2. Proc. Camb. Phil. Society, vol. i, p.83, 1849

3. Inglis, C. E.: Theory of Transverse Oscillations in Girders and its Relation to Live Load and Impact Allowances. Minutes of Proc. Inst. of Civil Engrs., 218, p. 225, 1923

4. Timoshenko, S.: Vibration Problems in Engineering. B. Van Nostrand Co., 2nd Ed., N.Y., 1937

5. Jeffcott, H. H.: On the Vibrations of Beams Under the Action of Moving Loads. Phil. Magazine, V.8, 1929

6. Hillerborg, A.: Dynamic Influences of Smoothly Running Loads on Simply Supported Girders. Institution of Structural Engineering and Bridge Building. Stockholm, Sweden

7. Brock, J. E.: Variation of Coefficients of Simultaneous Linear Equations. Quarterly of Applied Mathematics, vol.11, p.234, 1953

8. Korn, G. A. and Korn, T. M.: Electronic Analog Computors. McGraw-Hill Book Co., Inc., 1st Ed., 1952

9. Murray, F. J.: The Theory of Mathematical Machines. King's Crown Press, New York, 1947

10. Stelson, T. E.: Acceleration of Bodies in Fluids - A Study of Virtual Mass. D.Sc. Thesis, Carnegie Institute of Technology, 1952

11. Ibid., p.18

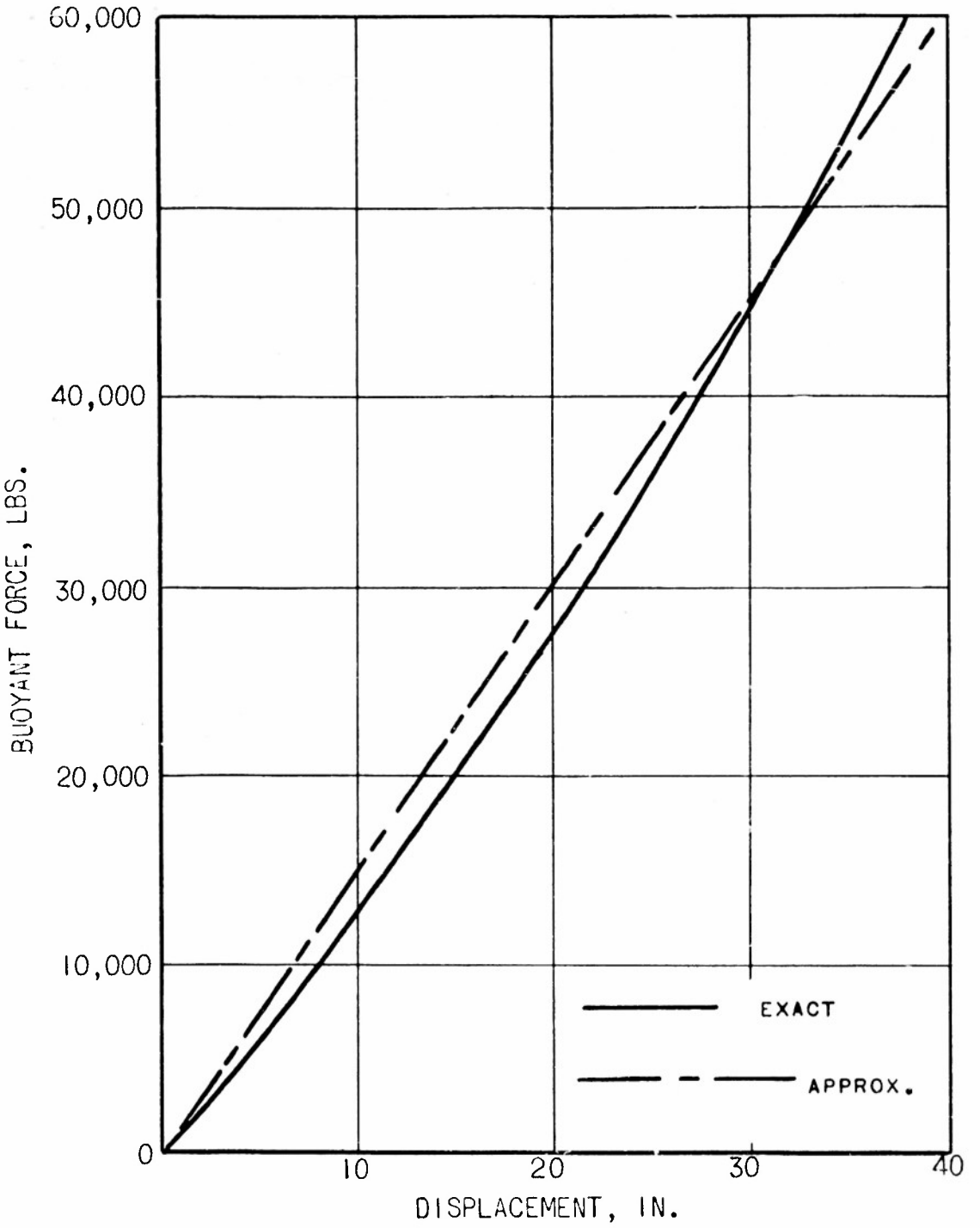

FIG. 5 BUOYANT FORCE—DISPLACEMENT RELATIONSHIP FOR AN M-4 PONTON

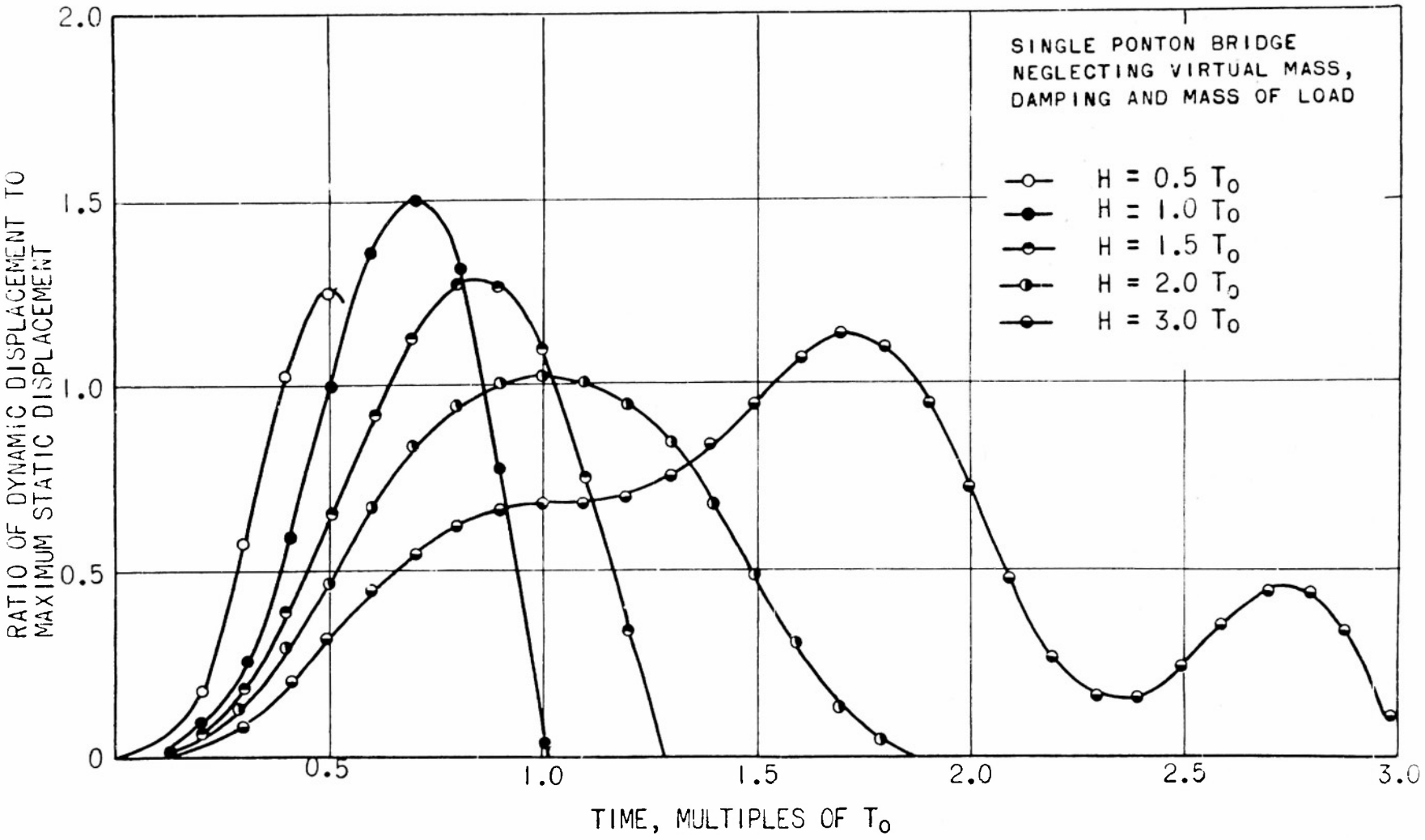

FIG. 7 DISPLACEMENT—TIME RELATIONSHIP FOR A SINGLE PONTON BRIDGE

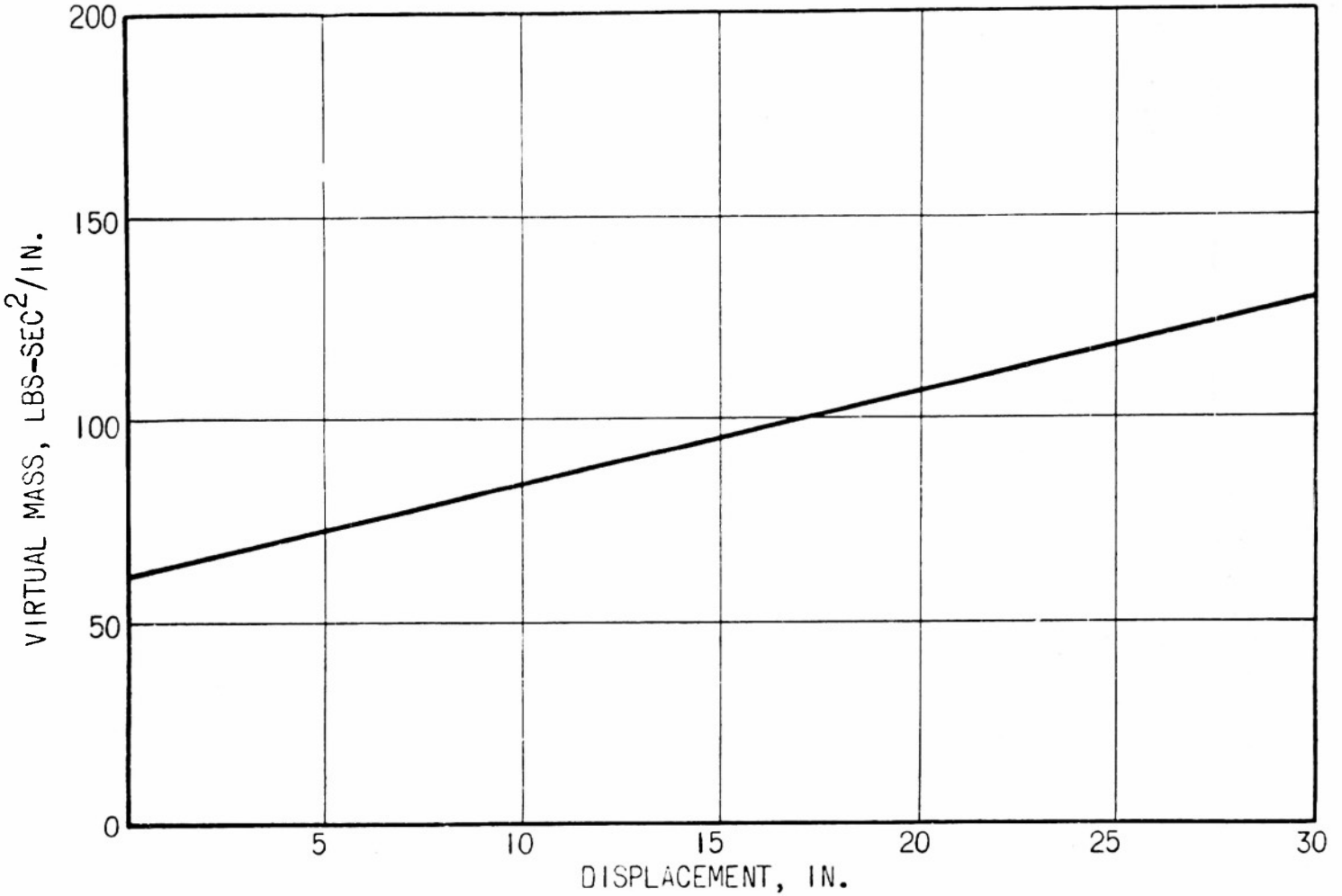

FIG. 8 VIRTUAL MASS—DISPLACEMENT RELATIONSHIP FOR AN M-4 PONTON

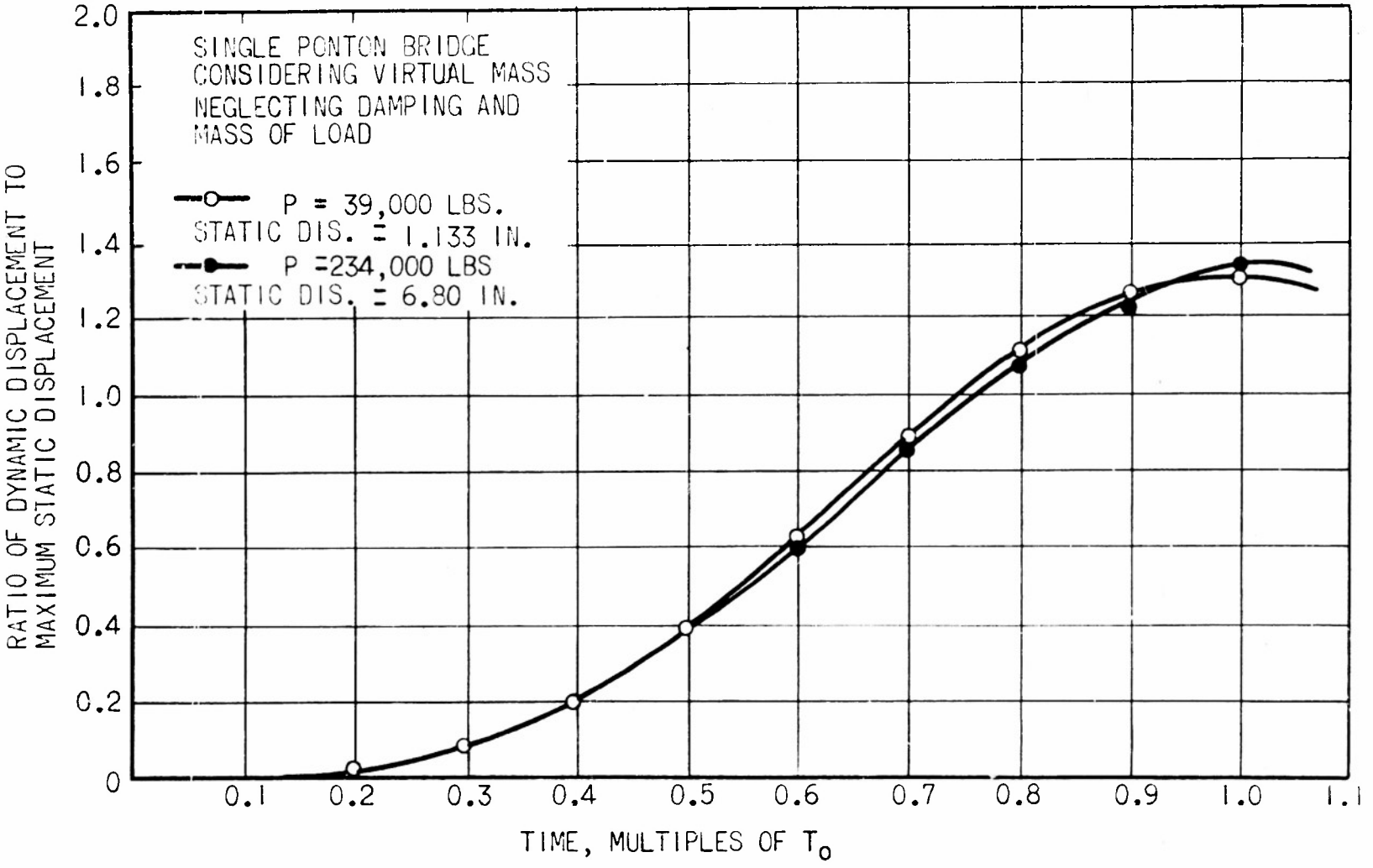

FIG. 9 DISPLACEMENT—TIME RELATIONSHIP FOR SINGLE PONTON BRIDGE CONSIDERING VIRTUAL MASS

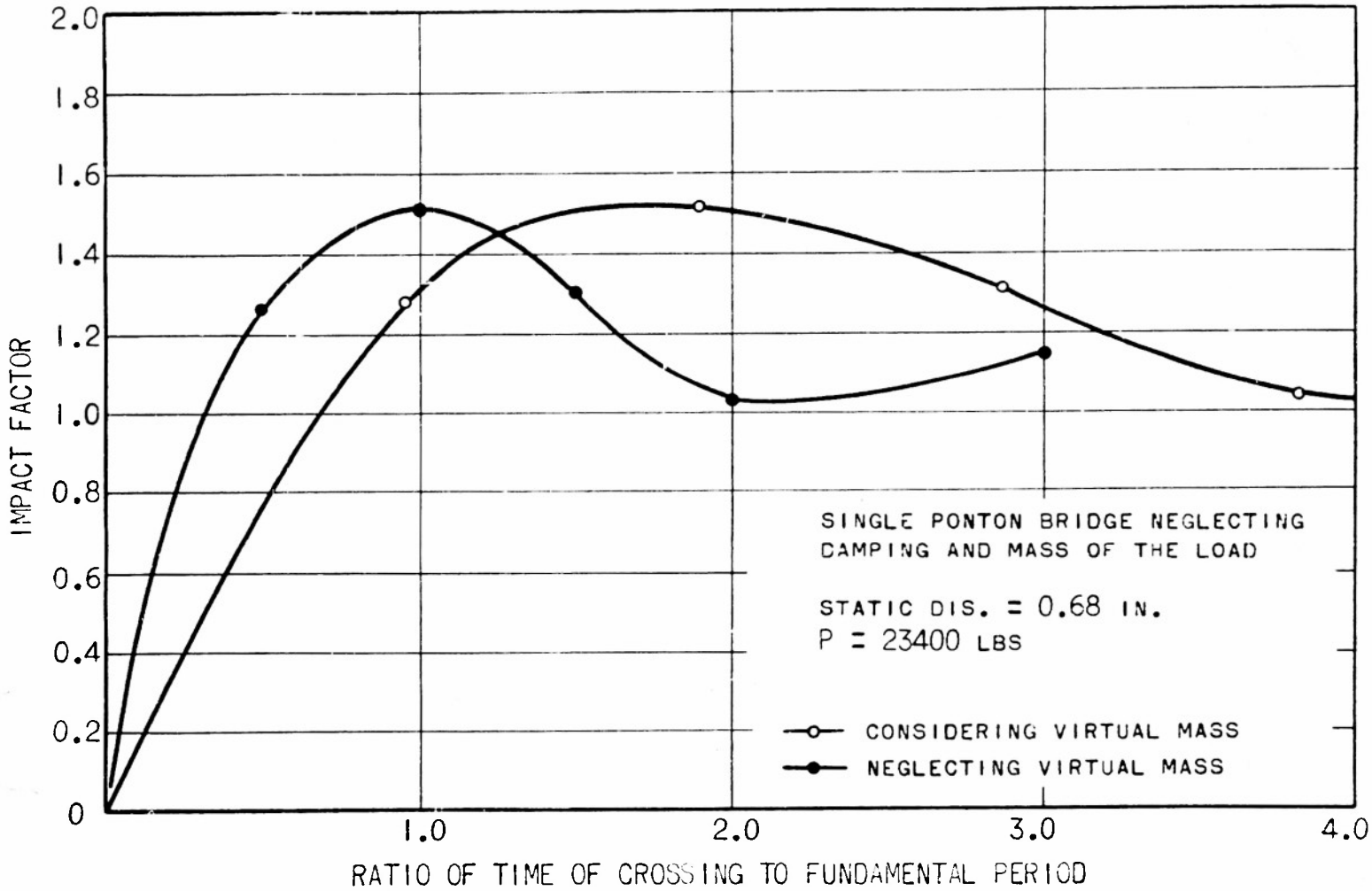

FIG. 10 RELATIONSHIP BETWEEN IMPACT FACTOR AND TIME OF CROSSING FOR SINGLE PONTON BRIDGE

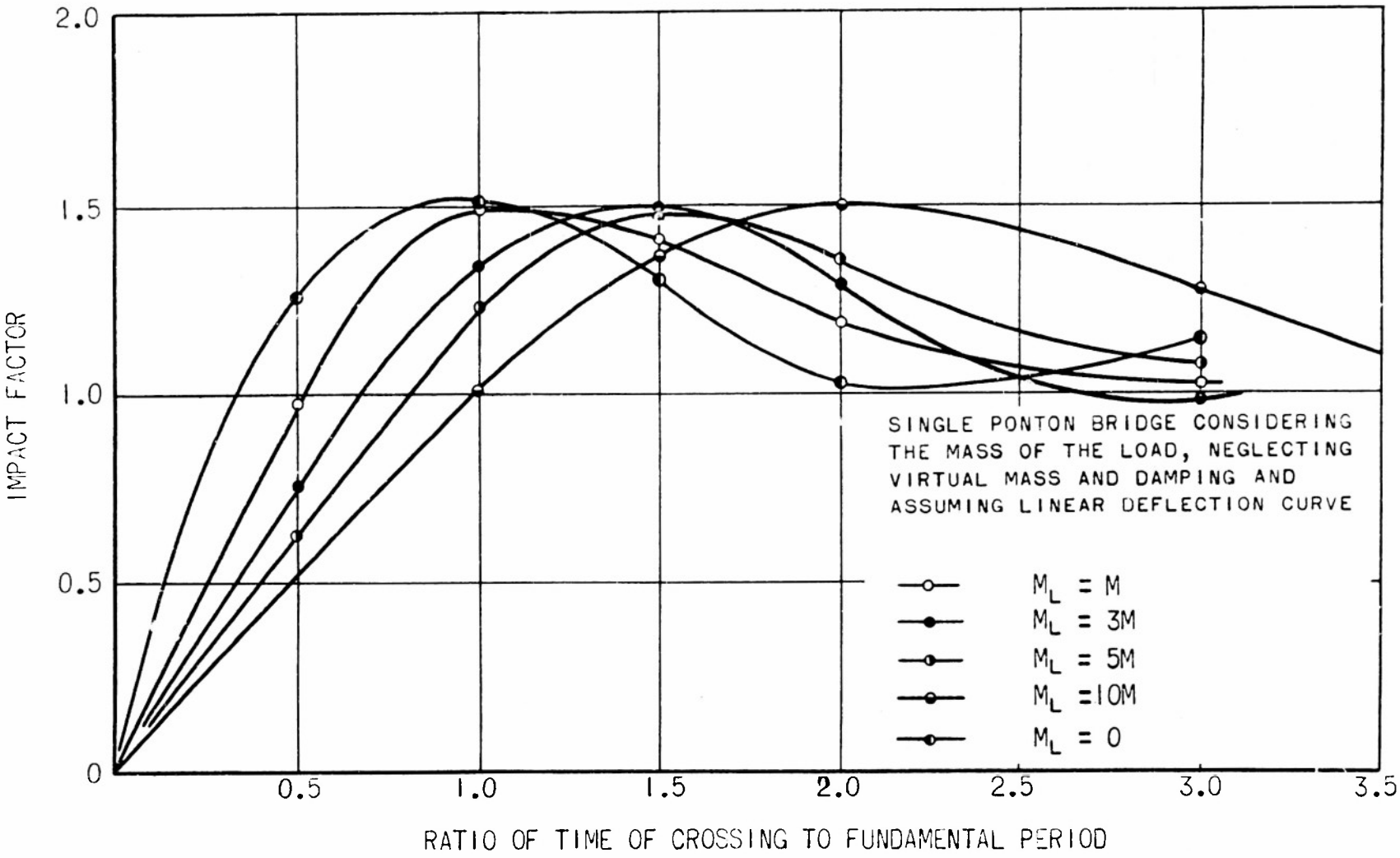

FIG. 11 RELATIONSHIP BETWEEN IMPACT FACTOR AND TIME OF CROSSING FOR SINGLE PONTON BRIDGE CONSIDERING MASS OF THE MOVING LOAD

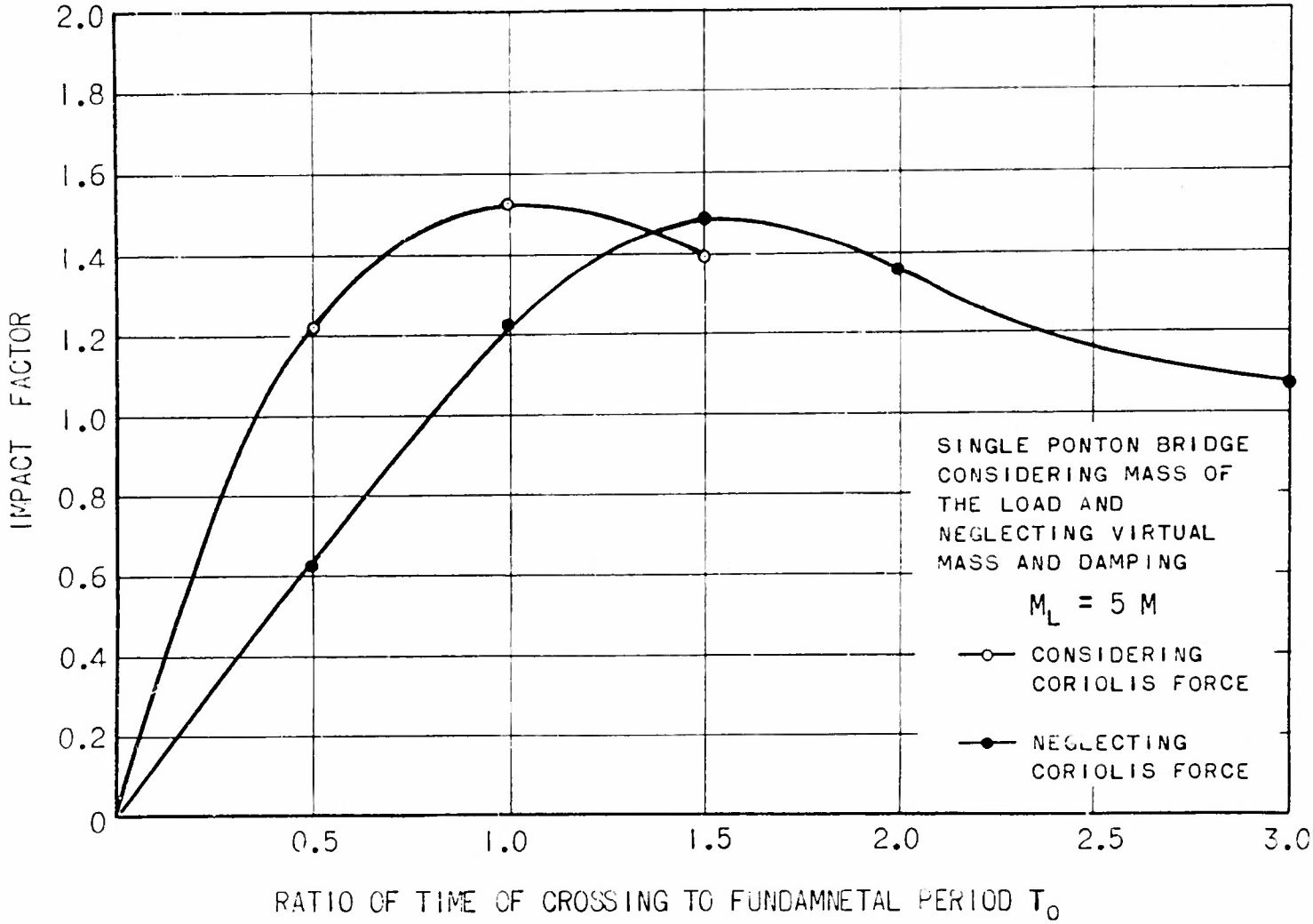

FIG. 11A RELATIONSHIP BETWEEN IMPACT FACTOR AND TIME OF CROSSING FOR SINGLE PONTON BRIDGE CONSIDERING MASS OF THE LOAD

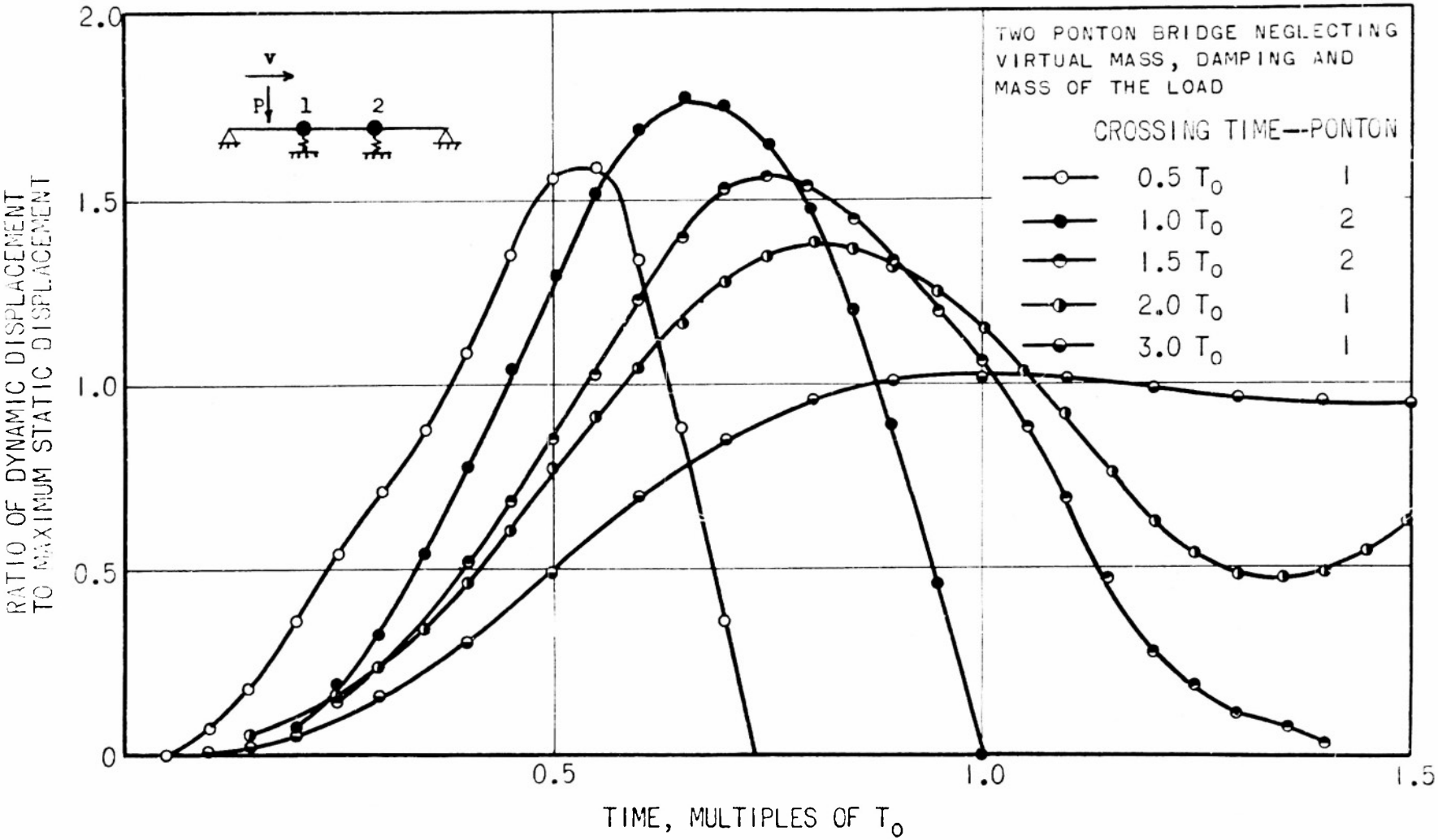

FIG. 13 DISPLACEMENT—TIME RELATIONSHIP FOR A TWO PONTON BRIDGE

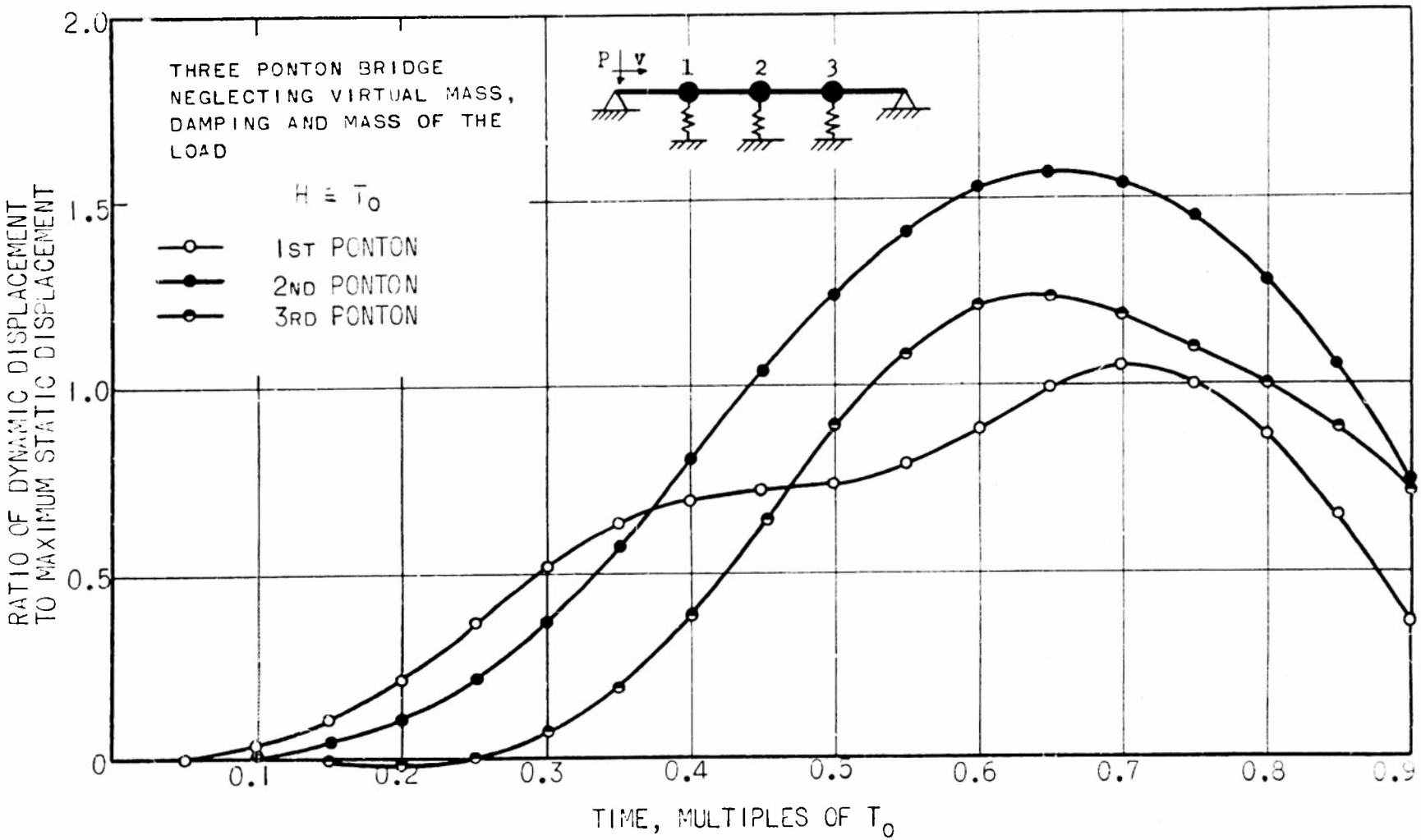

FIG. 14 DISPLACEMENT—TIME RELATIONSHIP FOR THREE PONTON BRIDGE

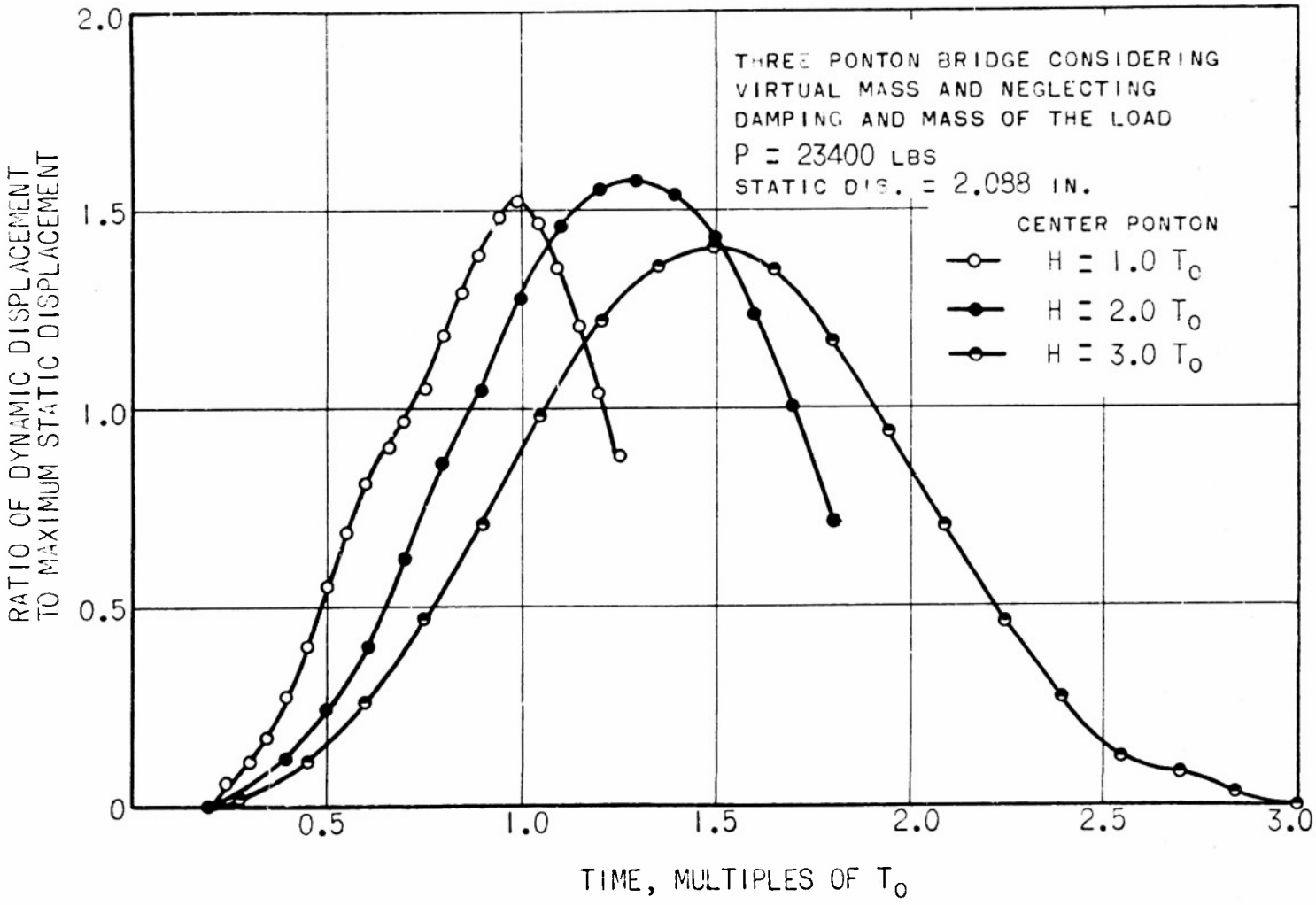

FIG. 15 DISPLACEMENT—TIME RELATIONSHIP FOR THREE PONTON BRIDGE CONSIDERING VIRTUAL MASS

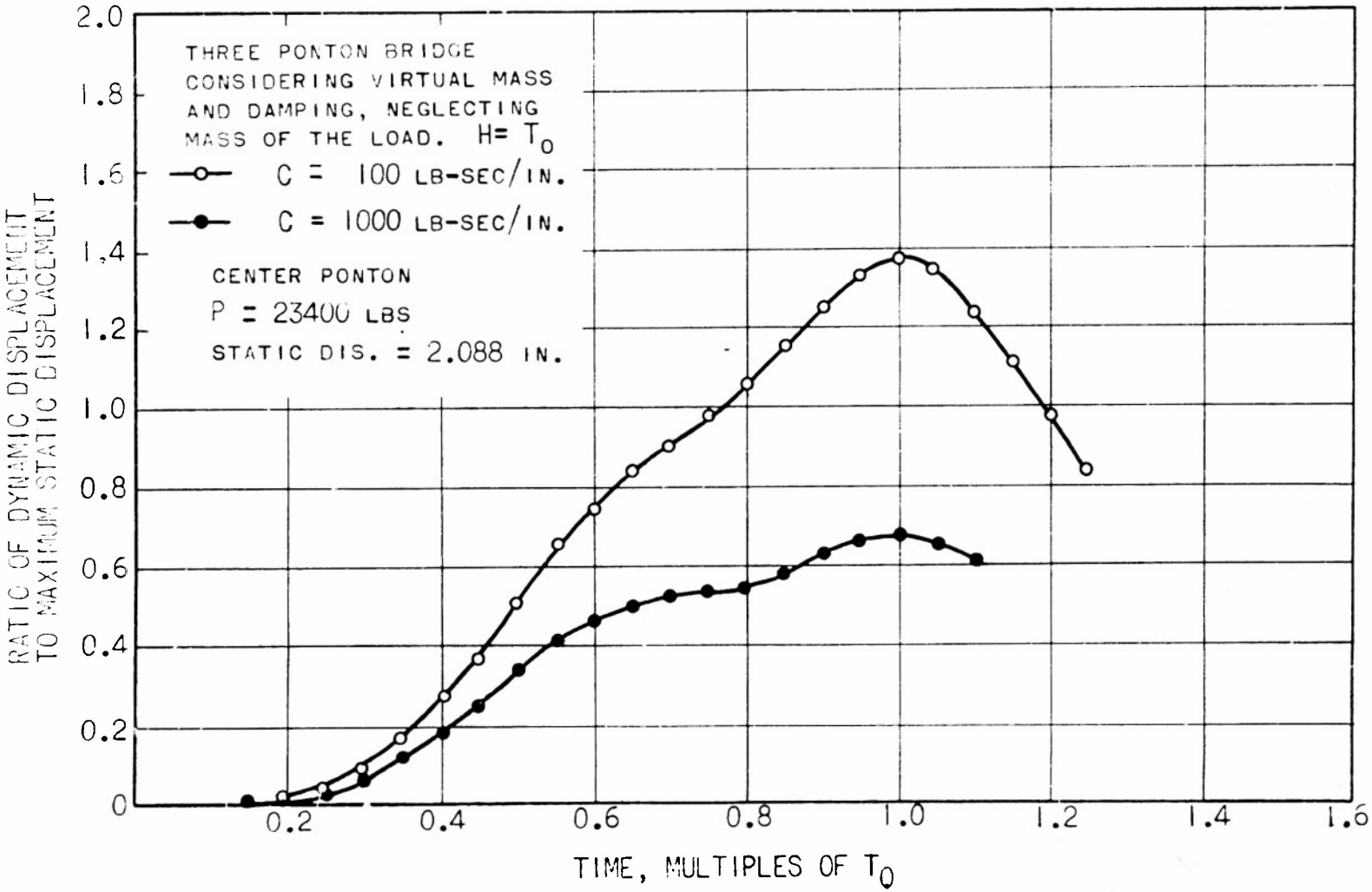

FIG. 16 DISPLACEMENT—TIME RELATIONSHIP FOR THREE PONTON BRIEGE CONSIDERING VIRTUAL MASS AND DAMPING

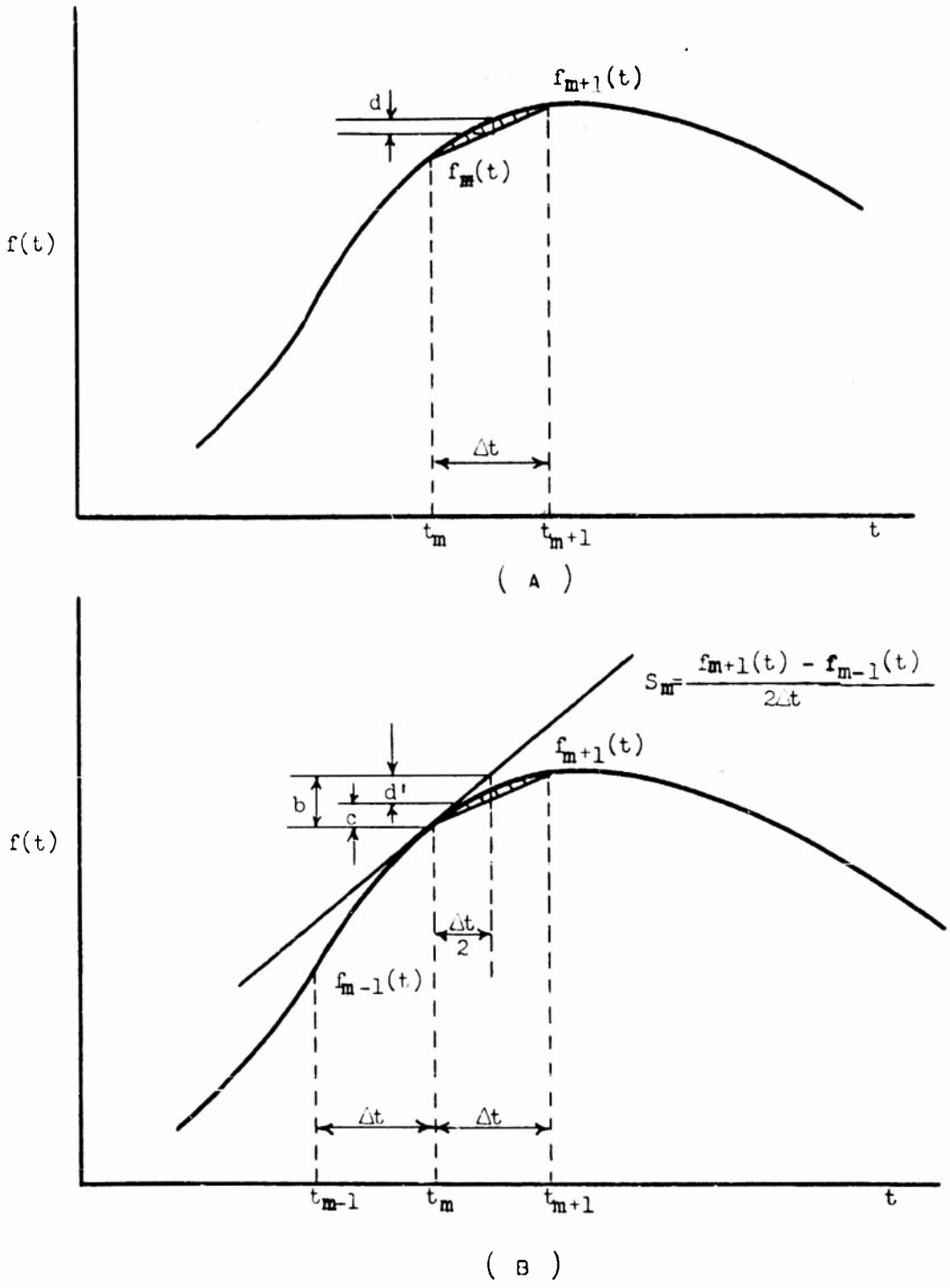

FIG. 17 NUMERICAL INTEGRATION

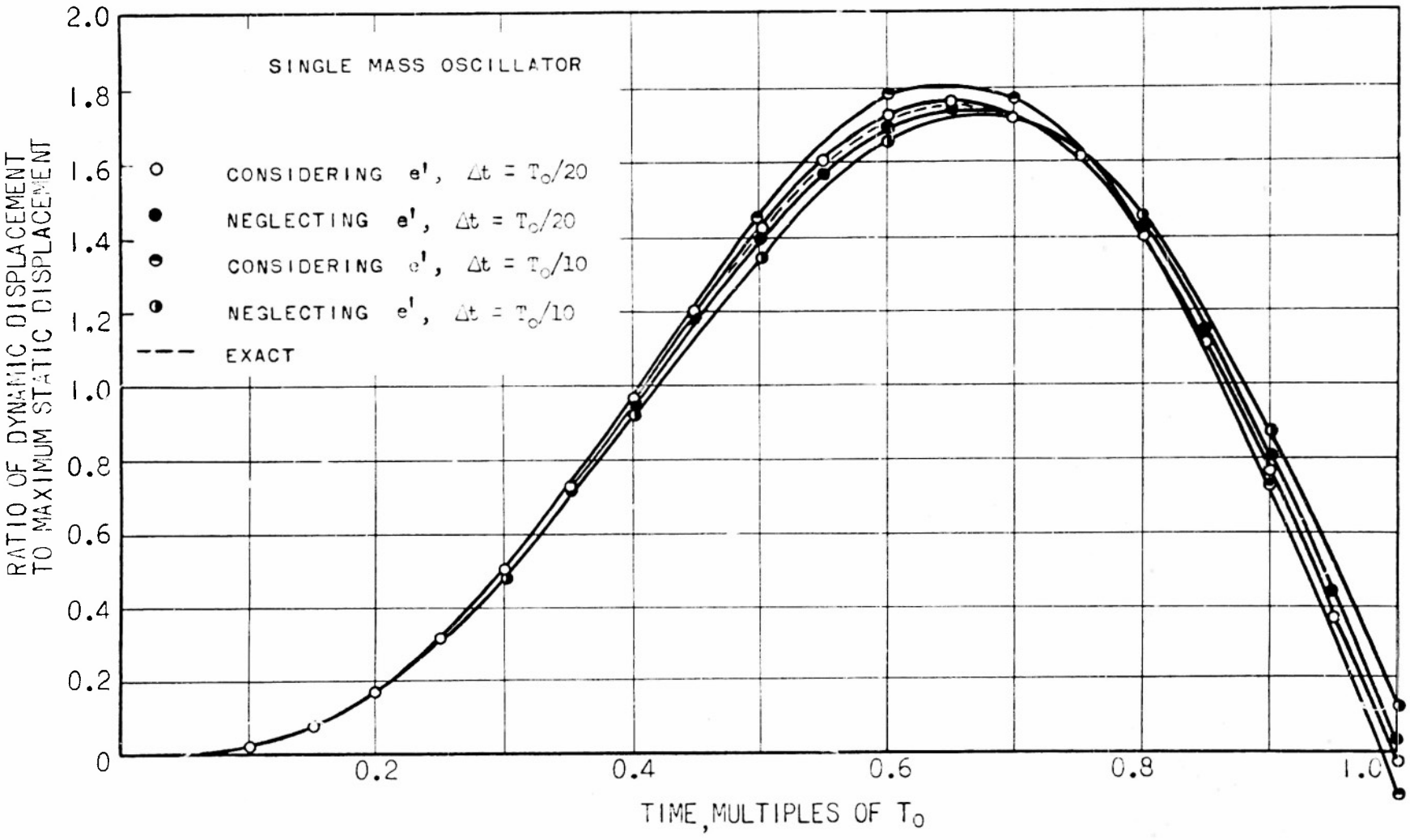

FIG. 18 DISPLACEMENT—TIME RELATIONSHIP FOR SINGLE MASS OSCILLATOR

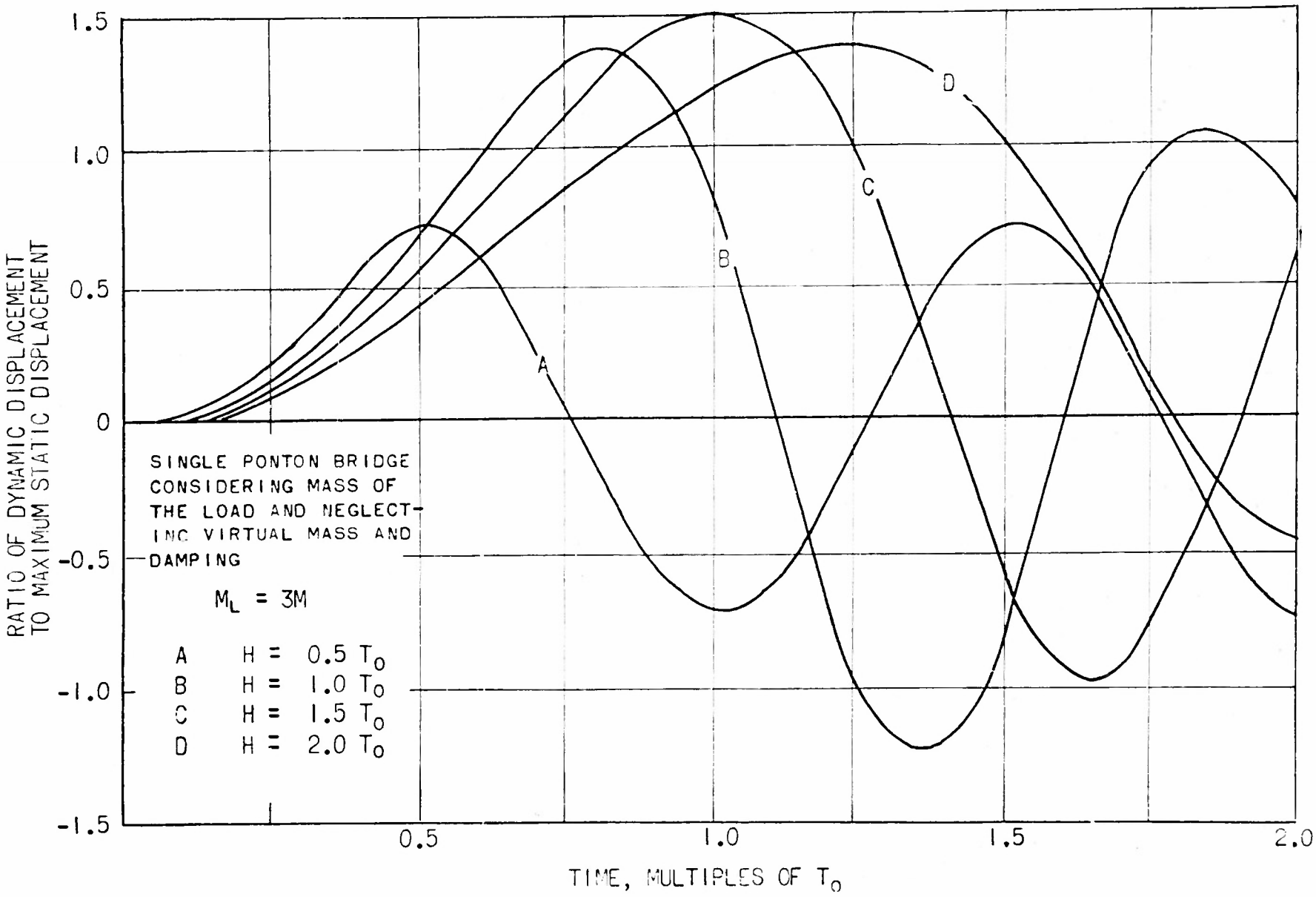

FIG. 20 DISPLACEMENT—TIME RELATIONSHIP FOR SINGLE PONTON BRIDGE CONSIDERING MASS OF THE LOAD

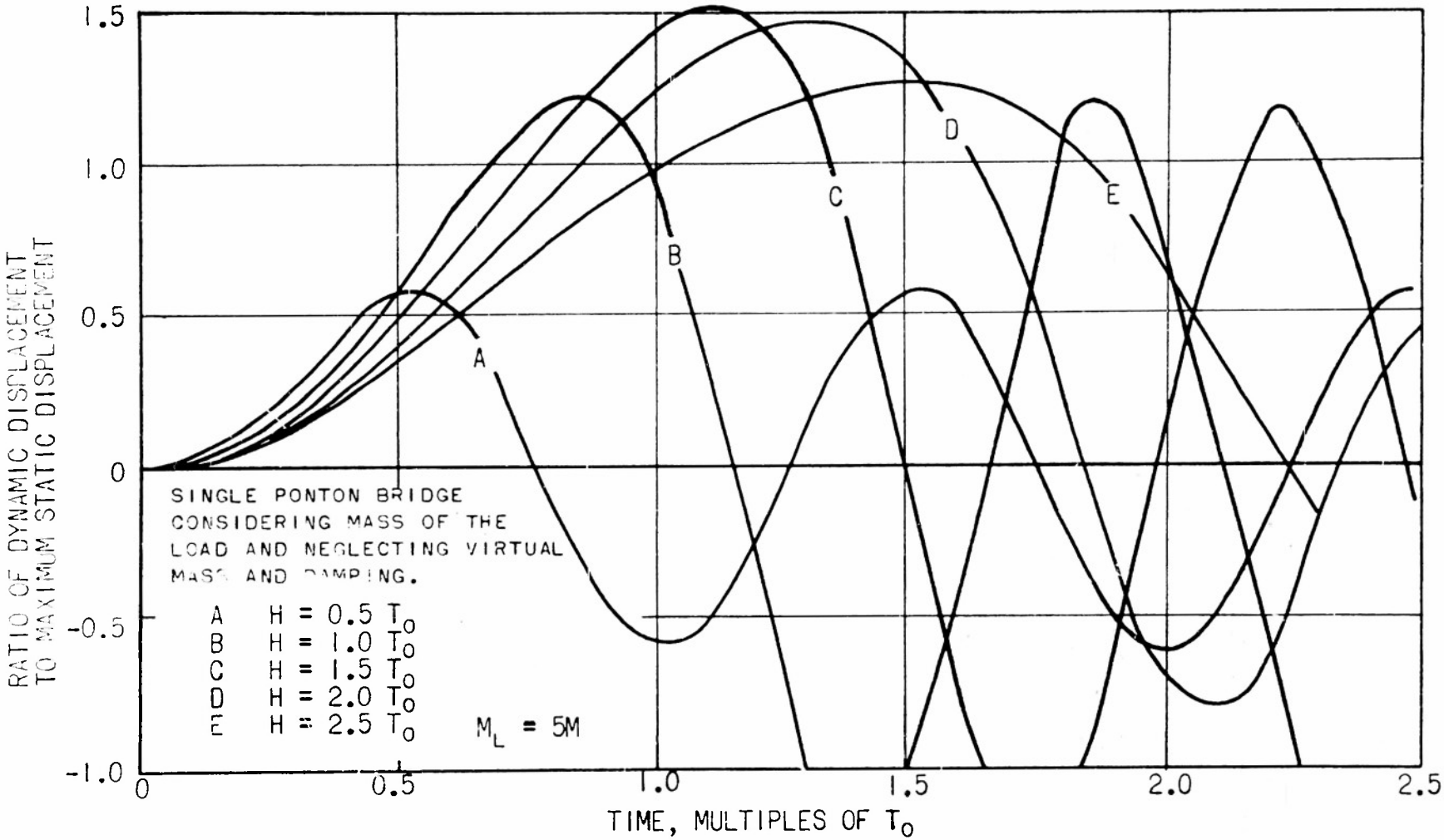

FIG. 21 DISPLACEMENT—TIME RELATIONSHIP FOR SINGLE PONTON BRIDGE CONSIDERING MASS OF THE LOAD

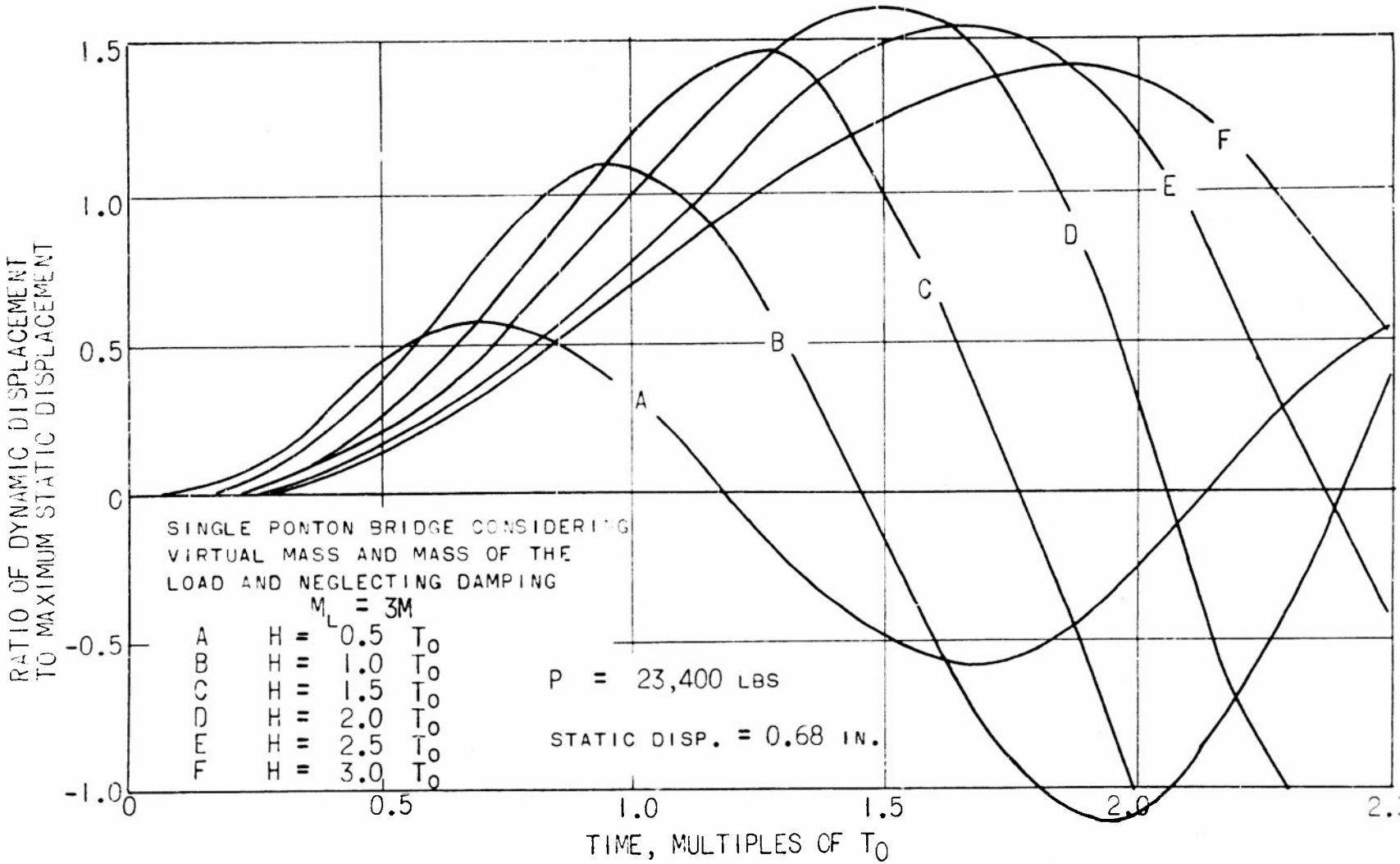

FIG. 22 DISPLACEMENT--TIME RELATIONSHIP FOR SINGLE PONTON BRIDGE CONSIDERING VITRUAL MASS AND MASS OF THE LOAD

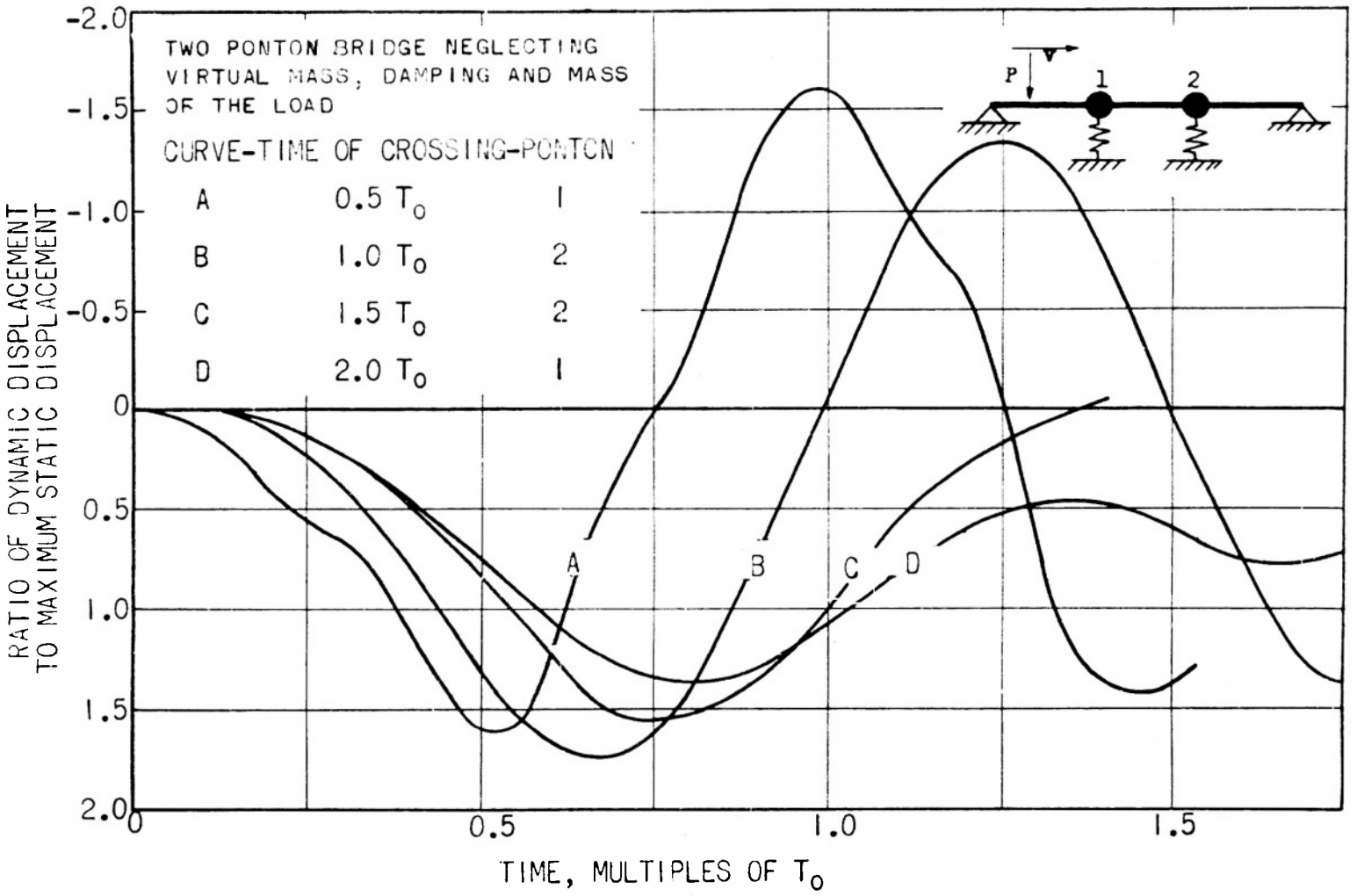

FIG. 24 DISPLACEMENT—TIME RELATIONSHIP FOR TWO PONTON BRIDGE

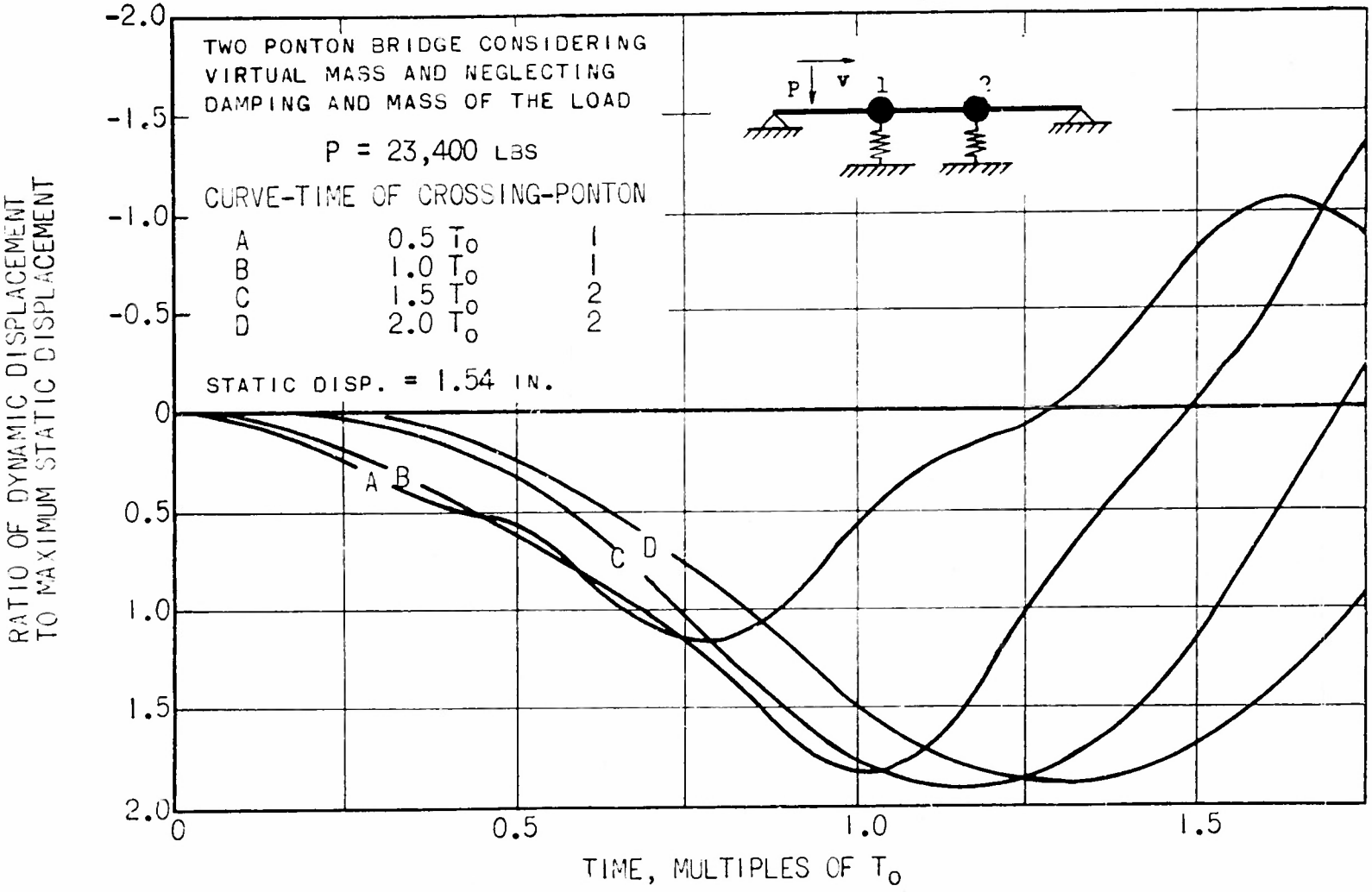

FIG. 25 DISPLACEMENT—TIME RELATIONSHIP FOR TWO PONTON BRIDGE CONSIDERING VIRTUAL MASS

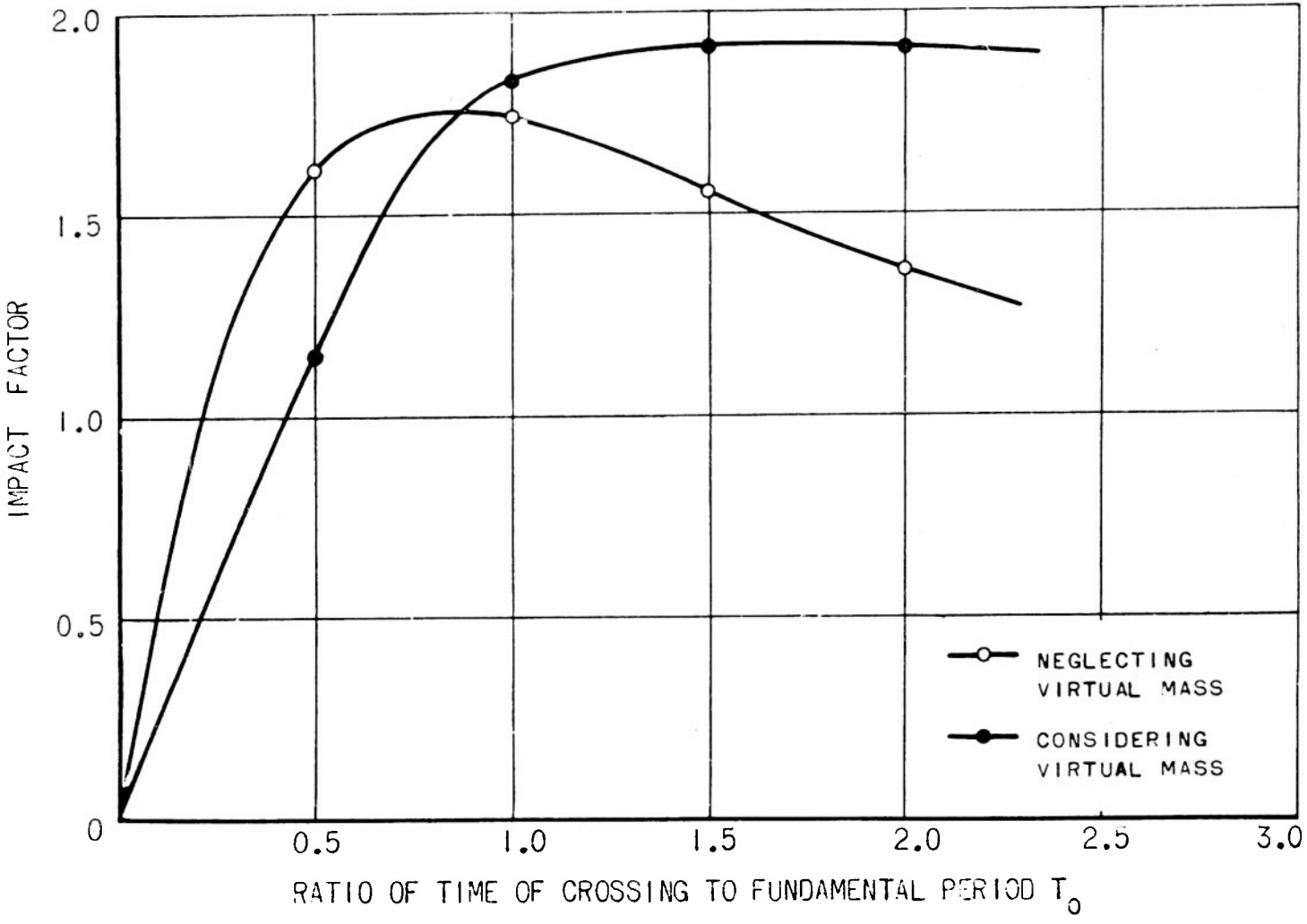

FIG. 25A RELATIONSHIP BETWEEN IMPACT FACTOR AND TIME OF CROSSING FOR TWO PONTON BRIDGE

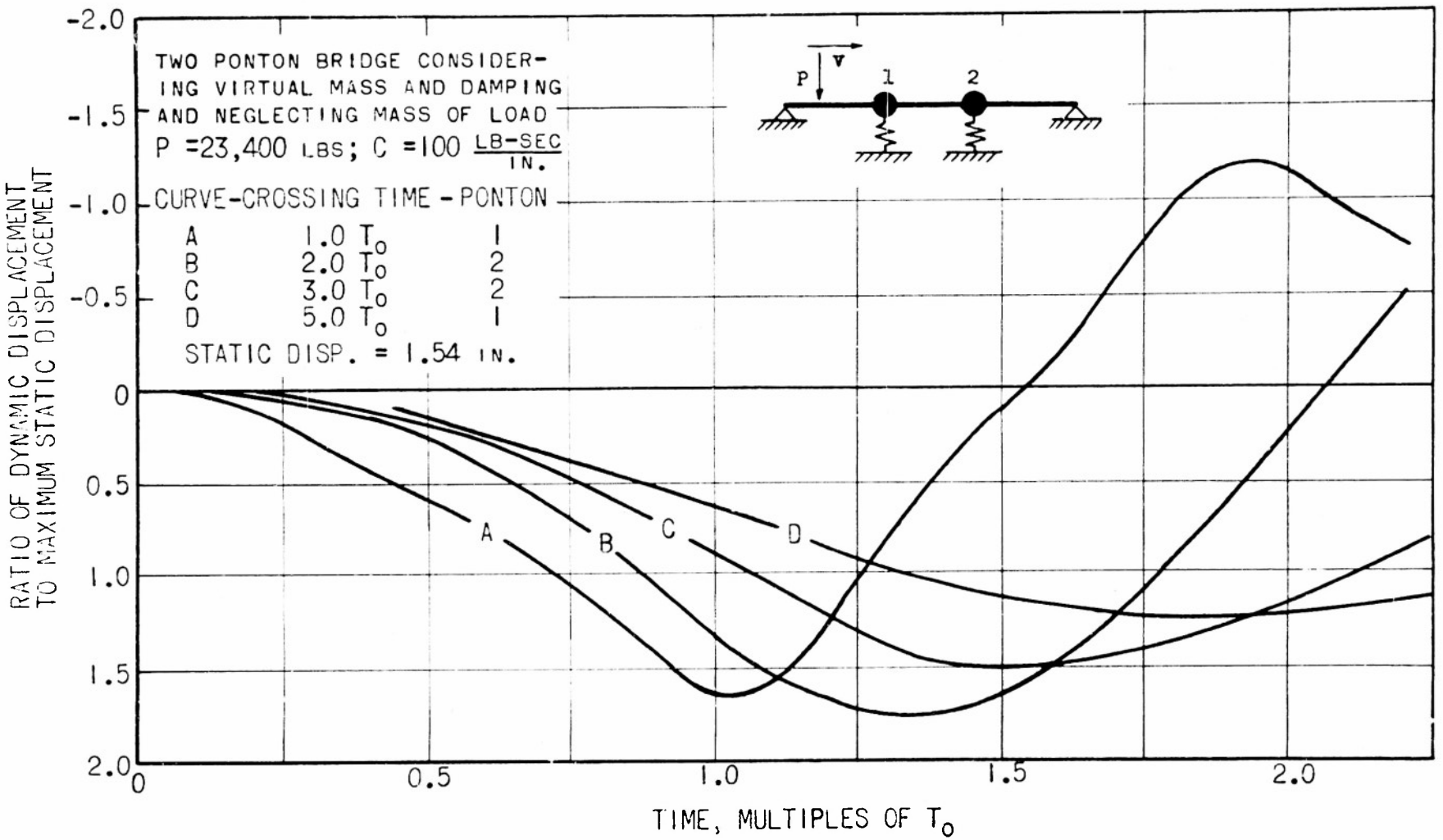

FIG. 26 DISPLACEMENT—TIME RELATIONSHIP FOR TWO PONTON BRIDGE CONSIDERING VIRTUAL MASS AND DAMPING, C = 100 LB-SEC/IN.

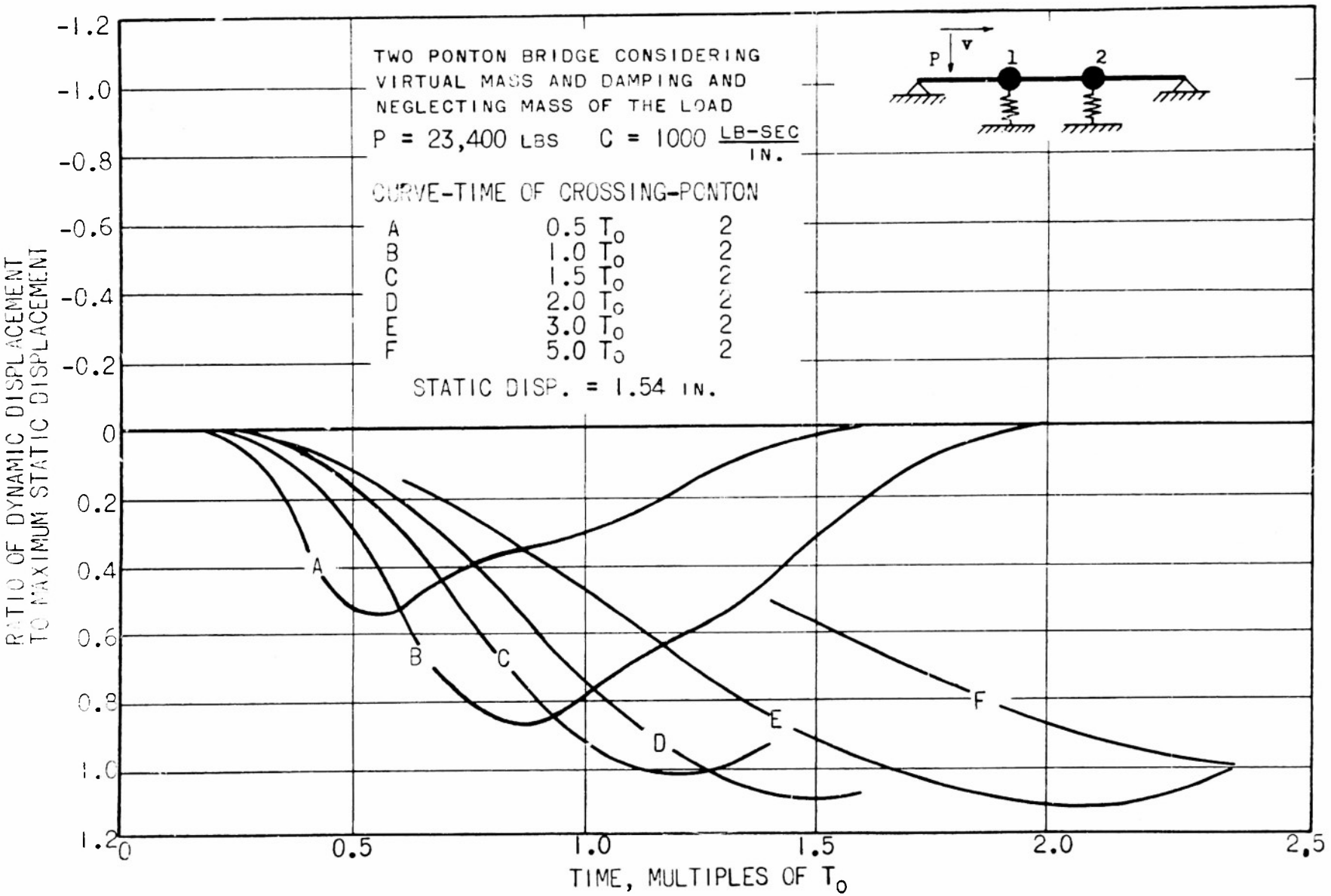

FIG. 27 DISPLACEMENT—TIME RELATIONSHIP FOR TWO PONTON BRIDGE CONSIDERING VIRTUAL MASS AND DAMPING, C= 1000 LB-SEC/IN.

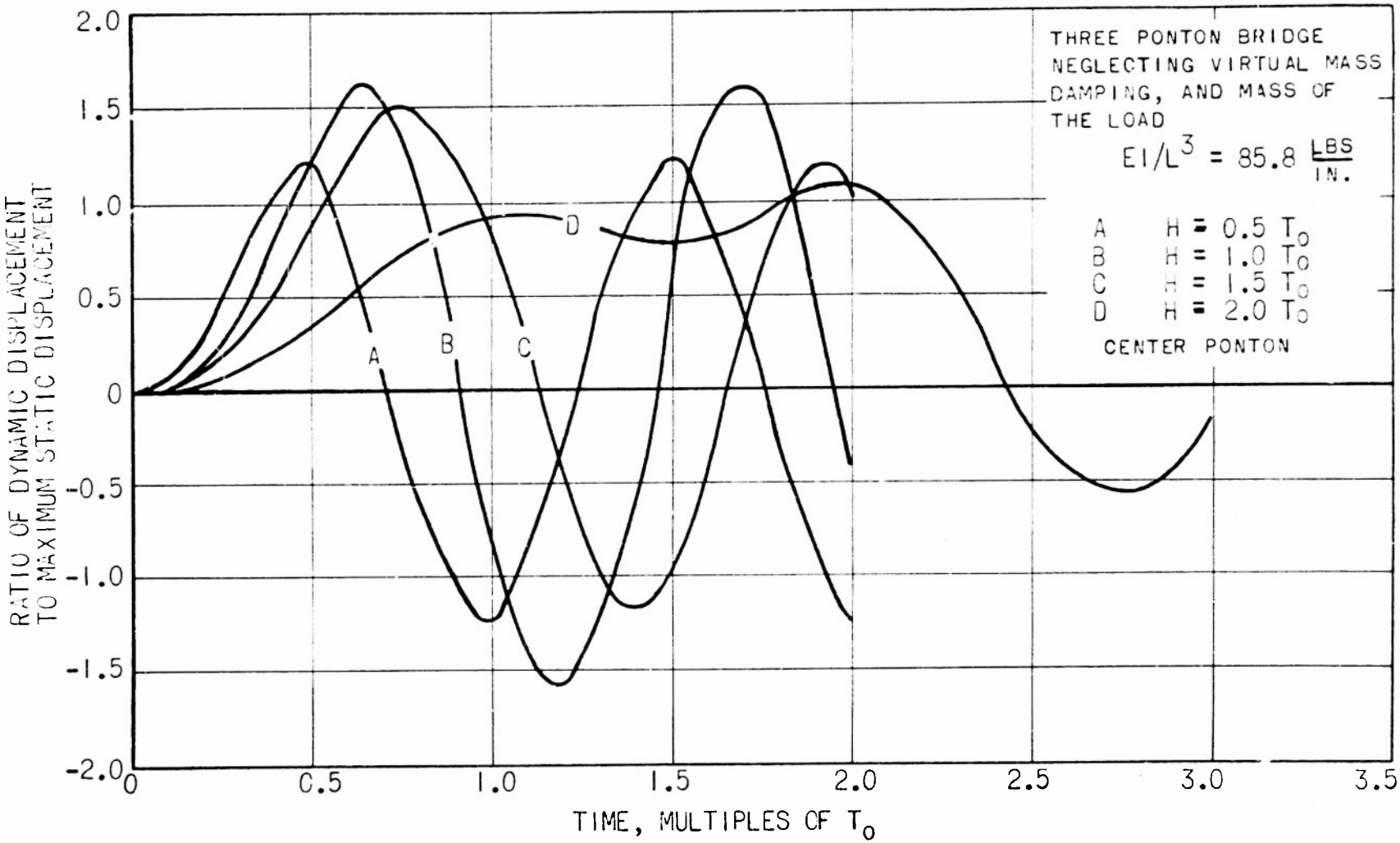

FIG. 29 DISPLACEMENT—TIME RELATIONSHIP FOR THREE PONTON BRIDGE, $EI/L^3 = 85.8 \frac{LB}{IN.}$

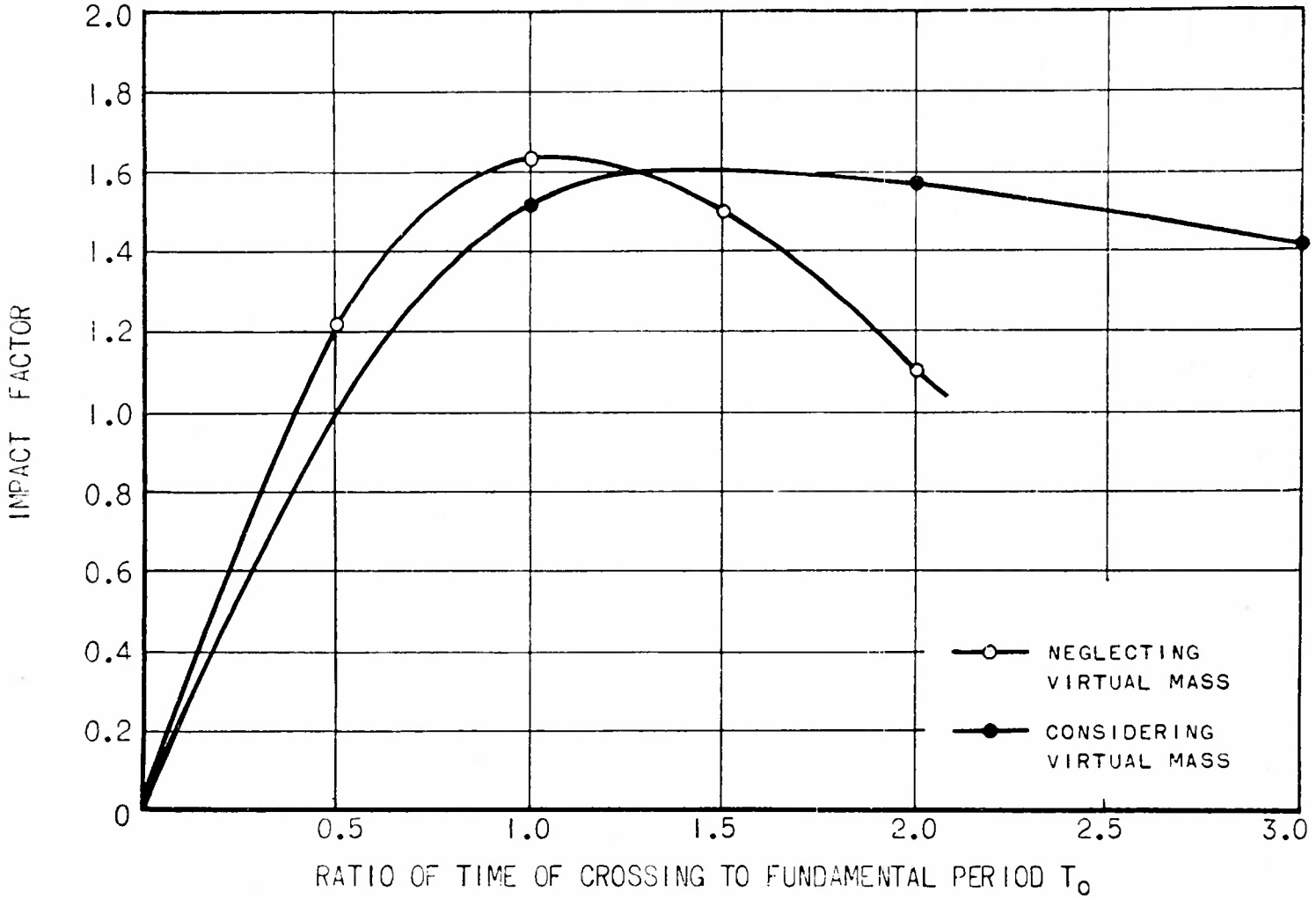

FIG. 29A RELATIONSHIP BETWEEN IMPACT FACTOR AND TIME OF CROSSING FOR THREE PONTON BRIDGE

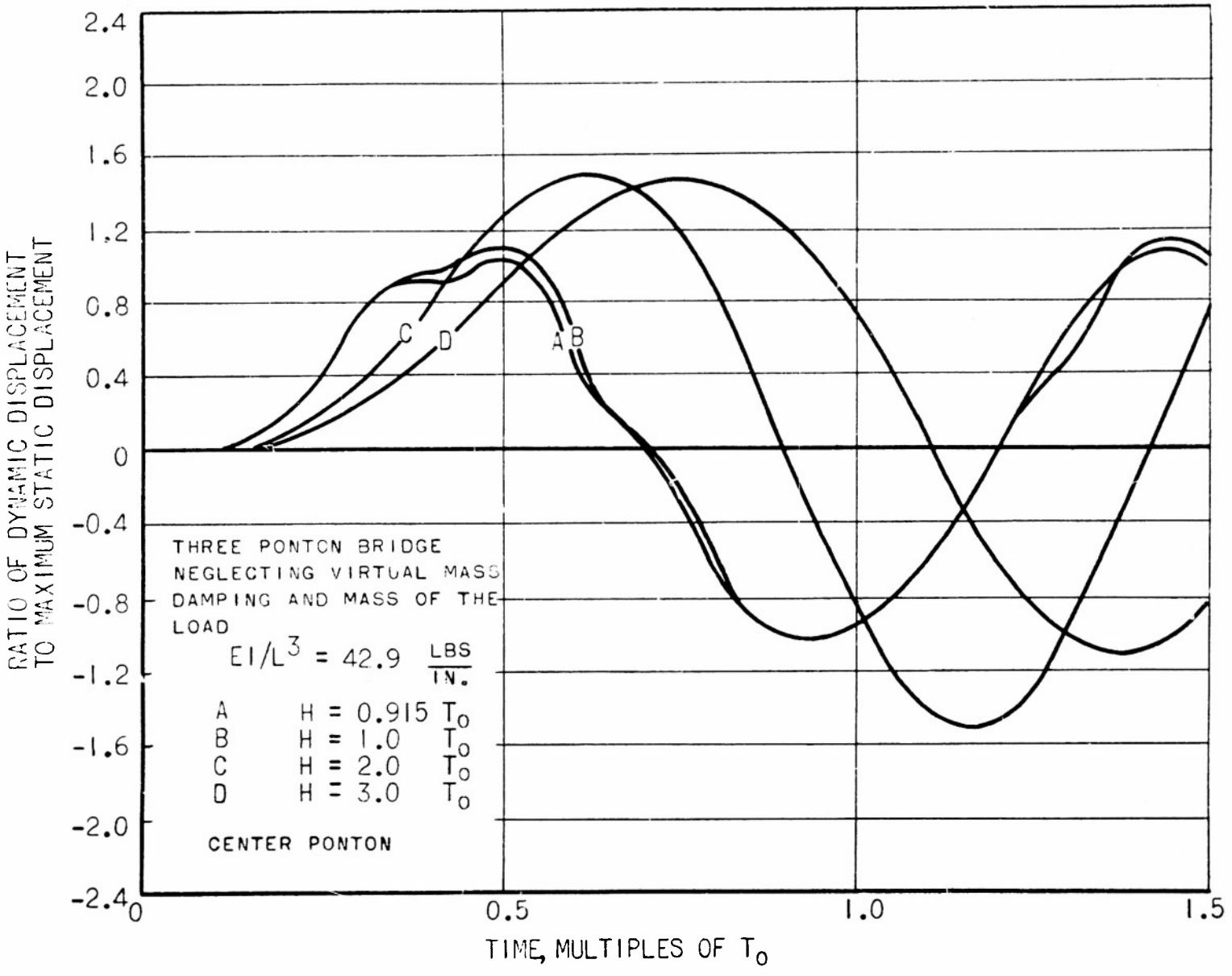

FIG. 30 DISPLACEMENT—TIME RELATIONSHIP FOR A THREE PONTON BRIDGE, $EI/L^3 = 42.9 \frac{LB}{IN.}$

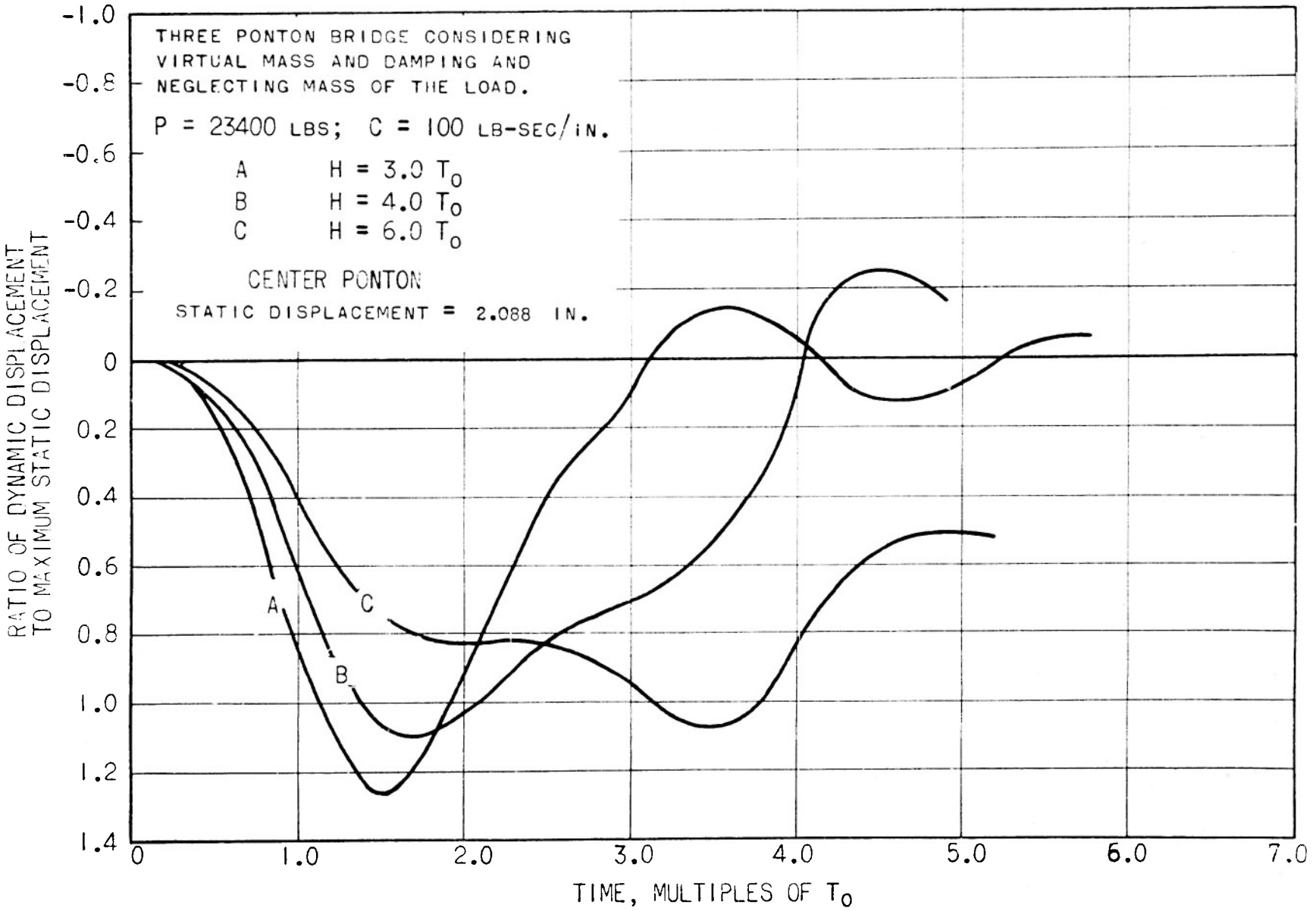

FIG. 31 DISPLACEMENT—TIME RELATIONSHIP FOR THREE PONTON BRIDGE CONSIDERING VIRTUAL MASS AND DAMPING, C = 100 LB-SEC PER IN

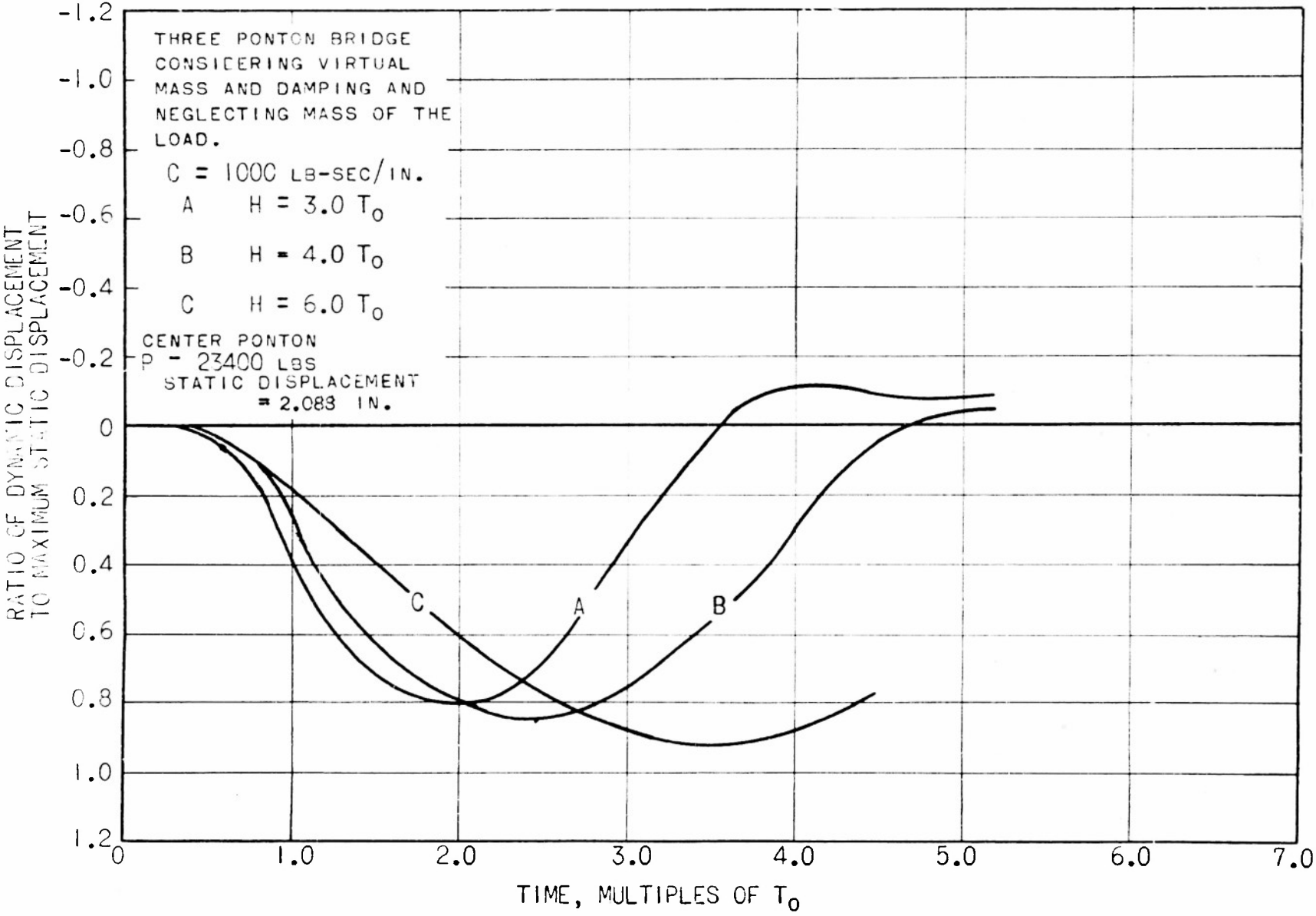

FIG. 32 DISPLACEMENT—TIME RELATIONSHIP FOR THREE PONTON BRIDGE CONSIDERING VIRTUAL MASS AND DAMPING, C = 1000 LB-SEC PER IN

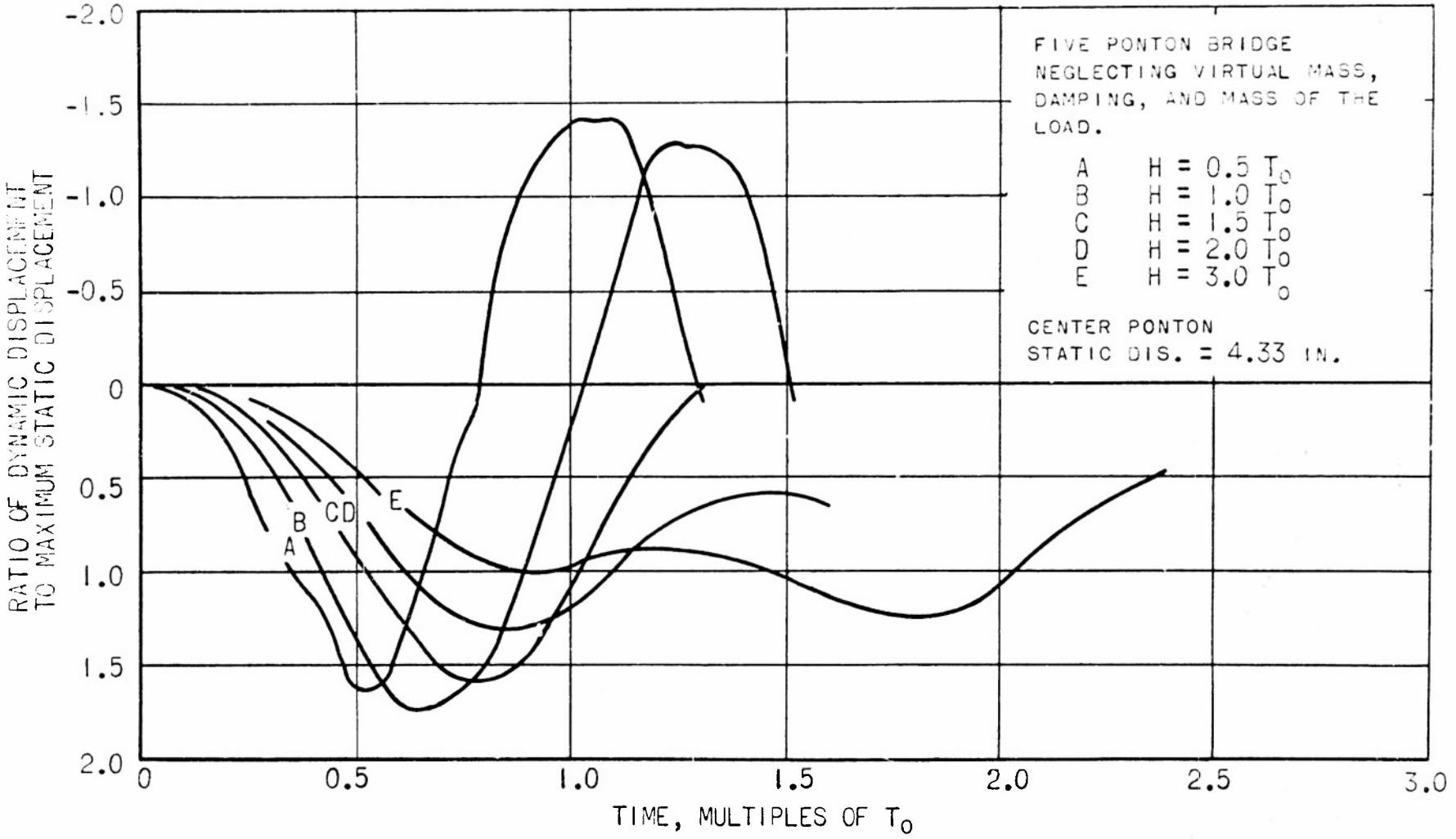

FIG 33 DISPLACEMENT—TIME RELATIONSHIP FOR FIVE PONTON BRIDGE

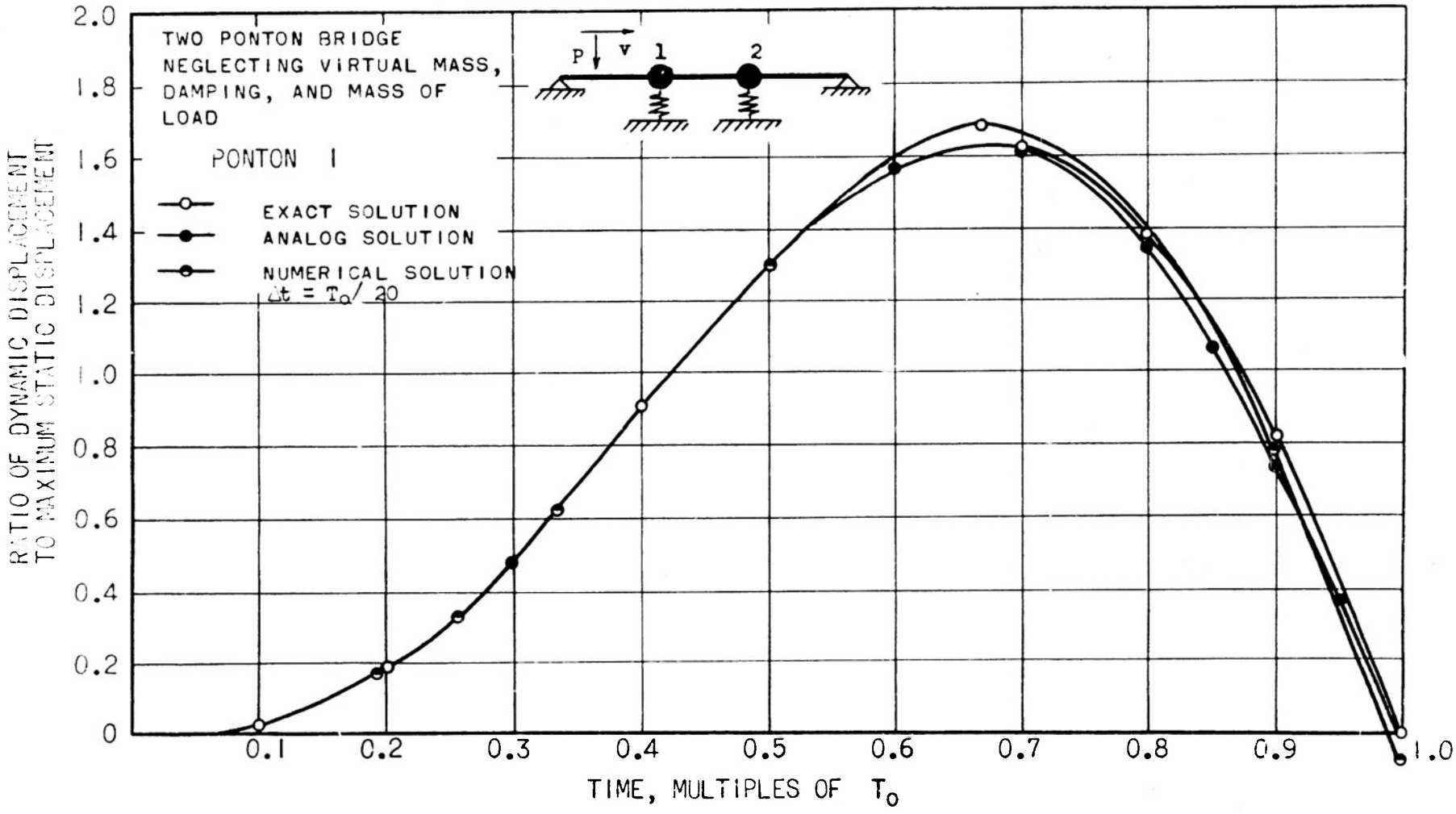

FIG 34 COMPARISON OF NUMERICAL, EXACT, AND ANALOG SOLUTIONS FOR A TWO PONTON BRIDGE

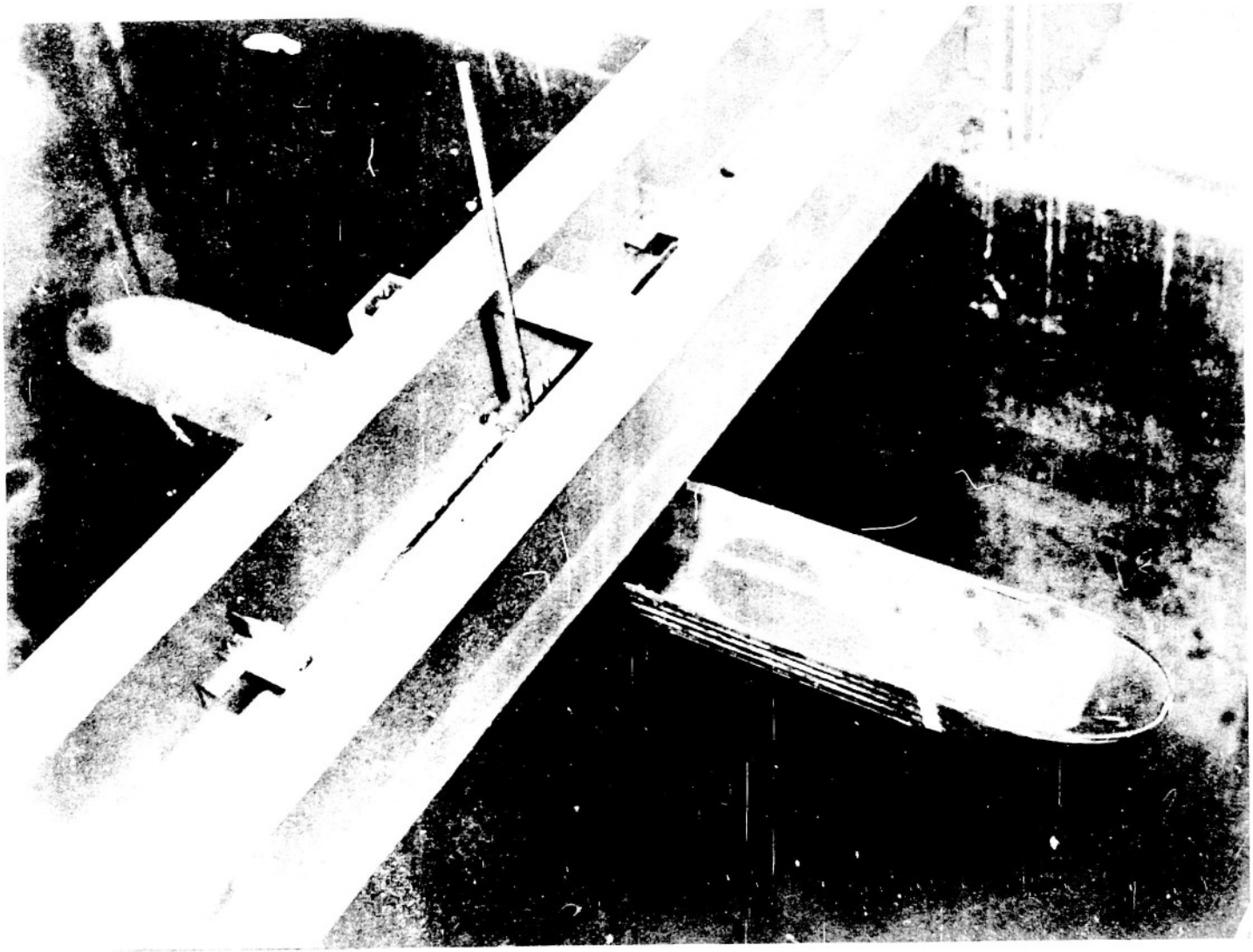

FIG. 35 VIRTUAL MASS APPARATUS

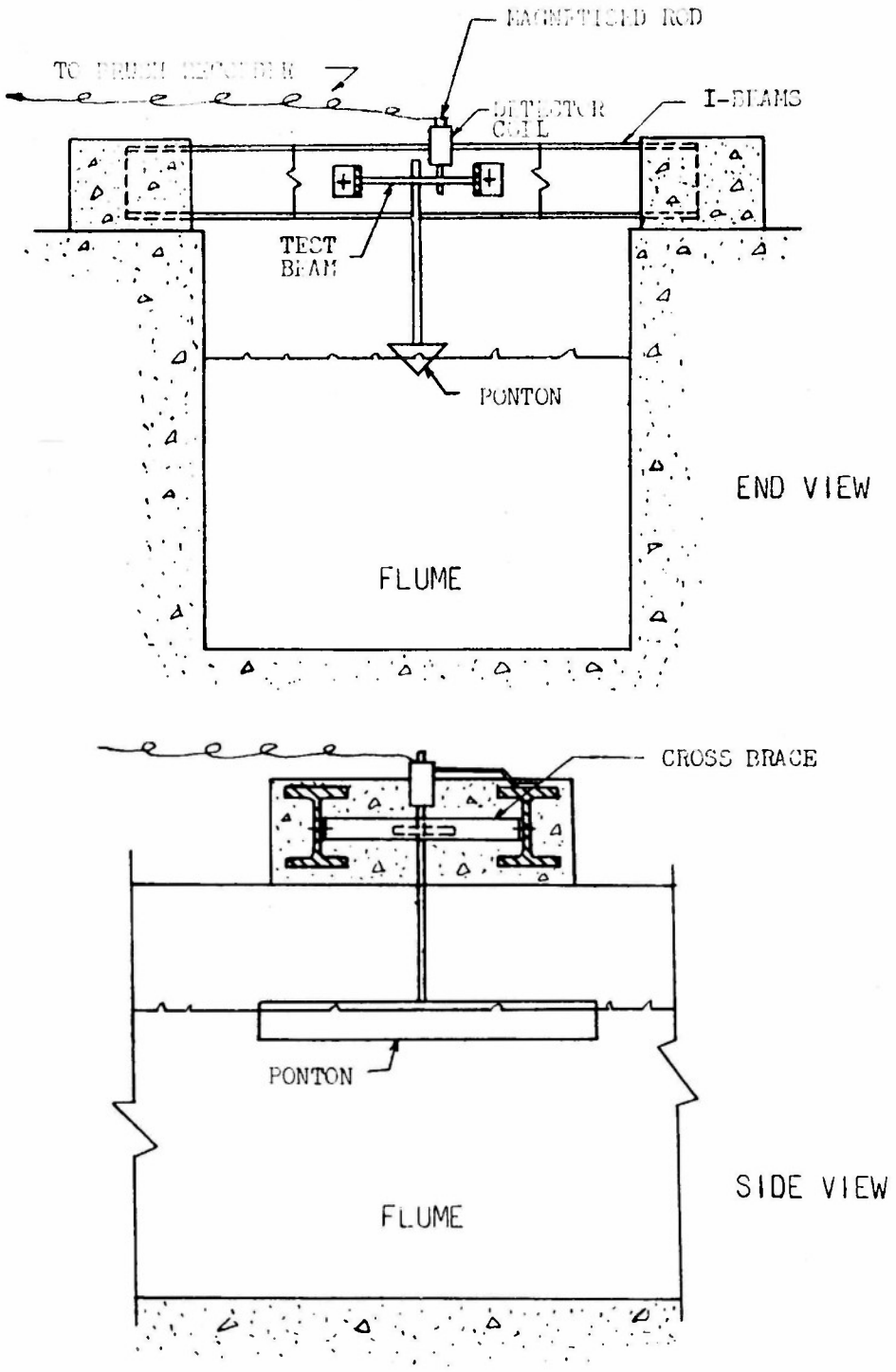

FIG. 36 SCHEMATIC DIAGRAM OF VIRTUAL MASS APPARATUS

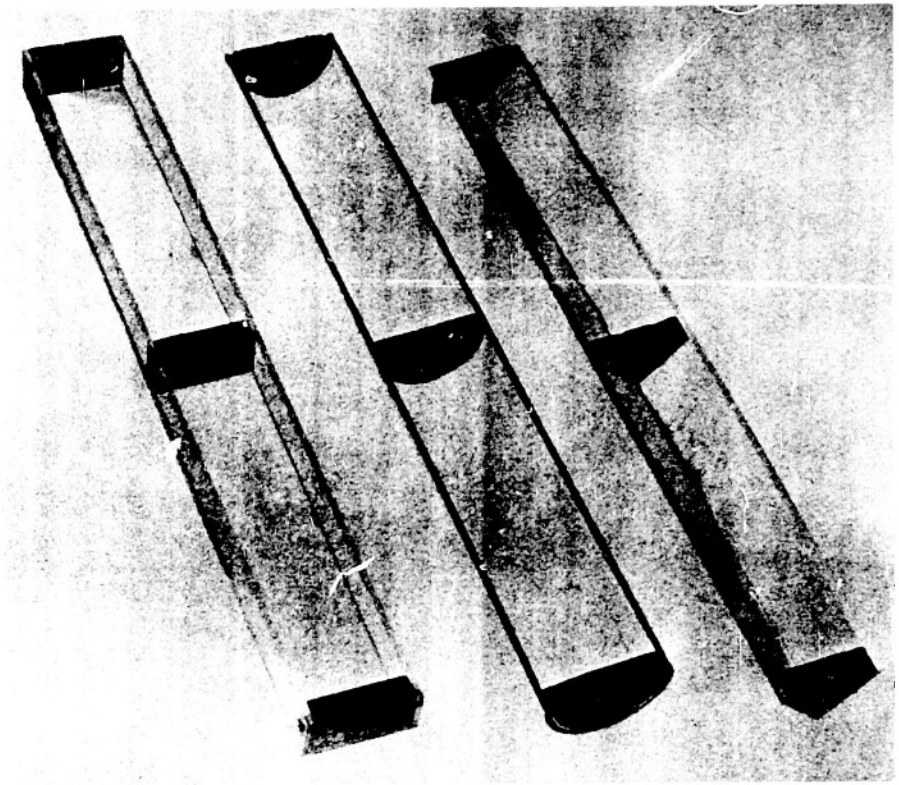

FIG. 37 TEST PONTONS

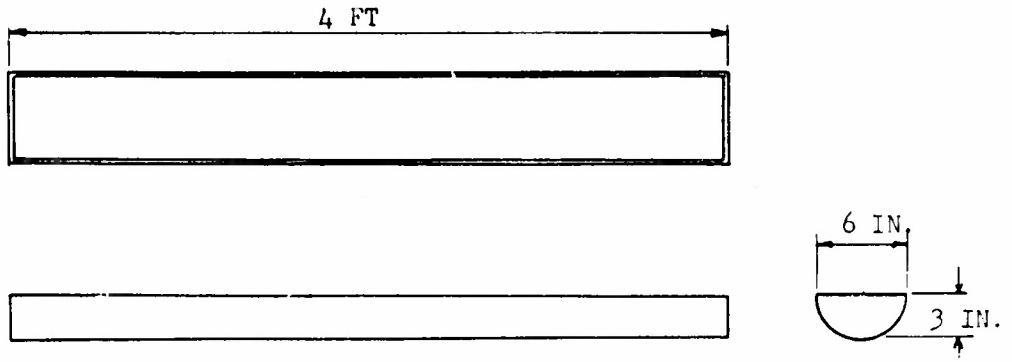

(a) CIRCULAR PONTON

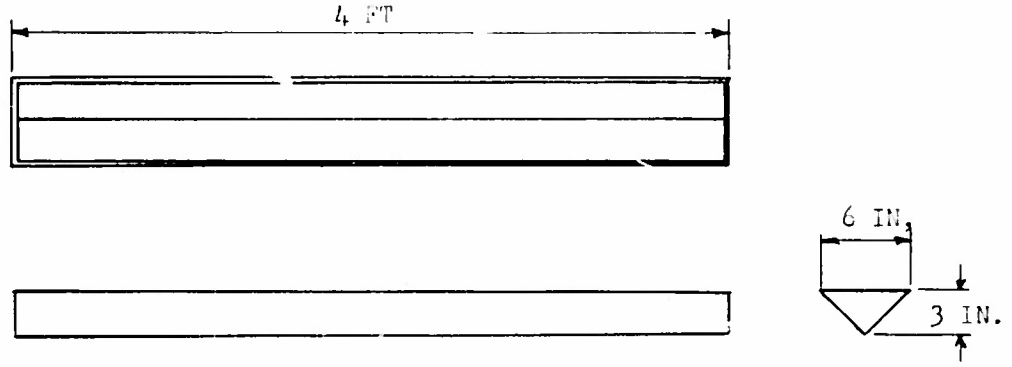

(b) TRIANGULAR PONTON

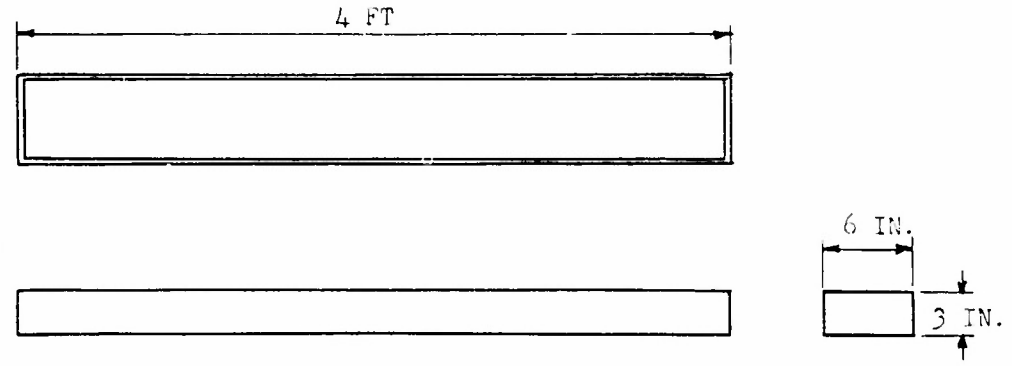

(c) RECTANGULAR PONTON

FIG. 38 SCHEMATIC DIAGRAM OF TEST PONTONS

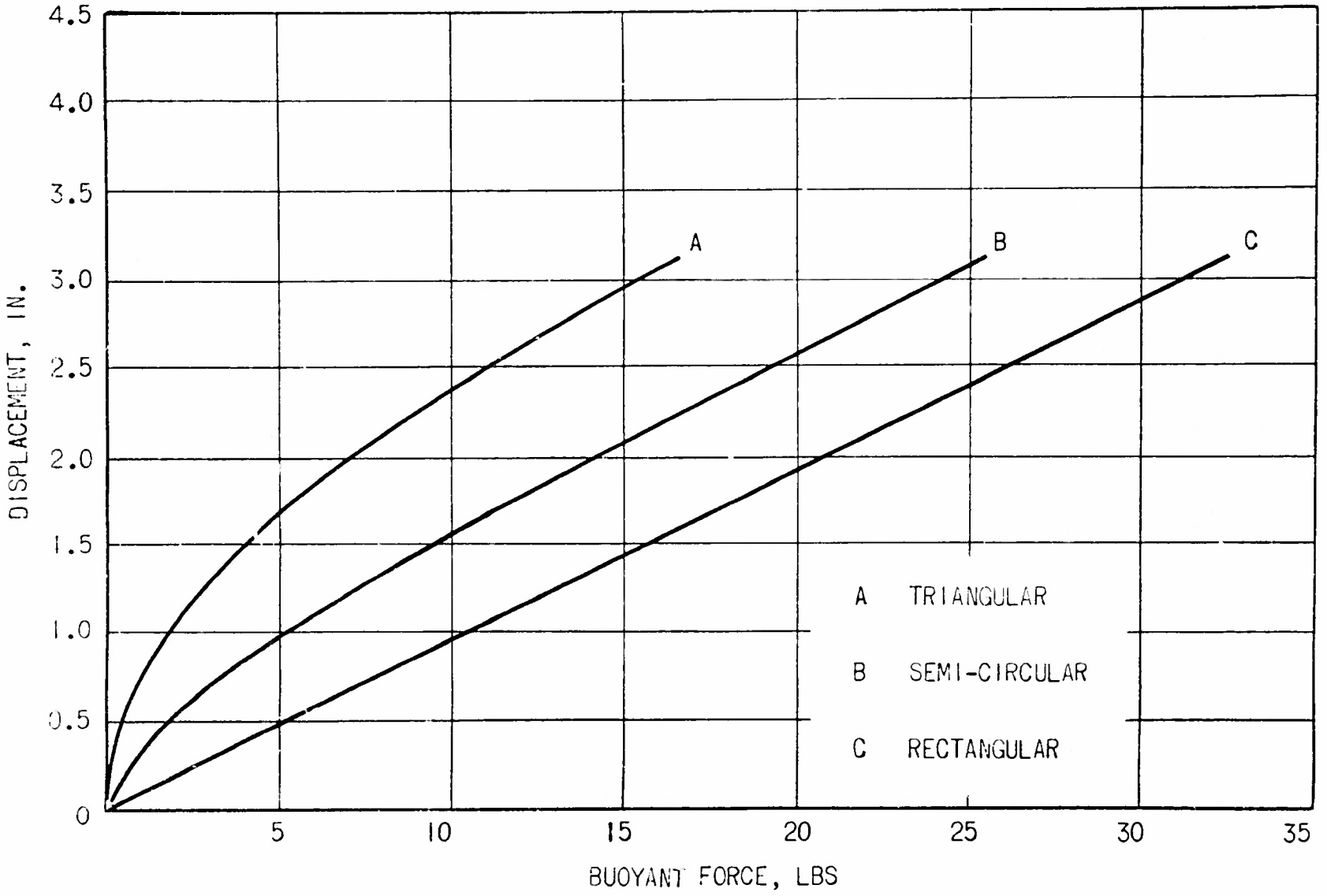

FIG. 39 BUOYANT FORCE—DISPLACEMENT RELATIONSHIP FOR TEST PONTONS

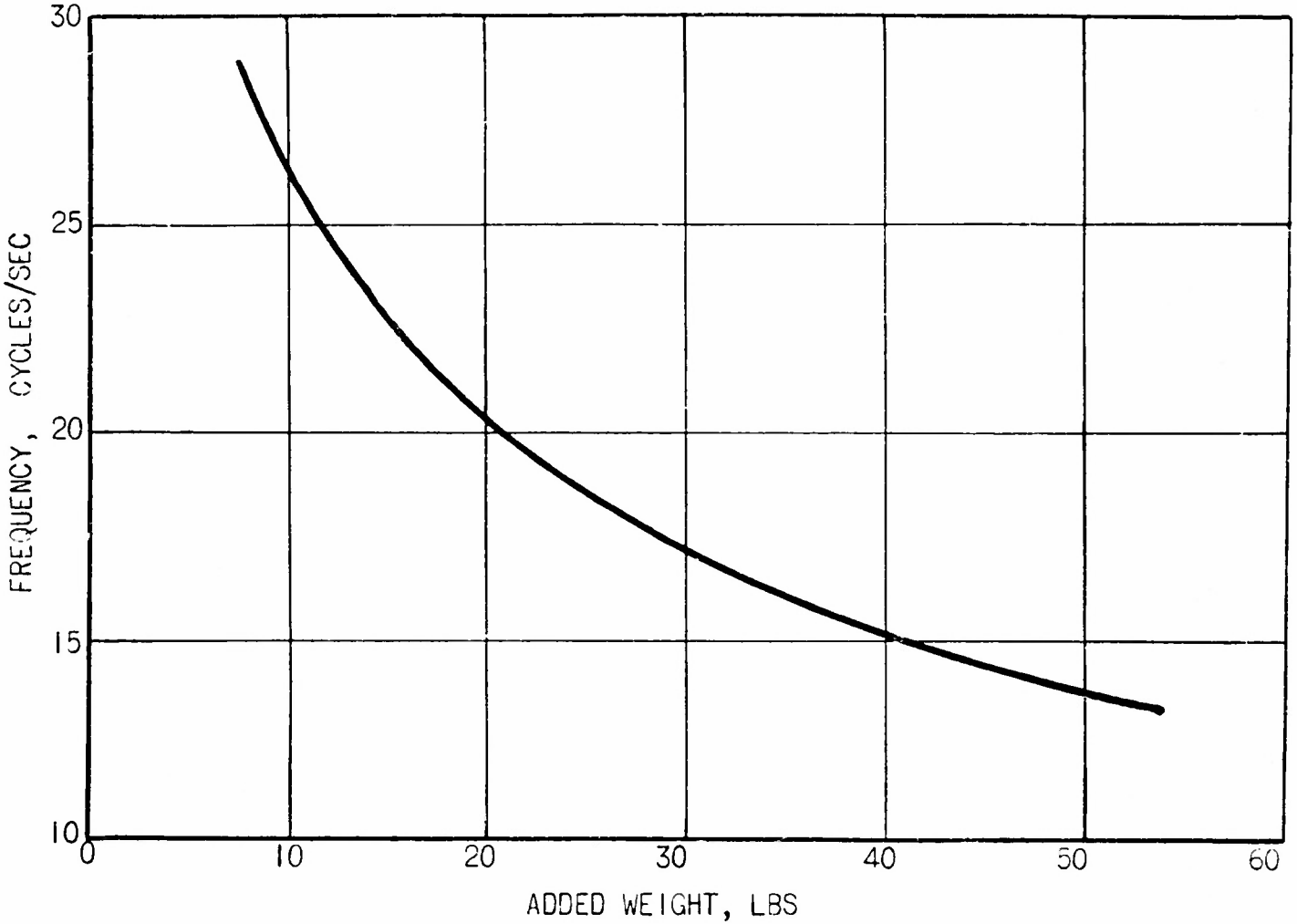

FIG. 40 CALIBRATION CURVE OF TEST BEAM

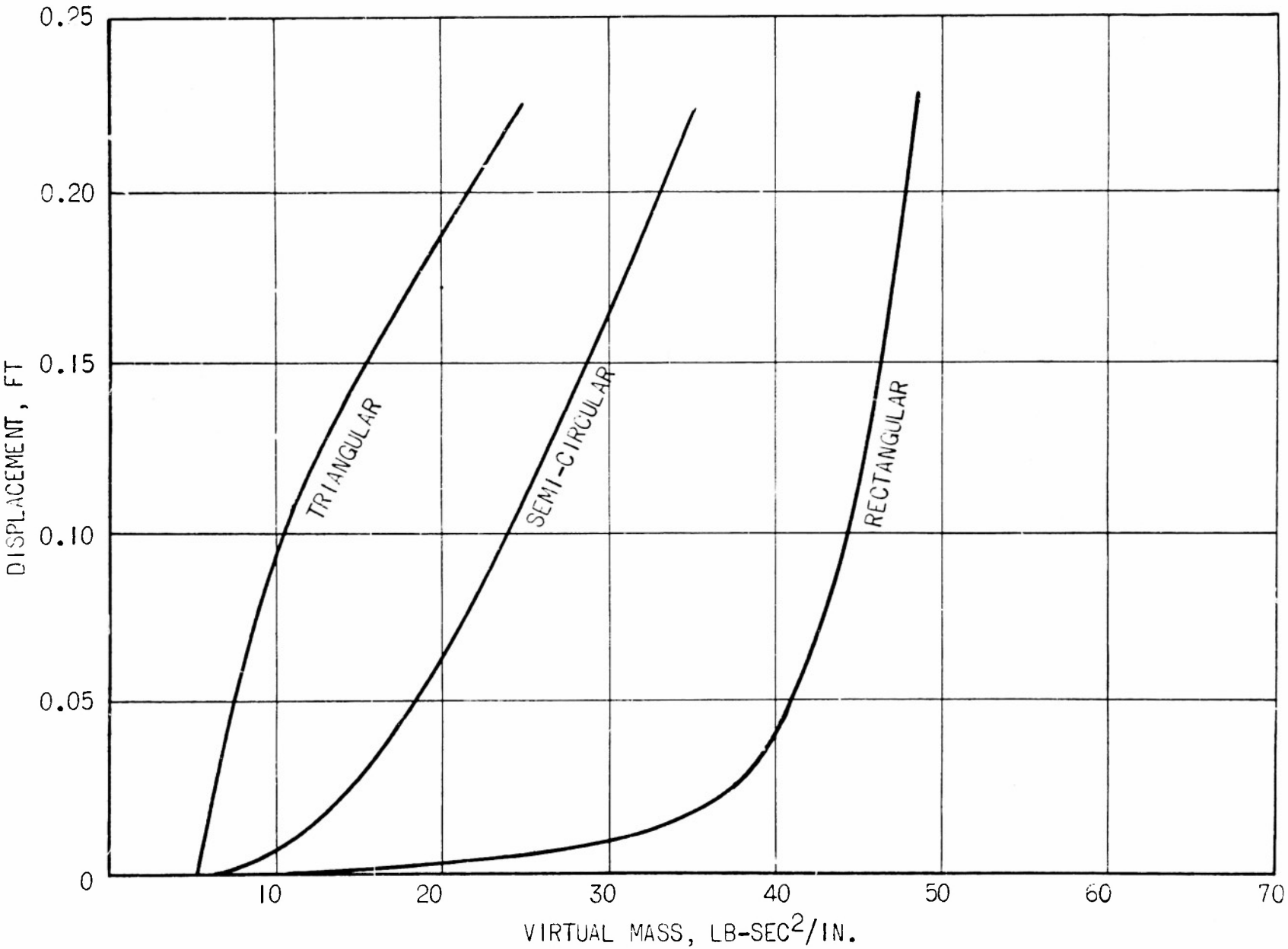

FIG. 41 VIRTUAL MASS—DISPLACEMENT RELATIONSHIP FOR TEST PONTONS

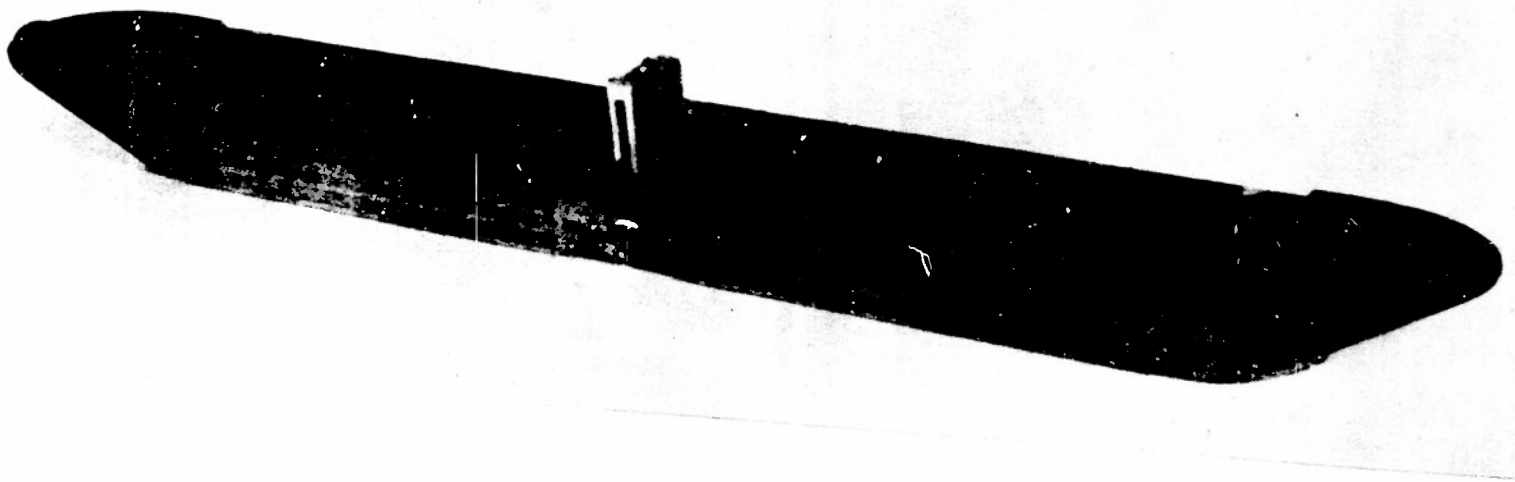

FIG. 42 MODEL OF M-4 MILITARY PONTON

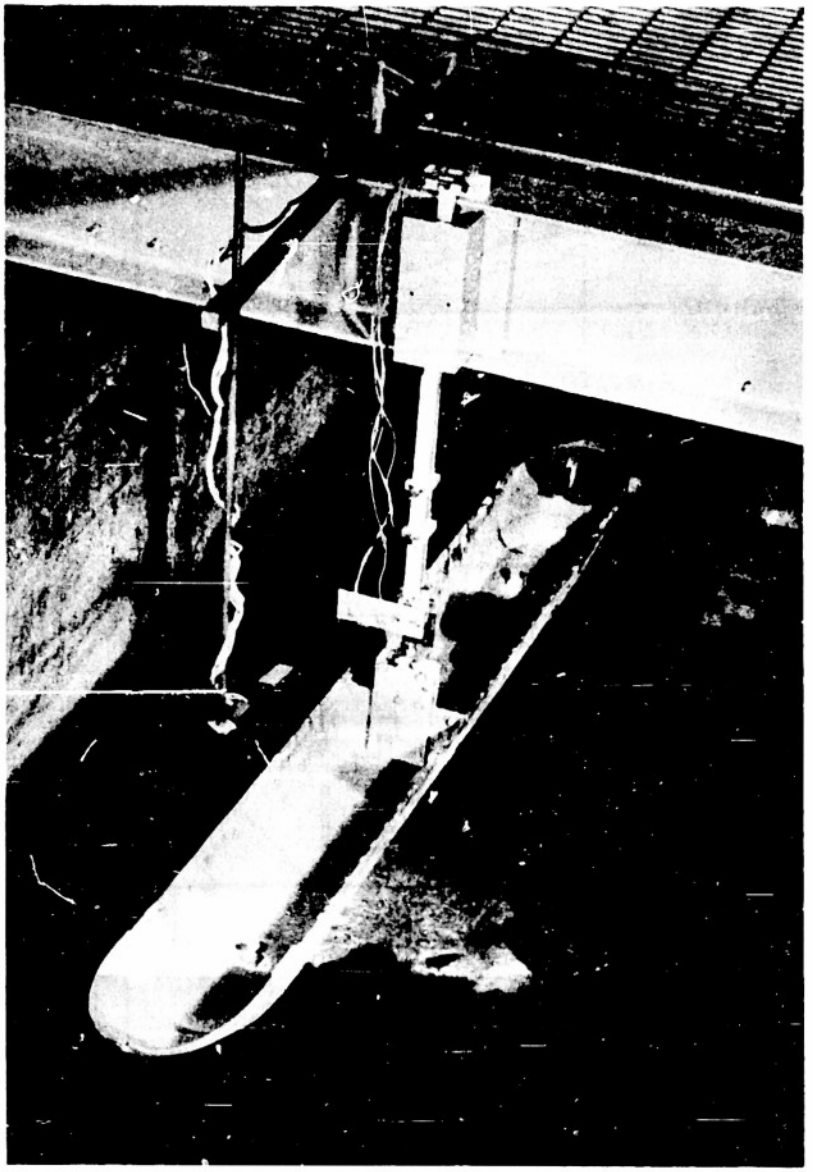

FIG. 43 IMPULSE-DISPLACEMENT APPARATUS

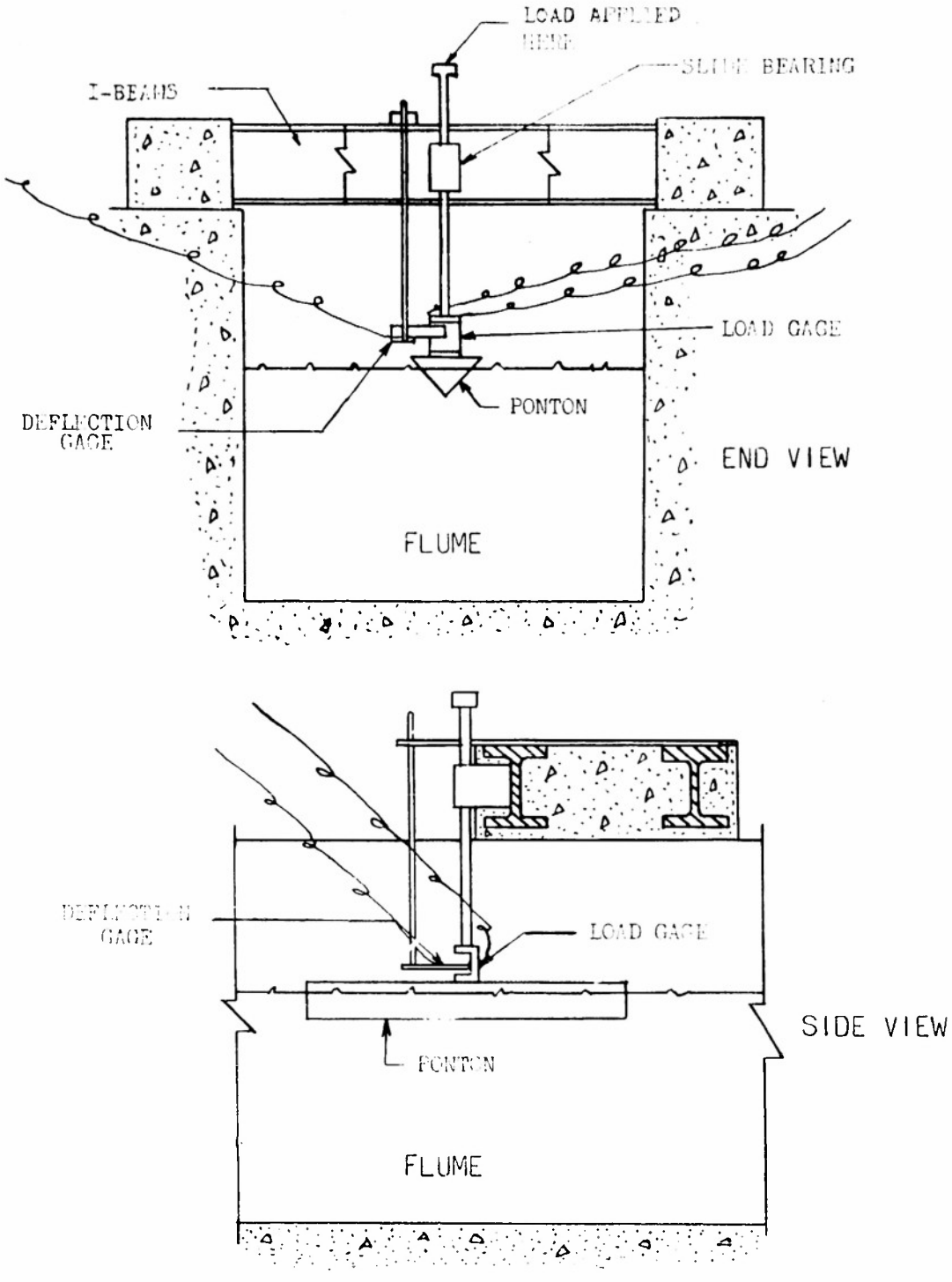

FIG. 44 SCHEMATIC DIAGRAM OF IMPULSE—DEFLECTION APPARATUS

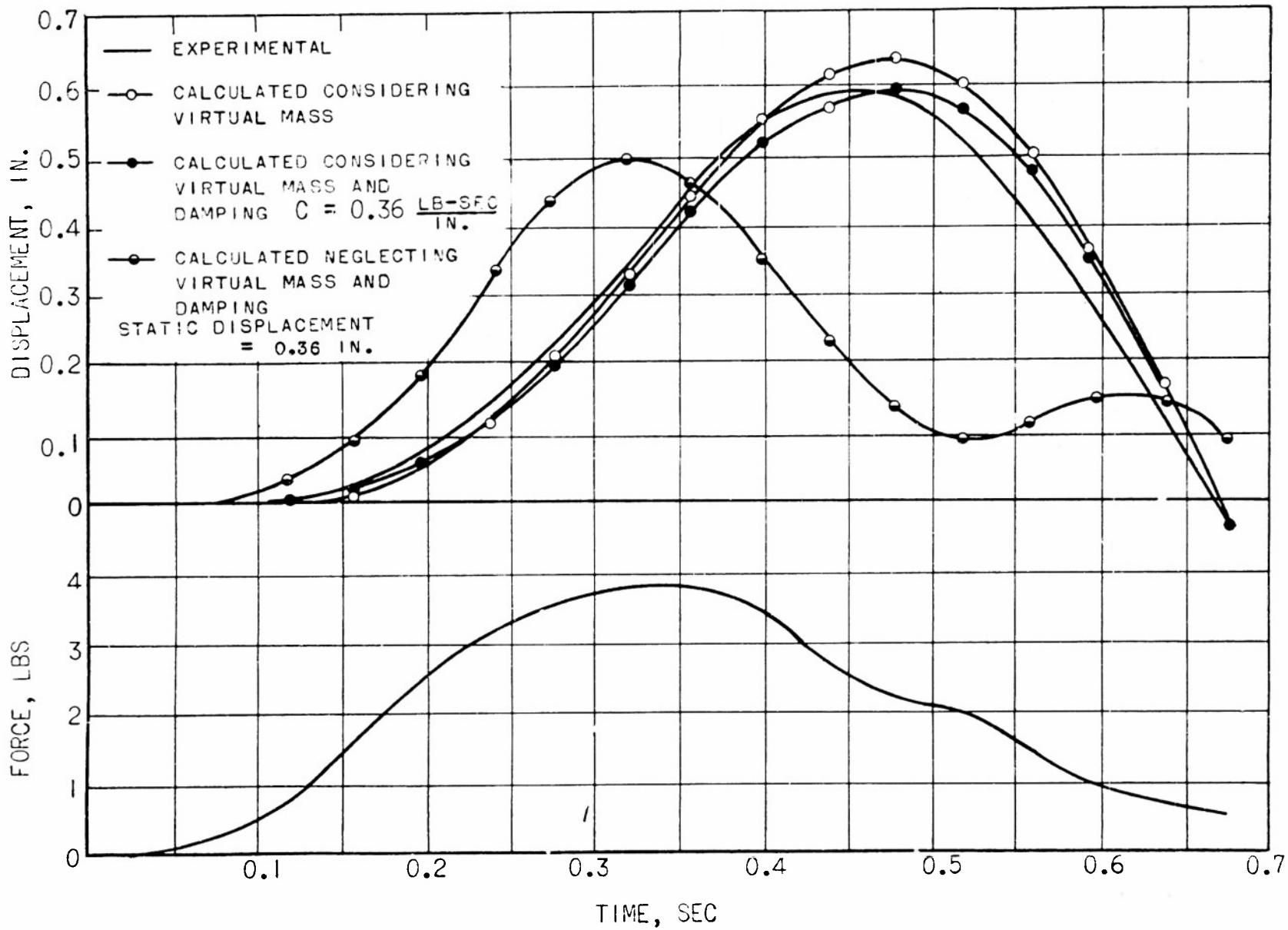

FIG. 45 RESULTS OF IMPULSE—DISPLACEMENT TEST ON RECTANGULAR PONTON

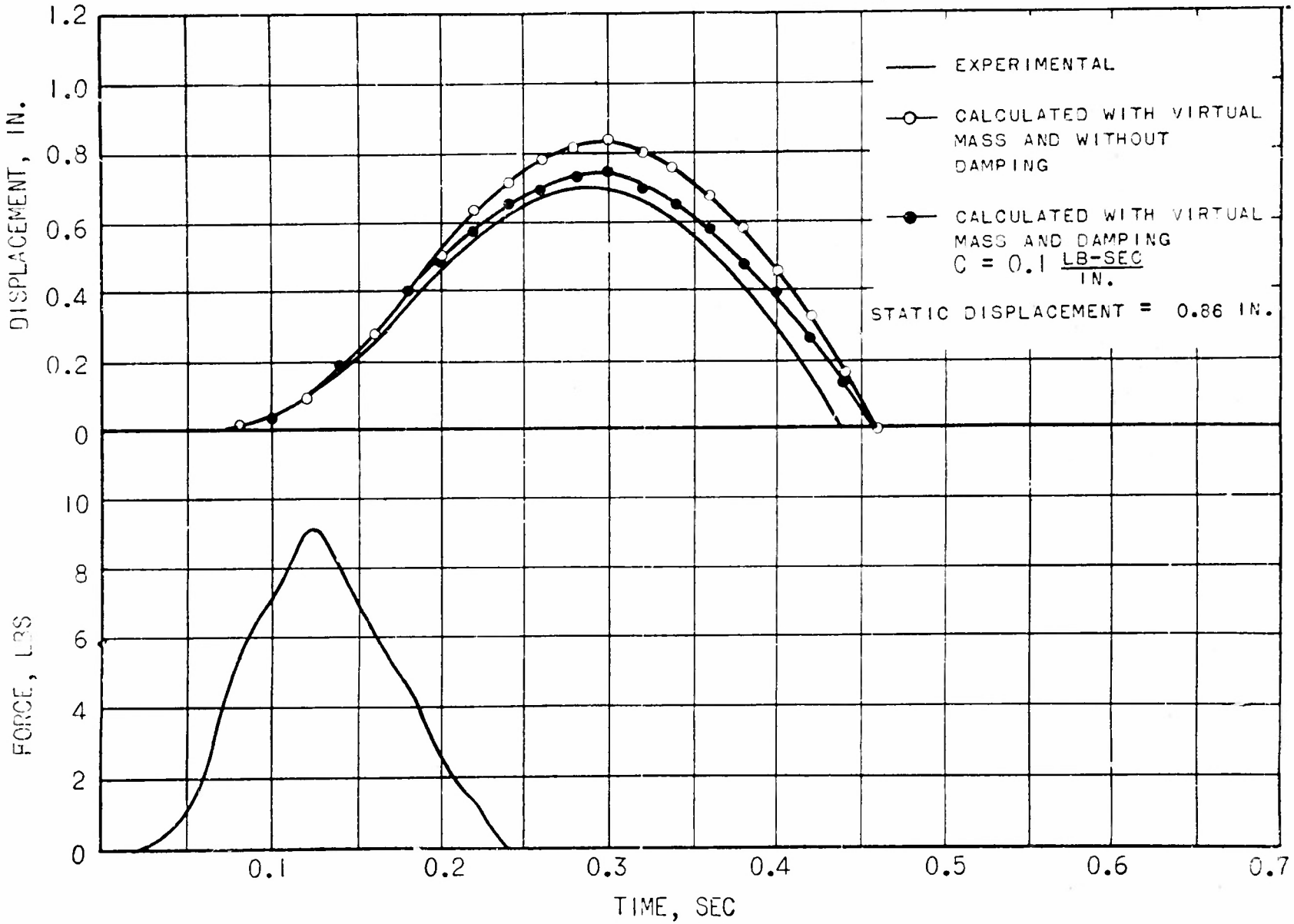

FIG. 46 RESULTS OF IMPULSE—DISPLACEMENT TEST ON RECTANGULAR PONTON

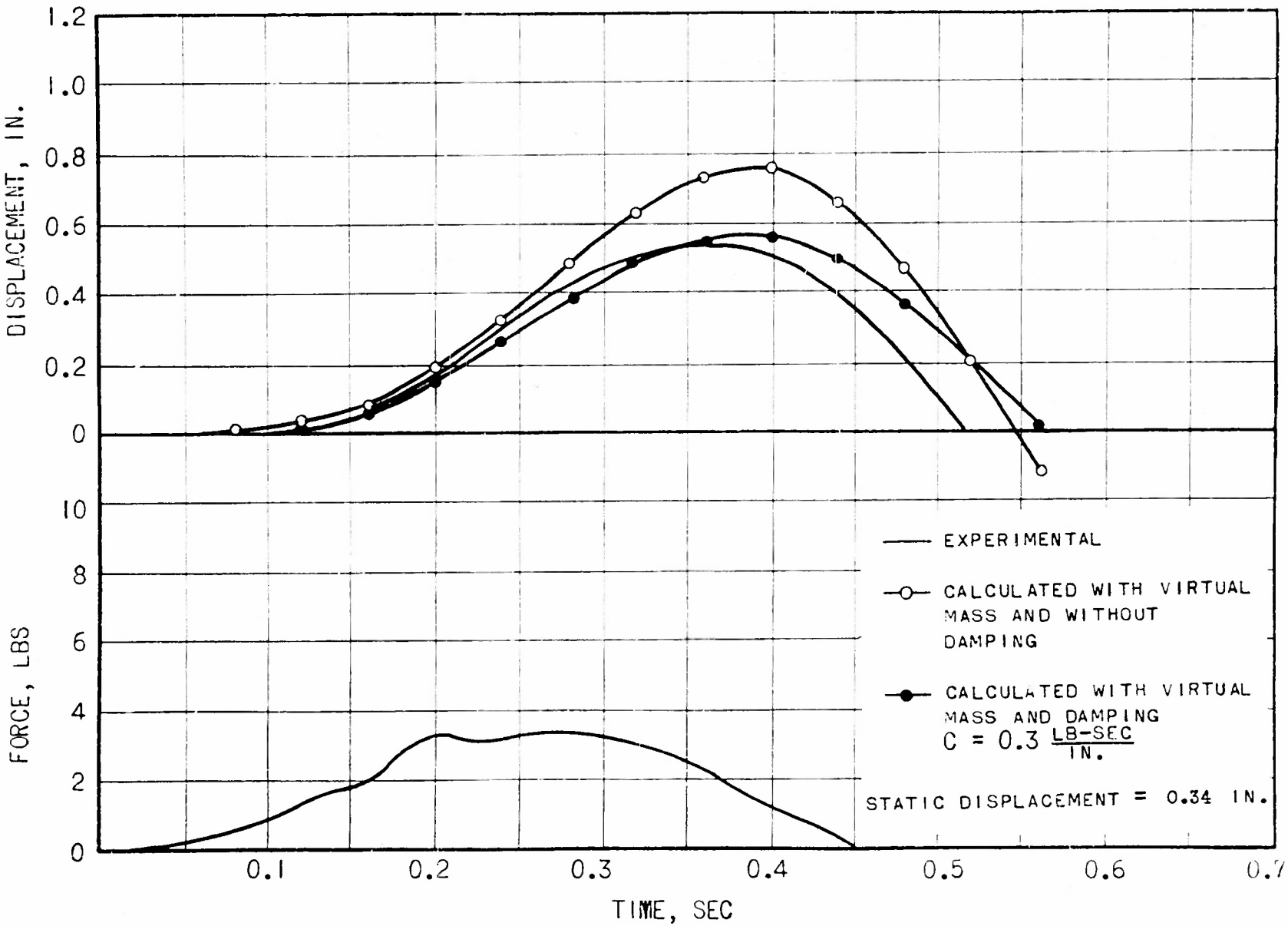

FIG. 47 RESULTS OF IMPULSE—DISPLACEMENT TESTS ON TRIANGULAR PONTON

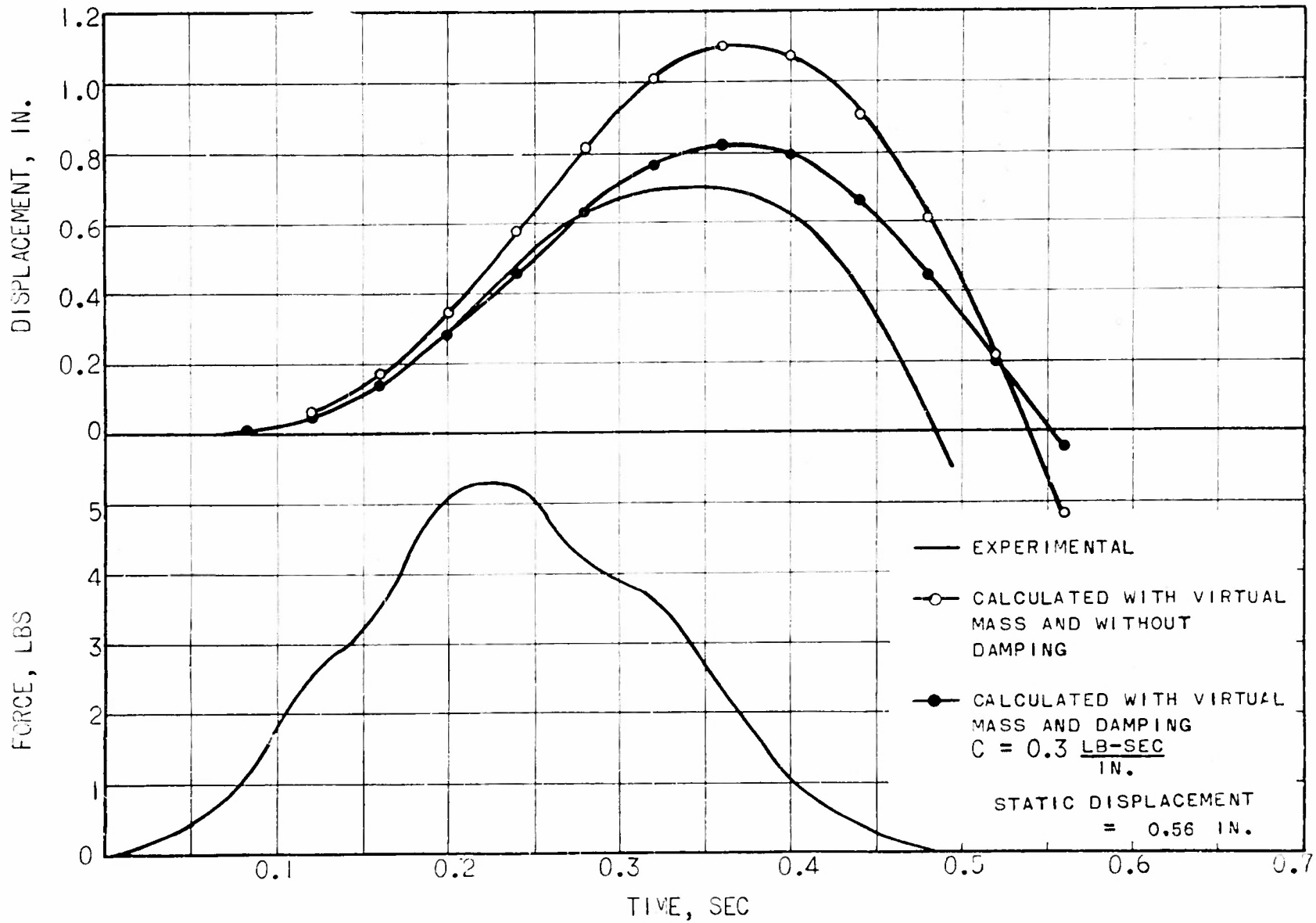

FIG. 48 RESULTS OF IMPULSE—DISPLACEMENT TEST ON TRIANGULAR PONTON

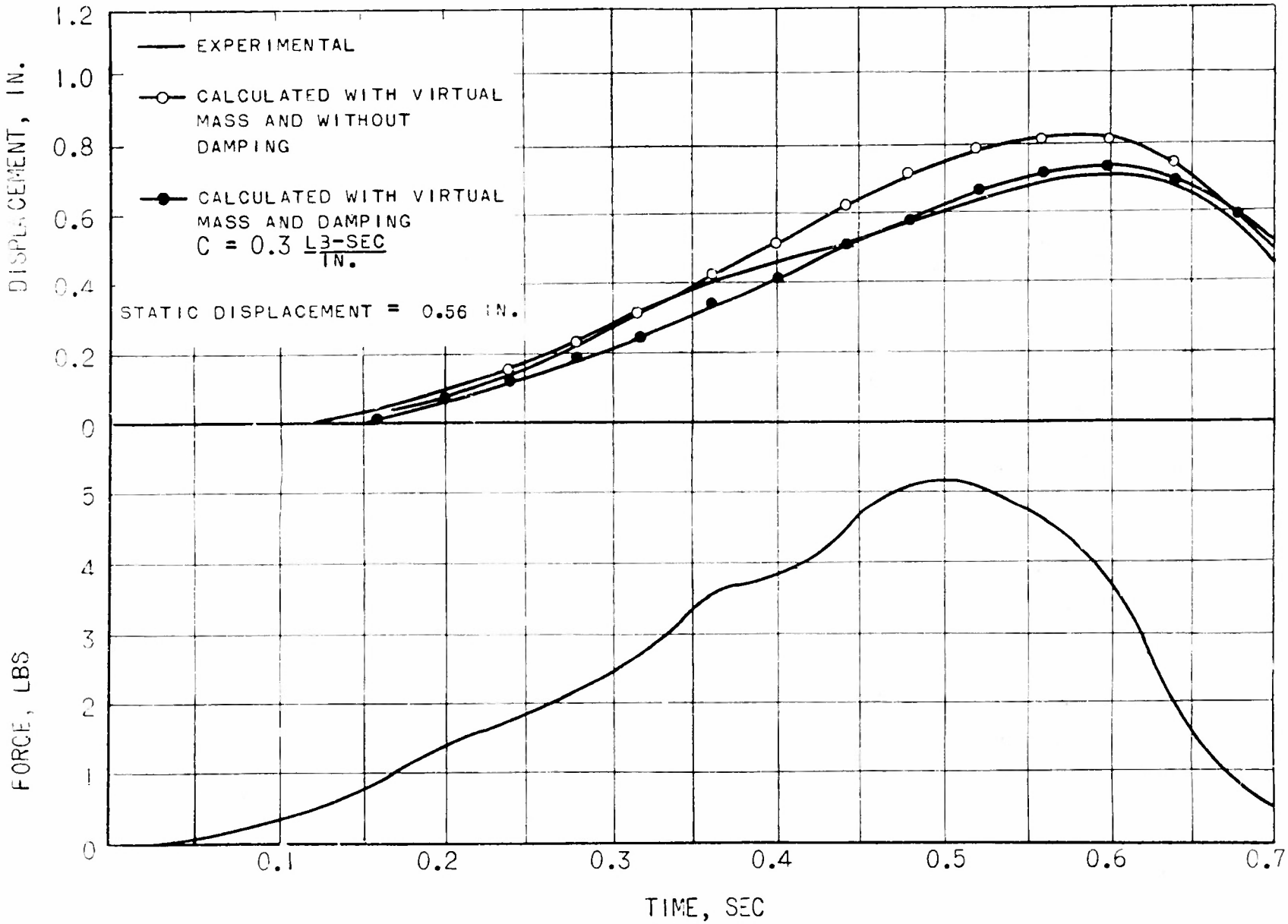

FIG. 49 RESULT OF IMPULSE—DISPLACEMENT TEST ON TRIANGULAR PONTON

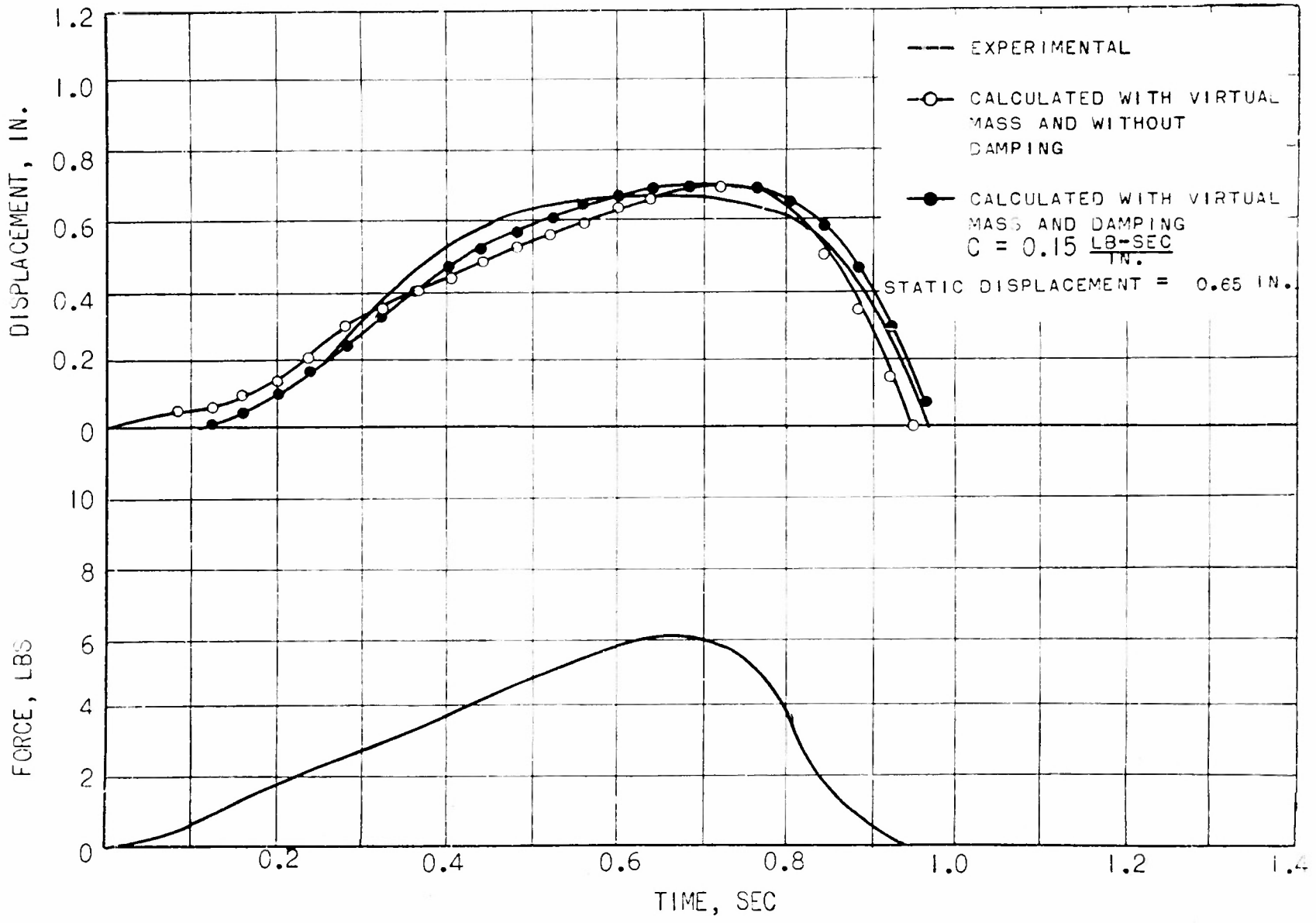

FIG. 50 RESULT OF IMPULSE—DISPLACEMENT TEST ON SEMI—CIRCULAR PONTON

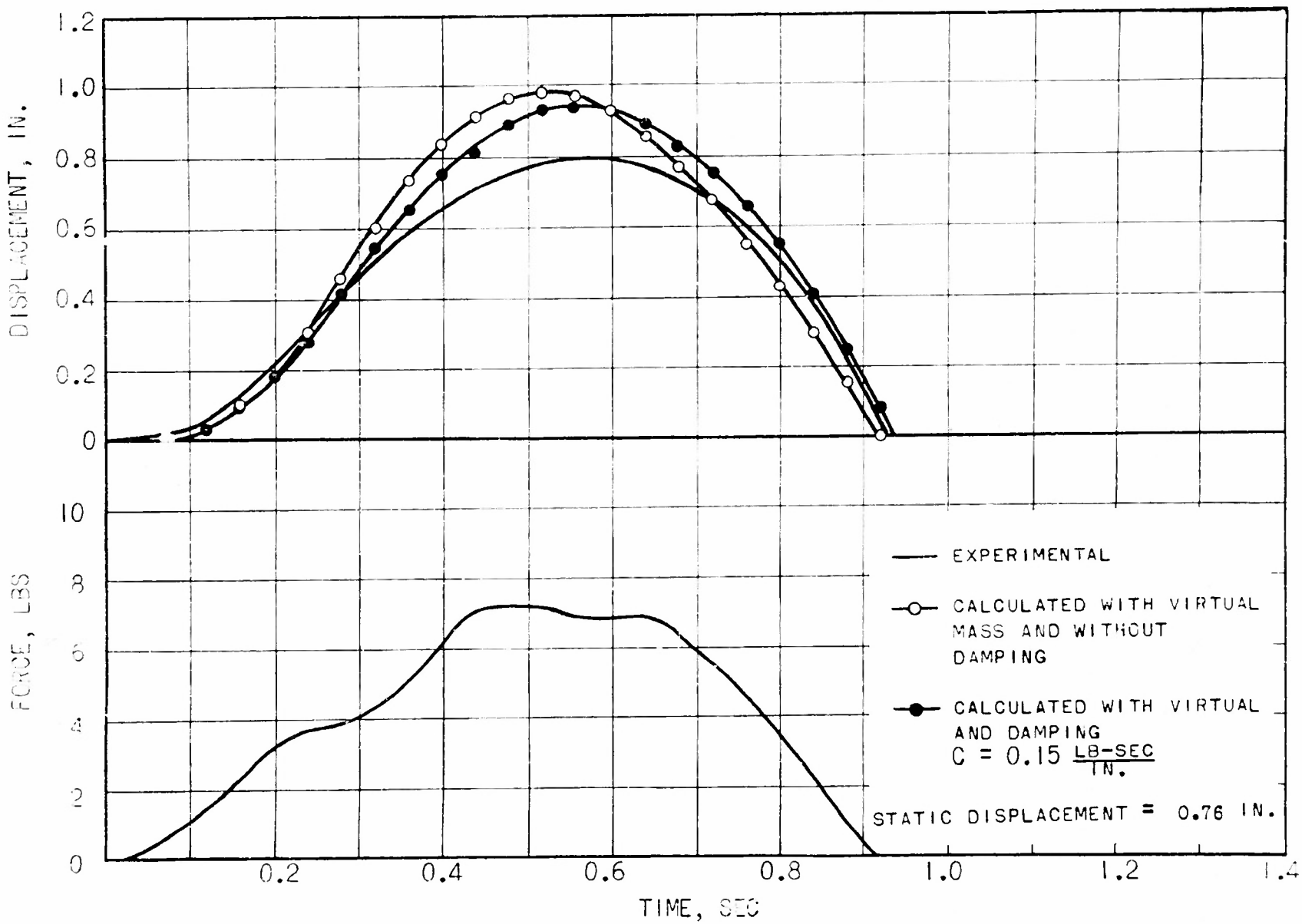

FIG. 51 RESULT OF IMPULSE—DISPLACEMENT TEST ON SEMI—CIRCULAR PONTON

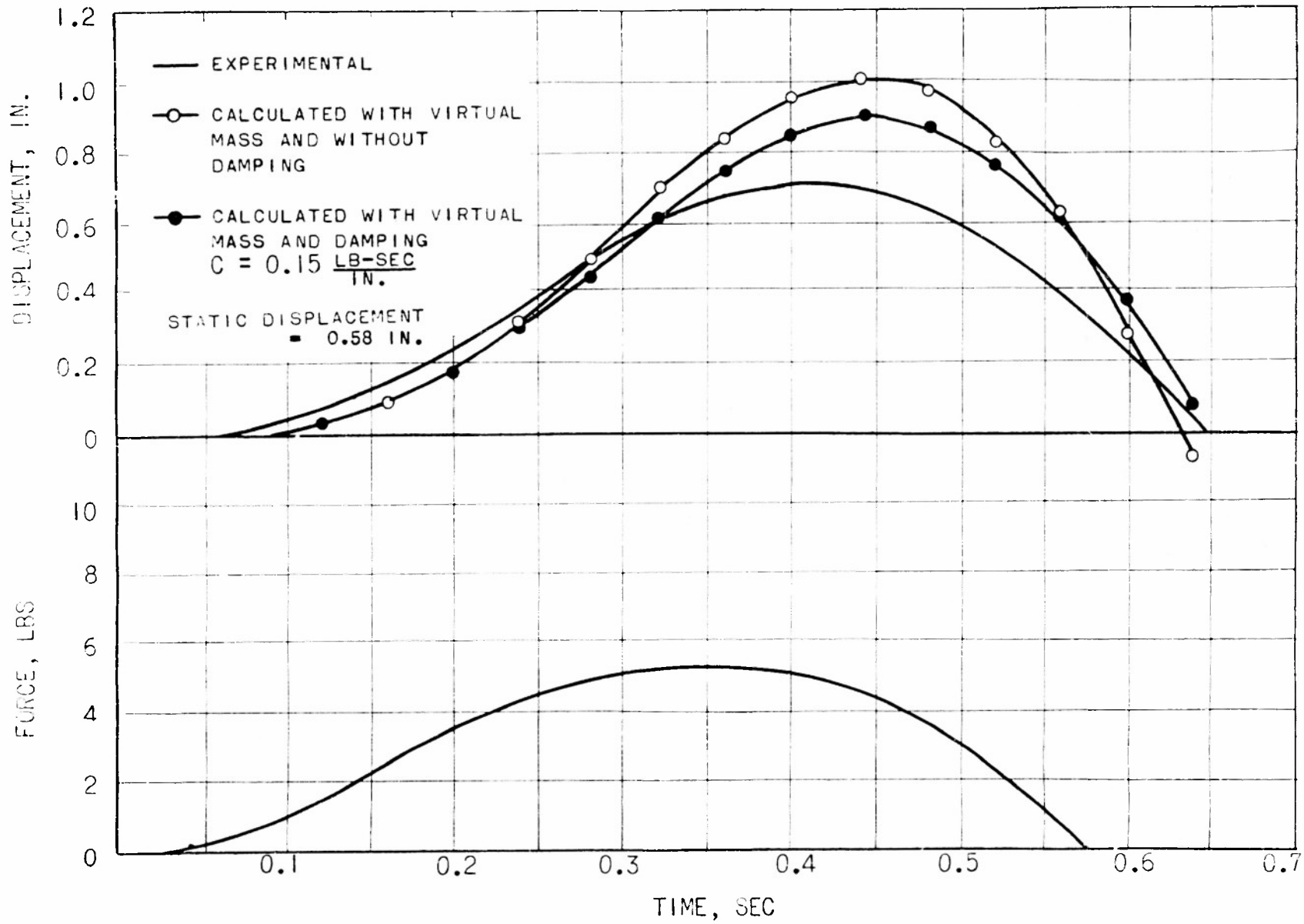

FIG. 52 RESULT OF IMPULSE—DISPLACEMENT TEST ON SEMI—CIRCULAR PONTON

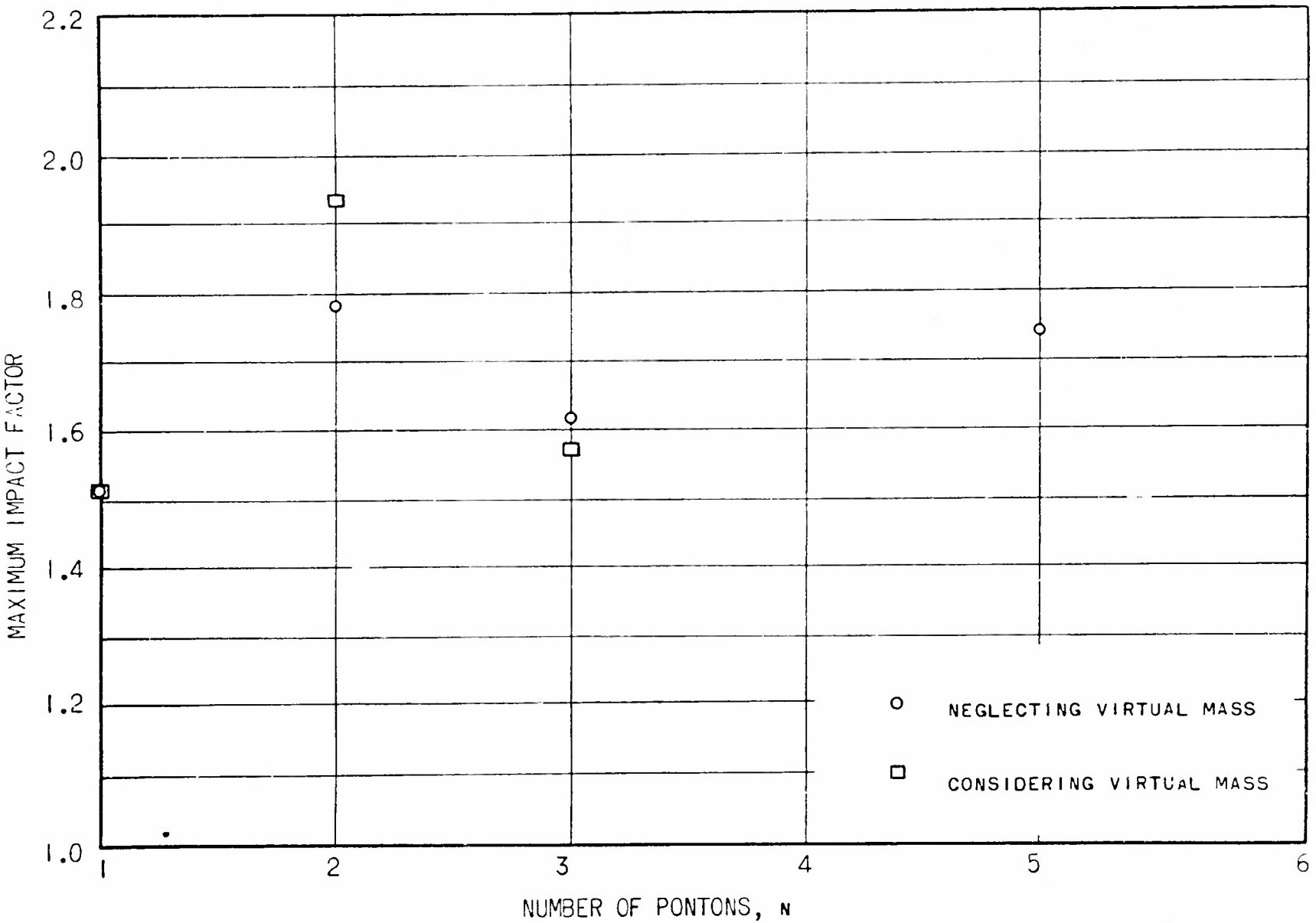

FIG. 53 RELATIONSHIP BETWEEN MAXIMUM IMPACT FACTOR AND NUMBER OF PONTONS

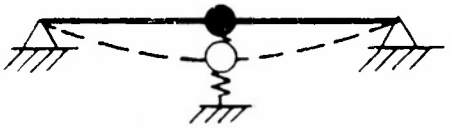

(a) ONE PONTON BRIDGE

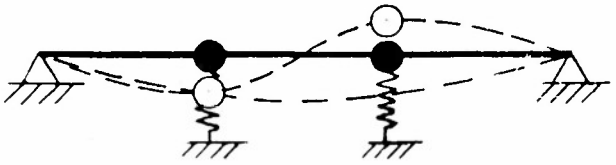

(b) TWO PONTON BRIDGE

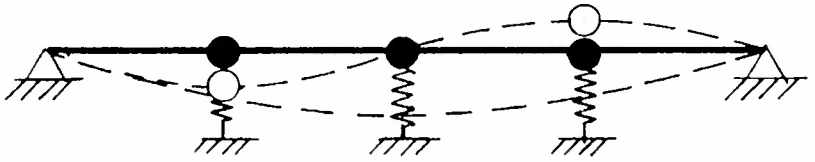

(c) THREE PONTON BRIDGE

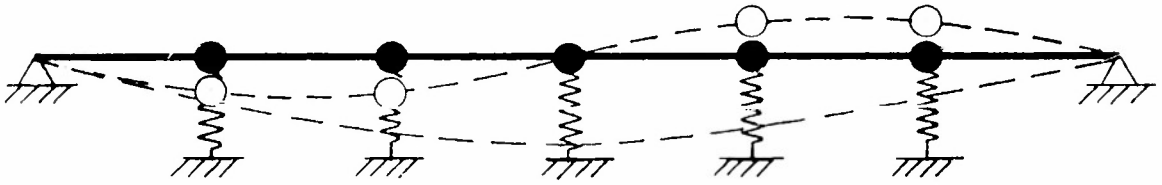

(d) FIVE PONTON BRIDGE

FIG. 54 FIRST AND SECOND MODES OF VIBRATION IN ONE, TWO, THREE AND FIVE PONTON BRIDGES

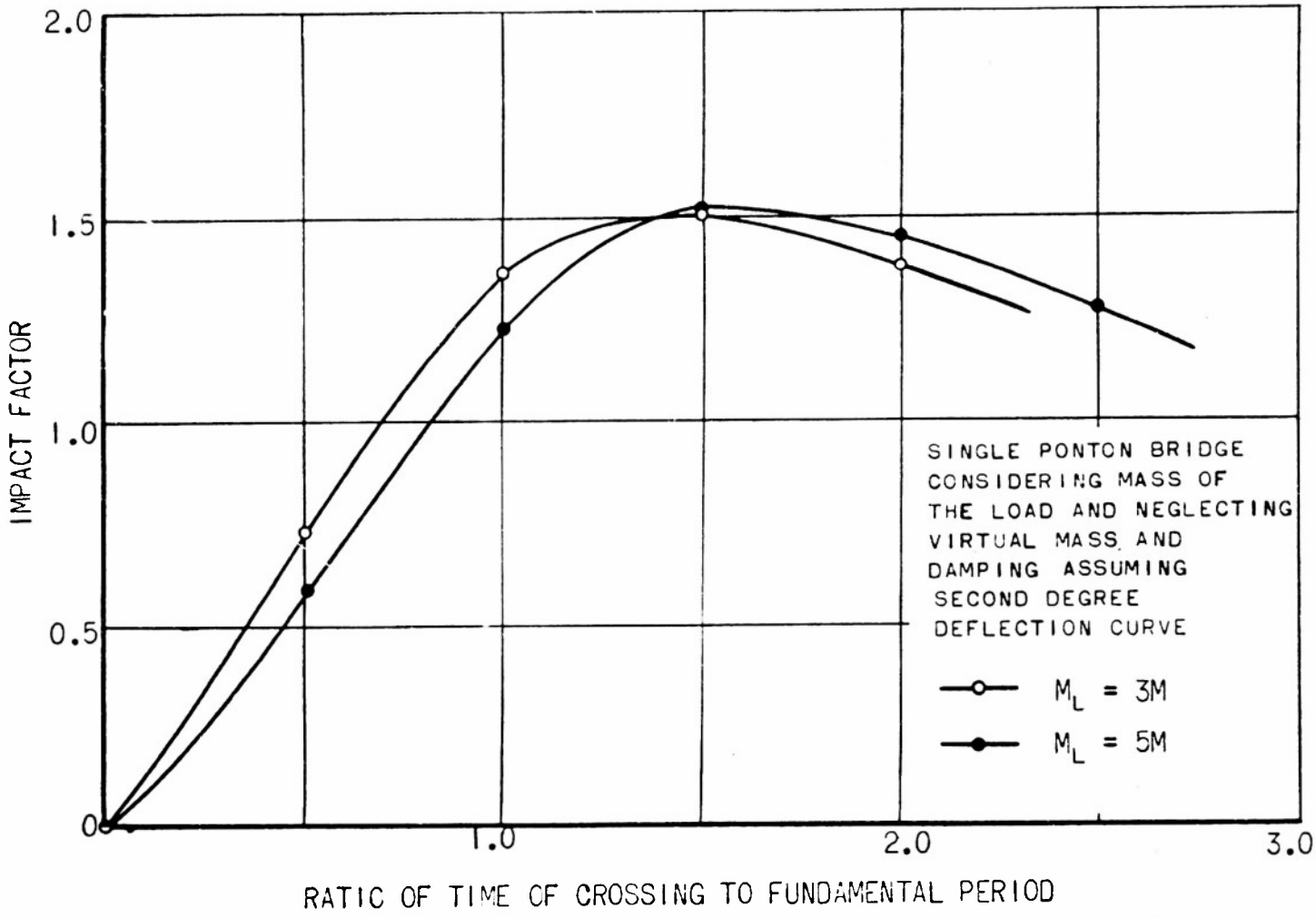

FIG. 55 RELATIONSHIP BETWEEN IMPACT FACTOR AND TIME OF CROSSING FOR SINGLE PONTON BRIDGE CONSIDERING MASS OF THE LOAD

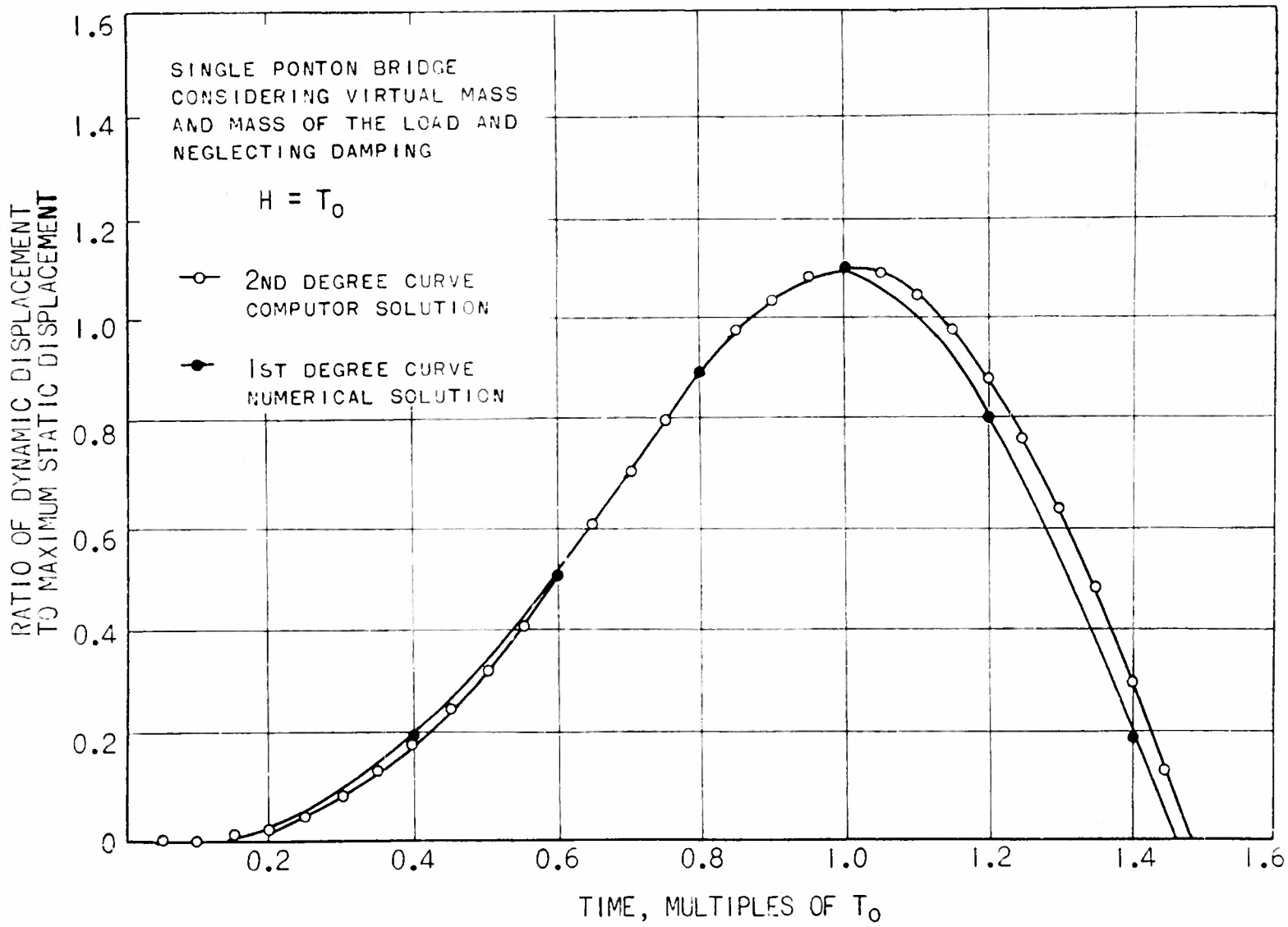

FIG. 56 DISPLACEMENT—TIME RELATIONSHIP FOR SINGLE PONTON BRIDGE CONSIDERING MASS OF THE LOAD

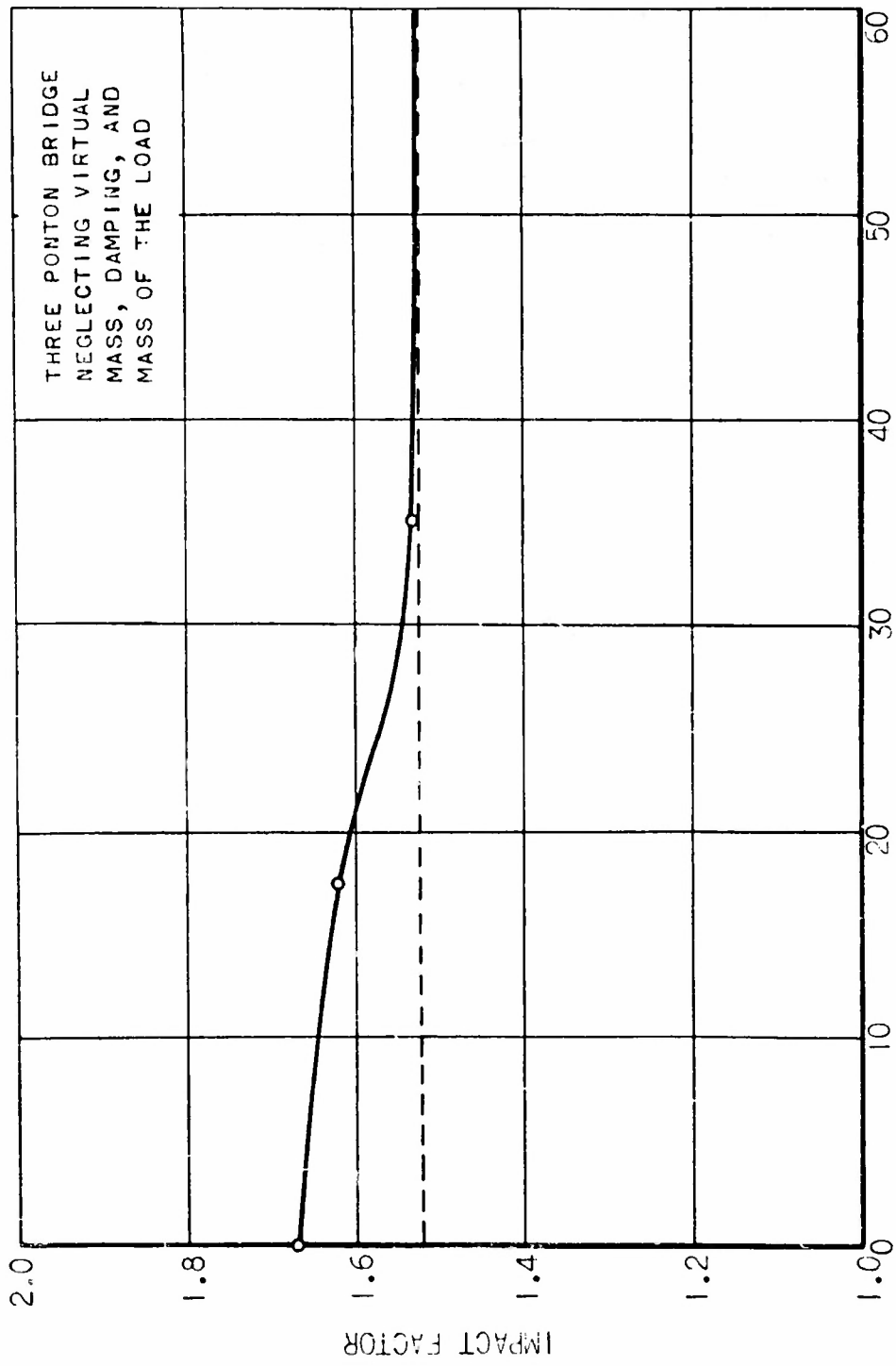

FIG.57 RELATIONSHIP BETWEEN IMPACT FACTOR AND RATIO OF K TO EI/L^3

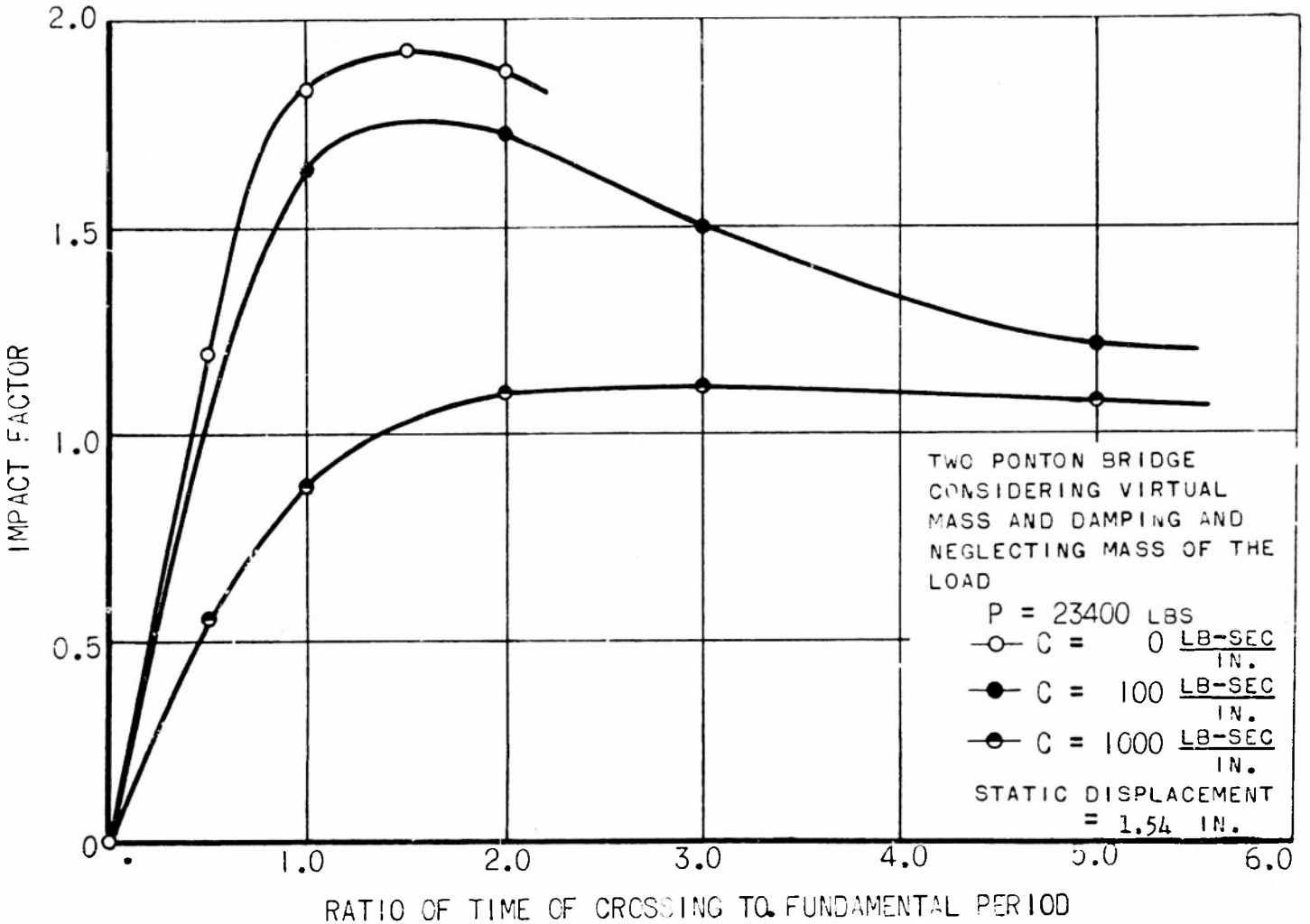

FIG. 58 RELATIONSHIP BETWEEN IMPACT FACTOR AND TIME OF CROSSING FOR TWO PONTON BRIDGE — C = 0, 100, AND 1000 LB-SEC PER IN

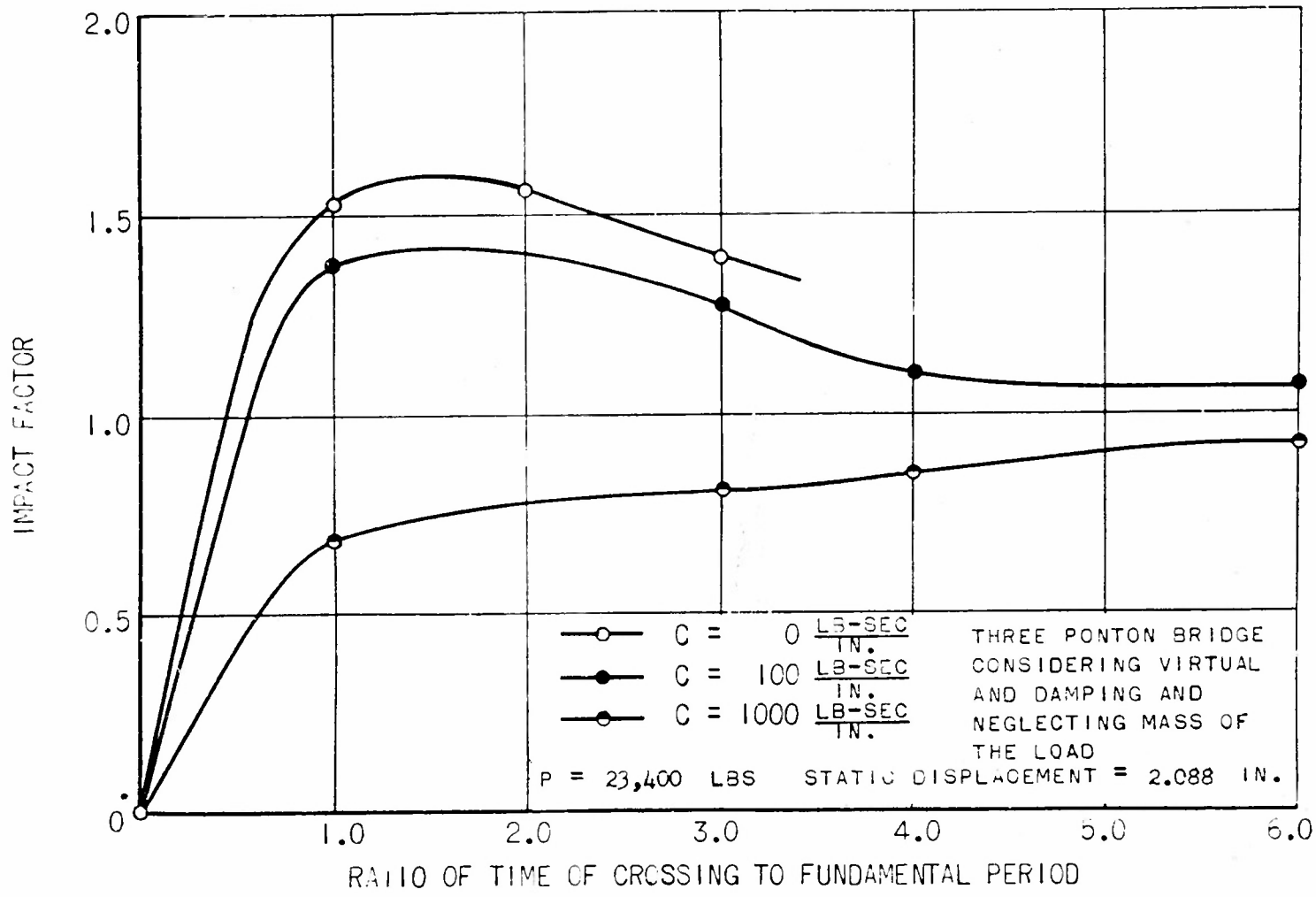

FIG. 59 RELATIONSHIP BETWEEN IMPACT FACTOR AND TIME OF CROSSING FOR THREE PONTON BRIDGE — C = 0, 100, AND 1000 LB-SEC PER IN

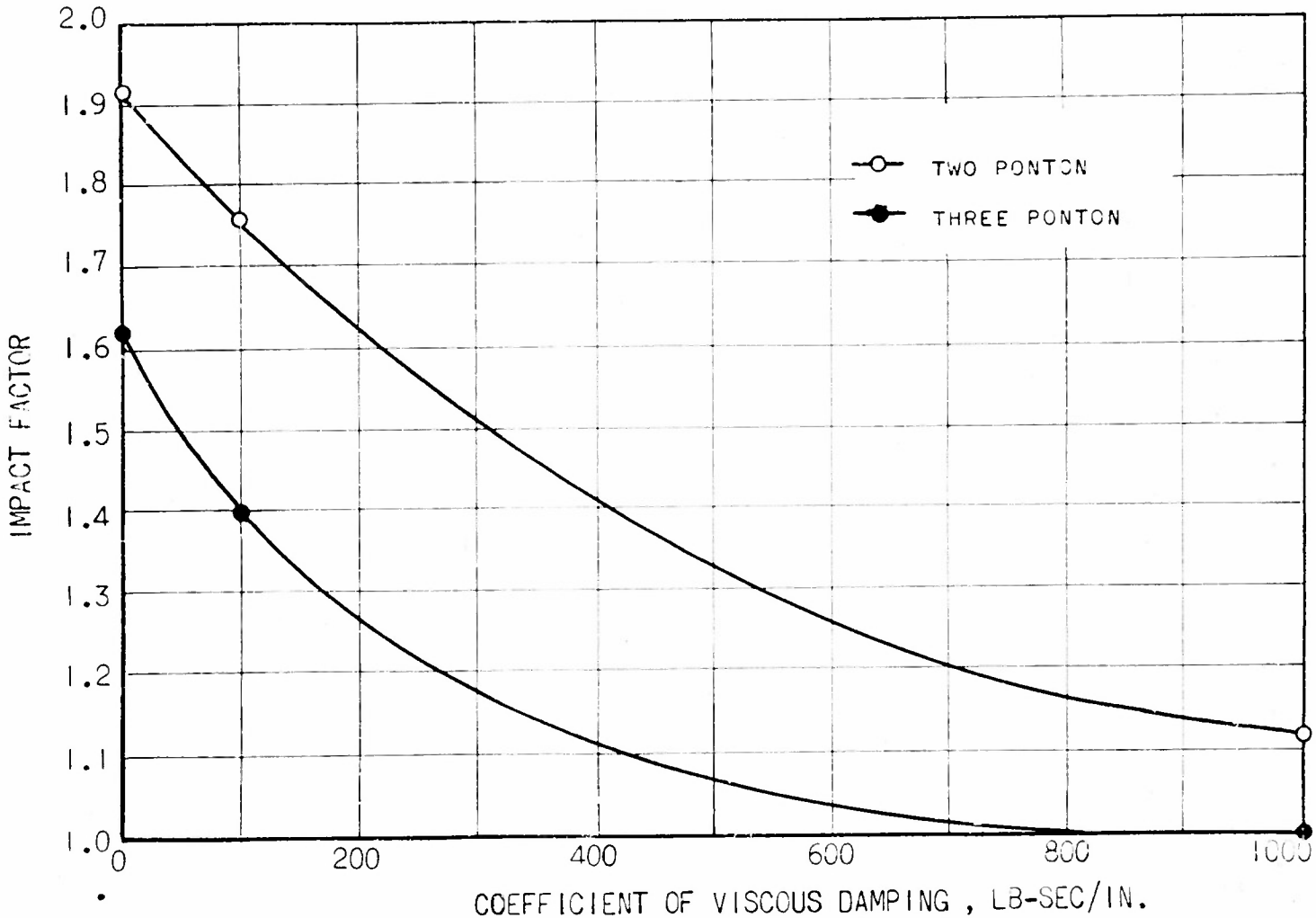

FIG. 60 RELATIONSHIP BETWEEN IMPACT FACTOR AND DAMPING FOR TWO AND THREE PONTON BRIDGES

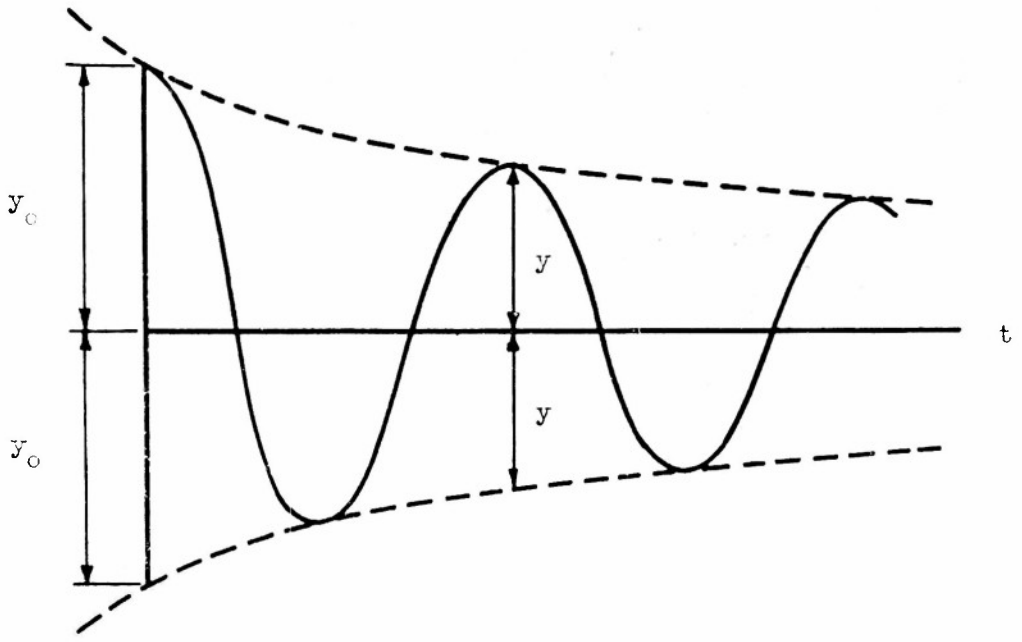

(a) SOLUTION OF EQUATION 78

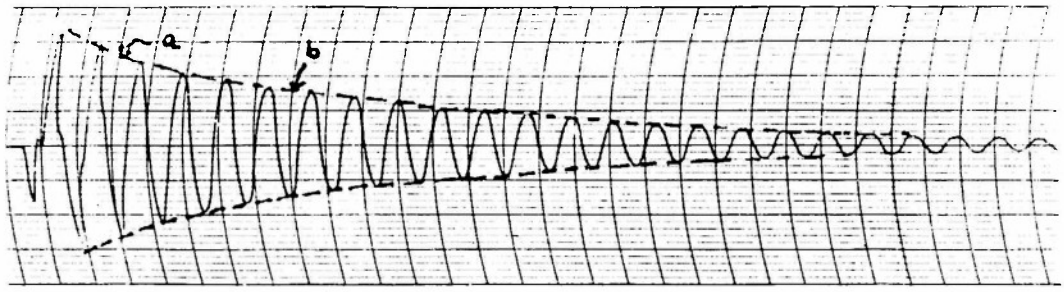

(b) TEST ON TRIANGULAR PONTON AT 2.06 IN. DISPLACEMENT

FIG. 61 DETERMINATION OF DAMPING COEFFICIENT

NETWORK

BLOCK REPRESENTATION

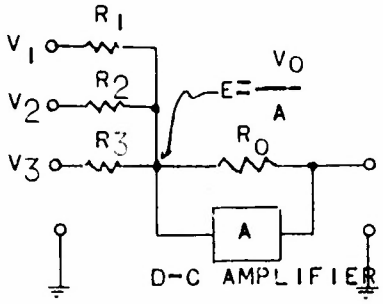

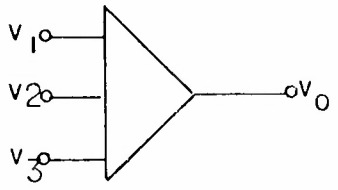

$V_0 = -(A_1V_1 + A_2V_2 + A_3V_3)$

(A) ADDITION

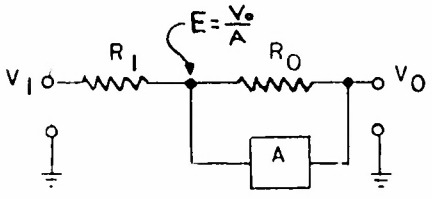

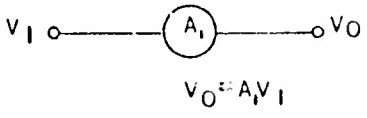

$V_0 = A_1V_1$

(B) MULTIPLICATION BY A CONSTANT

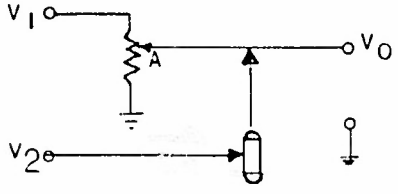

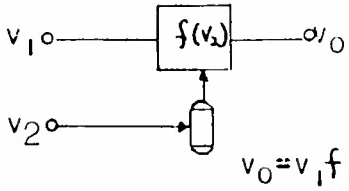

$V_0 = V_1 f(V_2)$

(C) MULTIPLICATION OF TWO VARIABLES

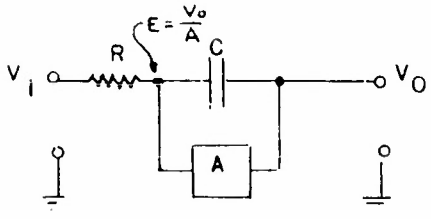

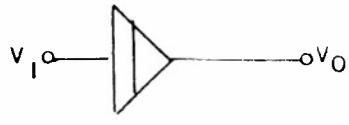

$V_0 = -\frac{1}{RCP} V_1$

(D) INTEGRATION

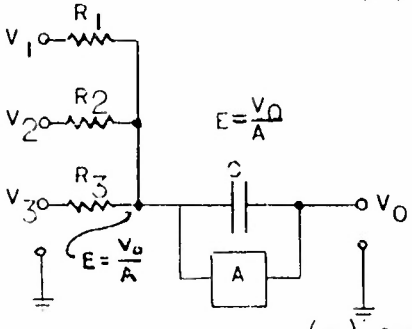

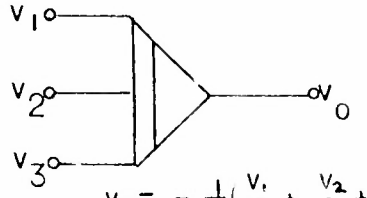

$V_0 = -\frac{1}{CP}\left(\frac{V_1}{R_1} + \frac{V_2}{R_2} + \frac{V_3}{R_3}\right)$

(E) SUMMING INTEGRATOR

FIG. 62 BASIC COMPUTING COMPONENTS

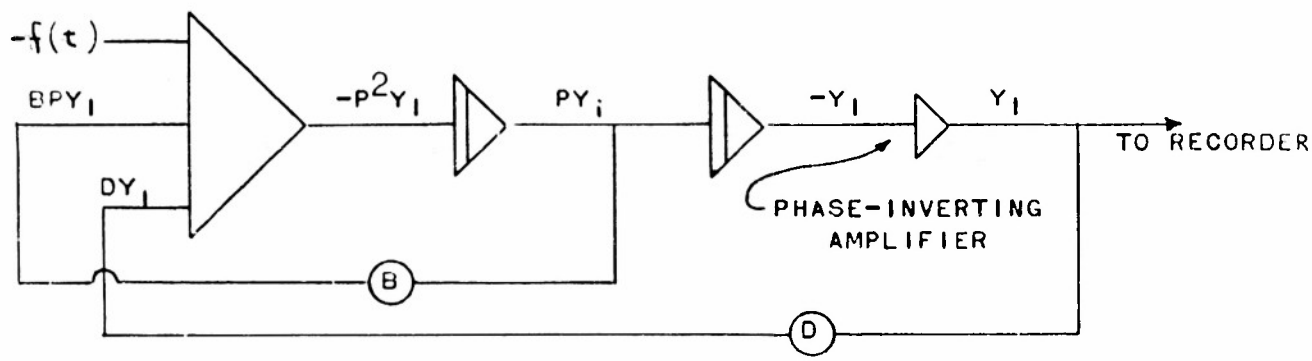

FIG. 65 SOLUTION OF THE DIFFERENTIAL EQUATION
$P^2Y_1+BPY_1+DY_1-f(t) = 0$

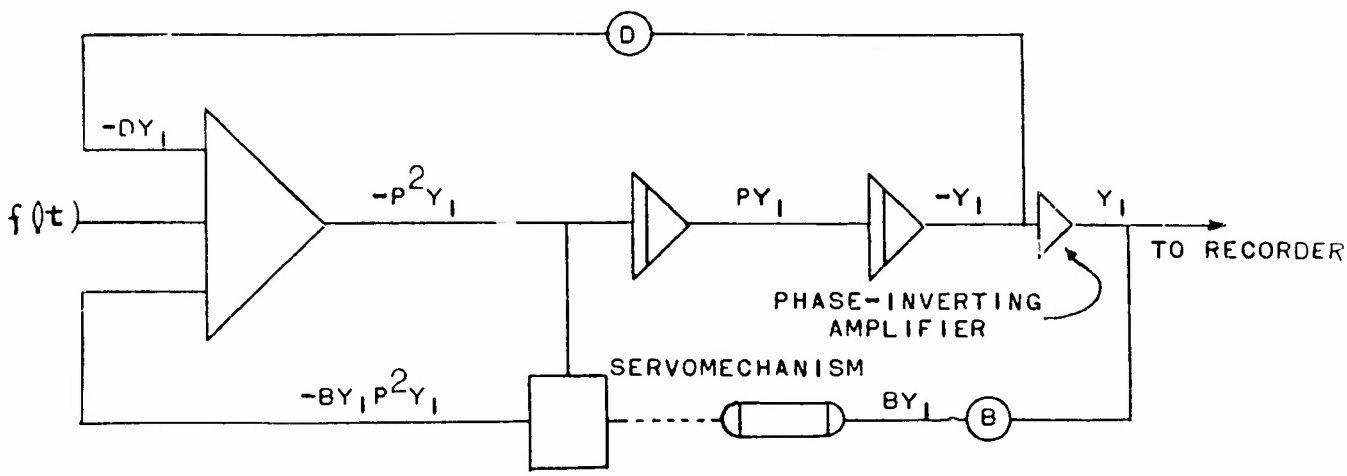

FIG. 66 SOLUTION OF THE DIFFERENTIAL EQUATION
$P^2Y_1+BY_1P^2Y_1+DY_1-f(t) = 0$

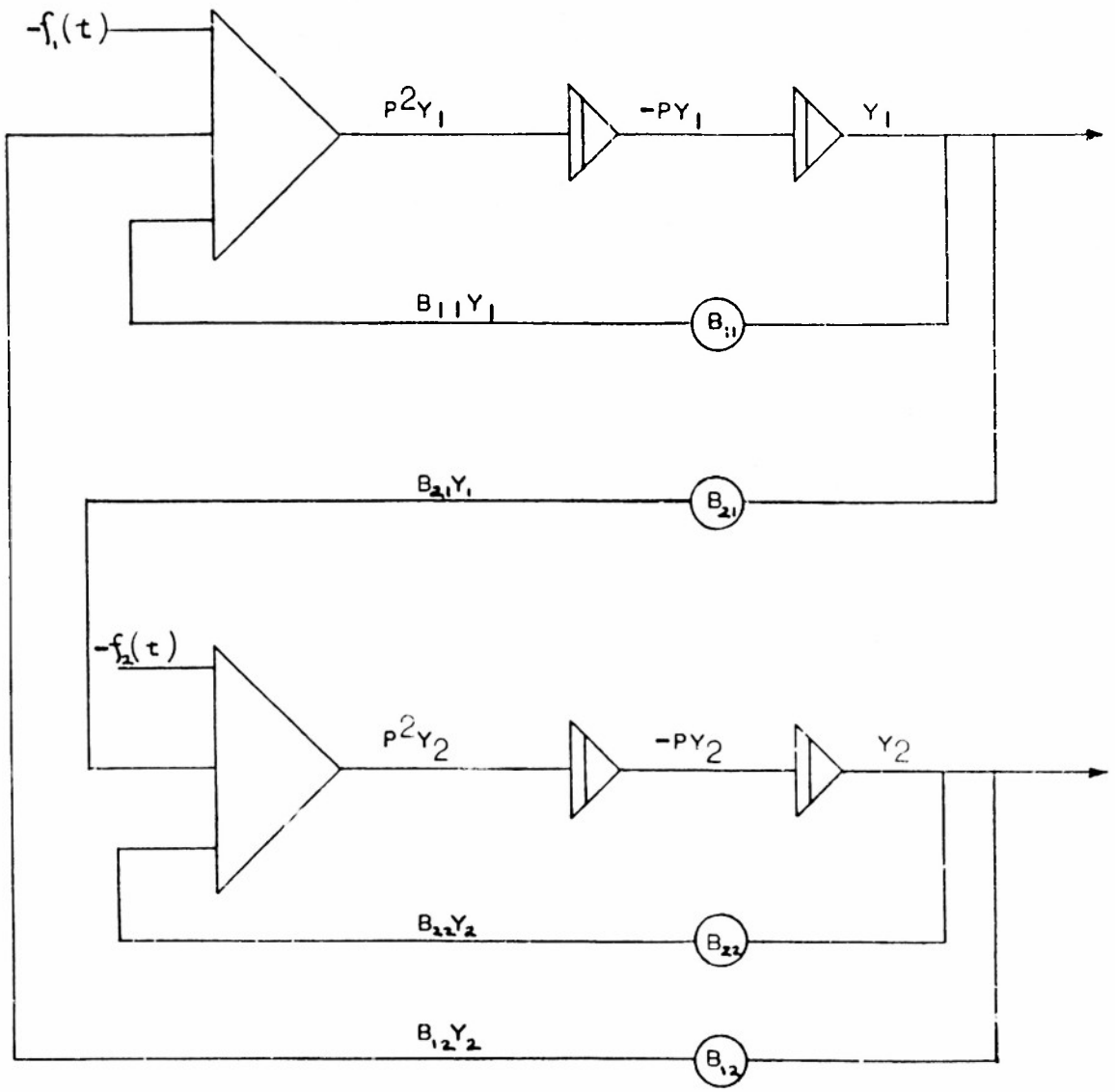

FIG. 67 PROGRAMING OF TWO PONTON BRIDGE